

**Zeitschrift:** IABSE reports of the working commissions = Rapports des commissions de travail AIPC = IVBH Berichte der Arbeitskommissionen

**Band:** 30 (1978)

**Rubrik:** Session IV: Seismic efficiency of large structures

### **Nutzungsbedingungen**

Die ETH-Bibliothek ist die Anbieterin der digitalisierten Zeitschriften auf E-Periodica. Sie besitzt keine Urheberrechte an den Zeitschriften und ist nicht verantwortlich für deren Inhalte. Die Rechte liegen in der Regel bei den Herausgebern beziehungsweise den externen Rechteinhabern. Das Veröffentlichen von Bildern in Print- und Online-Publikationen sowie auf Social Media-Kanälen oder Webseiten ist nur mit vorheriger Genehmigung der Rechteinhaber erlaubt. [Mehr erfahren](#)

### **Conditions d'utilisation**

L'ETH Library est le fournisseur des revues numérisées. Elle ne détient aucun droit d'auteur sur les revues et n'est pas responsable de leur contenu. En règle générale, les droits sont détenus par les éditeurs ou les détenteurs de droits externes. La reproduction d'images dans des publications imprimées ou en ligne ainsi que sur des canaux de médias sociaux ou des sites web n'est autorisée qu'avec l'accord préalable des détenteurs des droits. [En savoir plus](#)

### **Terms of use**

The ETH Library is the provider of the digitised journals. It does not own any copyrights to the journals and is not responsible for their content. The rights usually lie with the publishers or the external rights holders. Publishing images in print and online publications, as well as on social media channels or websites, is only permitted with the prior consent of the rights holders. [Find out more](#)

**Download PDF:** 09.12.2025

**ETH-Bibliothek Zürich, E-Periodica, <https://www.e-periodica.ch>**



## **SESSION IV**

### **Seismic Efficiency of Large Structures**

**CHAIRMAN:** R.T.G. Lane, London, England

**CO-CHAIRMAN:** Prof. Franco Capozza, Rome, Italy



Leere Seite  
Blank page  
Page vide



R.G.T. LANE, B.Sc., F.I.C.E., F.I.E.Aust.  
 Sir Alexander Gibb & Partners,  
 Reading,  
 England.

#### PROBLEMS IN ASSESSING THE EFFECTS OF EARTHQUAKE ON DAMS

It is difficult to assess future ground motion affecting large structures, failure of which would be catastrophic. The behaviour of mass concrete, and of earth and rockfill in embankments when subjected to earthquake is not well defined. There are few records of the effects of earthquake on dams. Extrapolation from model testing needs verification. The paper presents the problems and proposes further studies.

#### LA DIFFICULTE D'ESTIMER L'ACTION SISMIQUE SUR LES BARRAGES

Il est difficile d'estimer les mouvements futurs du terrain qui pourraient affecter des ouvrages de grandes dimensions dont la rupture serait catastrophique. Le comportement du béton cyclopéen, et des masses de terre et des enrochements dans des remblais, sous l'action de forces sismiques n'est pas bien défini. Il existe peu d'archives où sont enregistrés les effets des séismes sur des barrages. L'extrapolation des résultats d'essais sur modèles réduits demande à être vérifiée. Le présent article présente les problèmes et propose des études à poursuivre.

#### DIE BEURTEILUNG DER AUSWIRKUNG VON ERDBEBEN AUF DÄMME

Die Einwirkung von zukünftigen Erdbewegungen auf grosse Bauwerke, deren Zusammenbruch zu einer Katastrophe führen könnte, kann nur mit Schwierigkeiten eingeschätzt werden. Das Benehmen von Betonmassen, und von Erd- und Steinschüttung in Dämmen wird unter Erdbebenbedingungen nicht wohl erkannt. Es gibt wenige sorgfältig zusammengestellte Erfahrungen der Wirkung auf Talsperren von Erdbeben. Der Übergang in die Praxis von Modelluntersuchungen muss nachgewiesen werden. Im Papier werden die Probleme dargestellt und weitere Untersuchungen vorgeschlagen.



## CHAPTER 1 - DETERMINATION OF GROUND MOTION

1.1 Introduction

It is quite clear that it will never be possible to forecast the actual ground motion which will occur at the dam site due to a future major earthquake occurring close to site. It is therefore necessary to choose for design purposes an input of ground motion or force which will have a similar effect on the dam and the associated structures.

1.2 Pseudo-static methods

It has been known for many years that the simple pseudo-static approach using a seismic coefficient (a percentage of 'g', the acceleration of gravity) applied as a horizontal force, does not give a realistic answer when compared with a full dynamic analysis. A compromise solution can be adopted - such as that included in the U.S.S.R. regulations (ref. 1) in which a specified magnification of accelerations with height above ground is taken into account - but even this is not considered adequate for a large important structure for which failure could be catastrophic. A full dynamic analysis and model tests are recommended.

1.3 The problem

A two-fold problem is therefore presented :-

- specification for ground motion which is both realistic and is in a form which can be used in the computations,
- estimation of maximum magnitude (amplitude) of this motion.

1.4 Response spectrum method

It may be mentioned here that the "response spectrum" approach (ref. 2) as proposed for buildings has not yet been proven for large dams.

1.5 Design methods

The method often recommended uses an actual (or synthesized) ground motion based on records from a recording station which is considered from seismological and geological investigation to be similar to the dam site. The record may be scaled to have the maximum amplitude, predominate frequency and duration estimated as appropriate to the site (ref. 3). This requires skilled assessment by the Seismologist, Geologist and Engineer working together. Some dam designers have chosen to assume "white noise" with an estimated spectral density (ref. 4). The methods of computation which are used estimate (as well as the input data will allow) :

- principal stresses in the case of concrete dams,
- stresses and deformations for embankment dams.

In the latter case, some design methods use a finite element approach leading to the examination of critical zones where high shear stress could result in deformation (ref. 5) and others examine the conditions at critical slip surfaces (ref. 4 and 6).



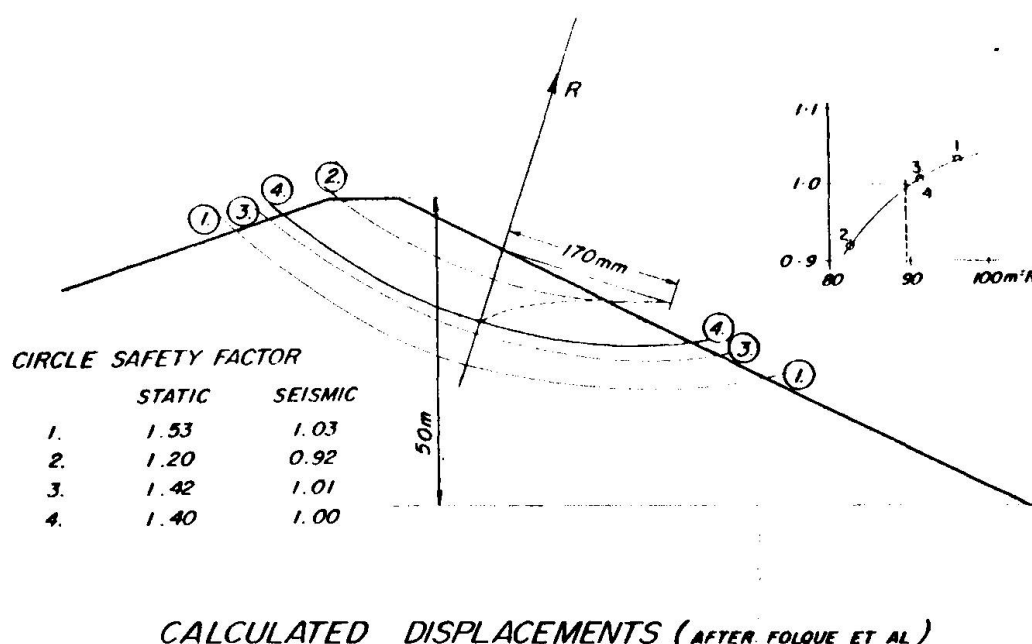


Fig. 1

#### 1.6 Further study and research

It is quite clear that further study and research are necessary before an agreed method of design can be recommended - indeed, it may be necessary to recommend more than one approach. For example, it is possible that different types of failure will become critical for different dams, or even for the same dam. Research work is in progress in many countries which includes the testing of existing dams using man-made vibrations (explosions), and instrumentation to record the effects of actual earthquakes. This will greatly improve our knowledge of dam behaviour within the elastic (or low-level stress) range. Further study of actual dam failures is also necessary related to the seismic events causing the failure and efforts are being made through the International Commission on Large Dams to assemble as much information as possible. For example,

1.6.1 - It is likely that the direction of approach of the ground vibration (horizontal, vertical or intermediate) will have a significant effect. Up to now vertical components of ground motion have usually been either neglected, or included in the design computations in an arbitrary manner; but there is theoretical evidence that the distribution of tensile stresses in an embankment due to vertical vibration is different from and perhaps more likely to be critical than due to horizontal vibration. The effect of vertical vibration on the stability of an unreinforced mass concrete structure is also likely to be significant.

1.6.2 - Examination of the frequency content of natural earthquake at the site could show resonance and the risk of causing resonance in the structure. For example, analysis of the ground motions recorded by instruments at the Lar scheme (embankment dam, tunnels etc.) in Iran has shown natural site resonance at Kalan at a frequency of about 3Hz. Also the frequency content of earthquake depends on geology, and on the distance to, and depth of the event. As another



#### IV.4

example, Ambraseys has shown that the acceleration response spectrum of the north-south component of motion in the Bucharest earthquake (March 4th, 1977) had an unusually long-period maximum, and structures with corresponding natural periods were worst affected (ref. 7). There is need for a better understanding of the relative effects of focal distances and depths on strong ground motion at sites of structures, both in regard to intensities and durations.

1.6.3 - The mode of failure needs critical examination, and the mathematical model should be able to demonstrate it. For example, earth slopes and escarpments can fail by lurching - i.e. the appearance of vertical cracks running parallel to the contours. Some embankment dams have failed in this manner. The seismic, topographic and soil conditions which lead to this phenomenon require further investigation.

#### 1.7 Seismic Zoning

For the purpose of regional planning in earthquake areas, the procedure of "seismic zoning" is adopted. Maps are prepared which usually divide the territory into zones corresponding to macroseismic intensity related to seismic coefficients tabulated in a code of practice. In recent seismic zoning the "intensity" is further specified on a "probability of occurrence" basis. This does not take into account local geologic or soil conditions, and at the scale of individual developments, micro-seismic zoning of the sites is required. It is a subject for discussion and further consideration as to which parameters should be shown on the microzoning maps, particularly for the sites of dams, where the engineer is interested in amplitude, frequency content and duration of ground motion; also the risk of soil failure with possible landslide, settlement or liquefaction.

#### 1.8 Induced seismicity

Local earthquakes have sometimes occurred after the impounding of large new reservoirs. If "large" is defined as depth of water exceeding 100 m and volume exceeding  $10^9$  cu. metres, then statistics indicate that this has happened in one out of every 14 such reservoirs. Magnitudes have in some cases exceeded 6 on the Richter scale.

These events may occur close to the dam and at shallow depth. They are therefore potentially dangerous even though the magnitude is not great; and at present there is only limited knowledge about the nature of such ground motions. It is probable that smaller, but important structures associated with the dam may be at greater risk than the dam itself (ref. 8).

### CHAPTER 2 - MATERIALS

#### 2.1 Concrete dams

2.1.1 The various gravity types and arch dams of concrete are built without general reinforcement, and the design for static conditions ensures compressive stresses throughout with few exceptions. Variable loading, the effects of temperature changes and gradients, and the variations in moisture content through the concrete often leads to minor cracks, usually at the surface and not very deep.

2.1.2 The addition of rapid and repeated stresses from earthquake can cause

new cracks or the propagation of existing cracks. On the other hand, materials are able to withstand higher stresses when the rate of application is high. At the present time the behaviour of concrete under these conditions is not well known.

2.1.3 The overall stability and safety of a structure subjected to earthquake depends on its ability to deform beyond the elastic limit without permanent damage, thus absorbing energy. Again there is little information available about the behaviour of mass concrete under these conditions.

## 2.2 Slopes and embankments

2.2.1 Natural slopes and embankments are prone to damage by lurching or landslide when subjected to earthquake. Lurching may be a failure in tension or perhaps shear between columns of material vibrating independently. Landslide is failure in shear, and the effect can be much worse if liquefaction occurs.

2.2.2 The properties of materials used for embankment dam construction include the following :-

- Deformation which is not reversible
- Significant volume changes
- Properties which change under wet conditions
- Properties which depend on previous stress history

2.2.3 The deformations therefore depend on the combined static and cyclic conditions of loading, and the laws governing the behaviour of these materials in a three dimensional static stress field when subjected to rapid and repeated stresses, as from earthquake, are not yet fully understood. The representation of soil properties as a visco-elastic continuum is not complete.

2.2.4 Two other particular aspects should be included in further investigations:

- The inertia effect which enables a soft material to resist a sudden blow,
- The failure which occurs at the tension phase of a stress reversal.

## CHAPTER 3 - STRUCTURES

### 3.1 Structure stability

The stability of a structure when subjected to earthquake is largely determined by its ability to withstand stresses beyond the elastic limit. This implies that there will be permanent deformation under severe conditions, as stress beyond the elastic limit leads to some strain which is not recoverable. It has even been suggested that concrete and steel structures should be designed with a factor of safety based on allowable deformation.

### 3.2 Concrete dams

3.2.1 Concrete dams are a special case in that unreinforced mass concrete is used. The risk of cracking and crack propagation has been referred to above



#### IV. 6

- but perhaps the greater risk is that movement will take place at construction joints. This is clearly dependant on stress across the joints, and high compression - as for example in a fully loaded arch dam - is going to reduce the risk of movement - either opening or sliding at the joints. It seems therefore that design should particularly take account of vertical dynamic forces combined with horizontal forces, and especially in the case of arch dams (when unloaded) and gravity dams.

##### 3.2.2 Examples of damage to concrete are :-

- Koyna (Maharashtra, India), a concrete gravity dam, which developed horizontal cracks on both upstream and downstream faces at about the level of the change of slope of the downstream face (ref. 1).

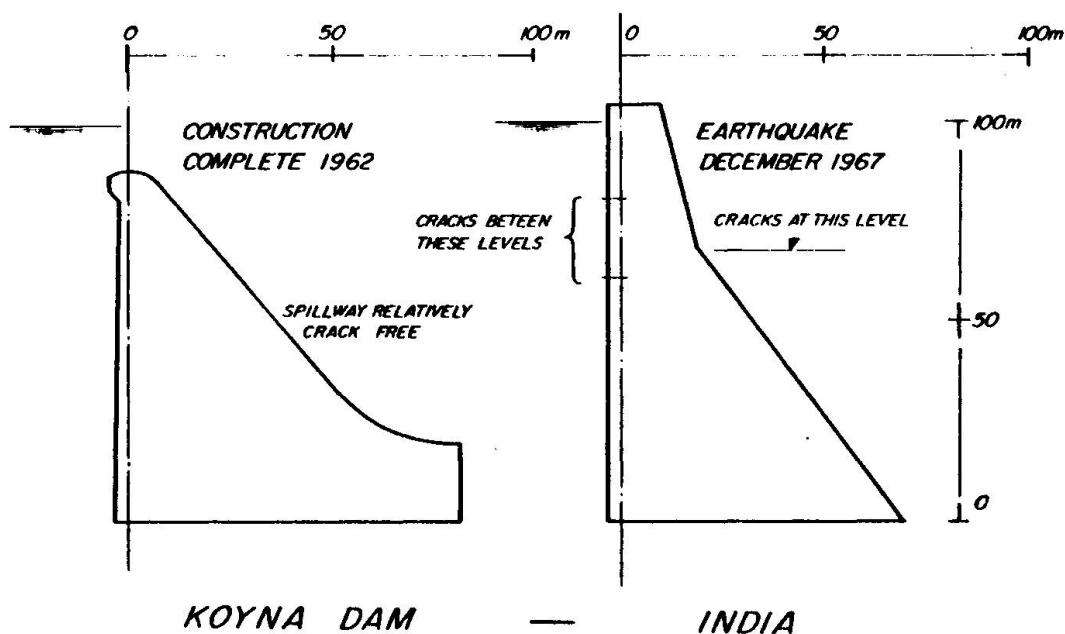


Fig. 2

- Murayama - Upper dam (Japan), an embankment dam, but the parapet wall developed a horizontal crack through it, and some of the concrete facing blocks above water level moved. (ref. 1)

##### 3.3 Embankments

3.3.1 Some embankment dams have been damaged by the development of approximately vertical cracks parallel to the axis of the dam (e.g. Ono dam, Japan, Murayama Lower dam, Japan, and Otani-ike dam, Japan). Other dams have failed by landslide, e.g. Sheffield Dam (U.S.A.) and the Lower San Fernando Dam (U.S.A.) (ref. 1).

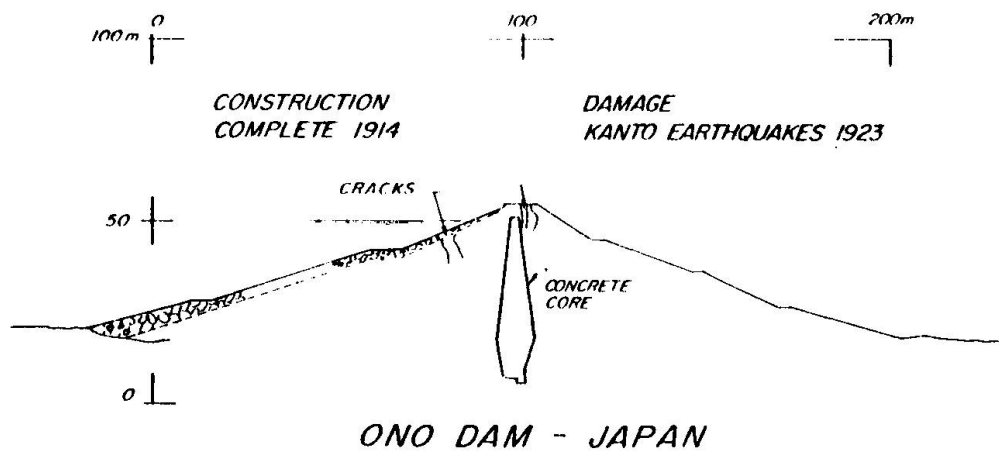


Fig. 3

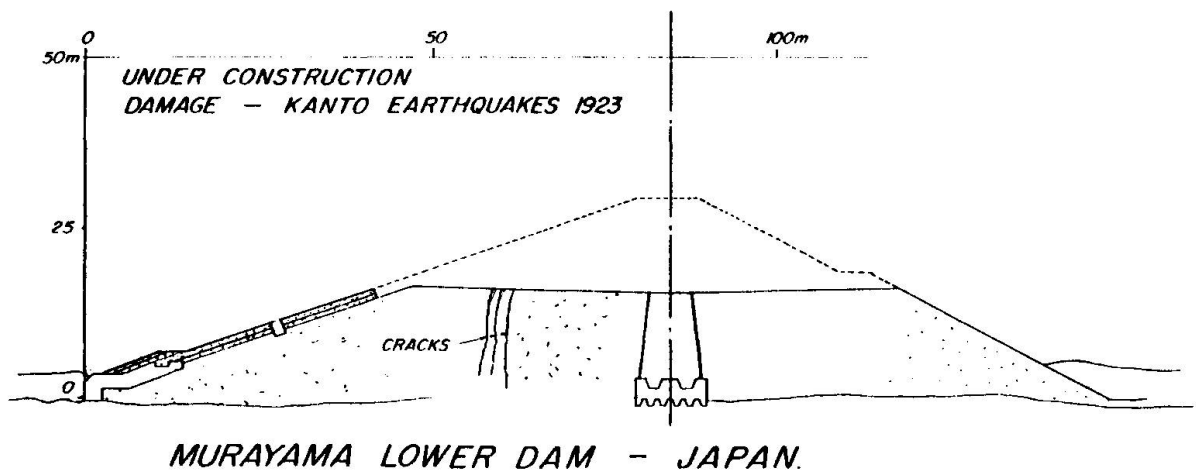


Fig. 4

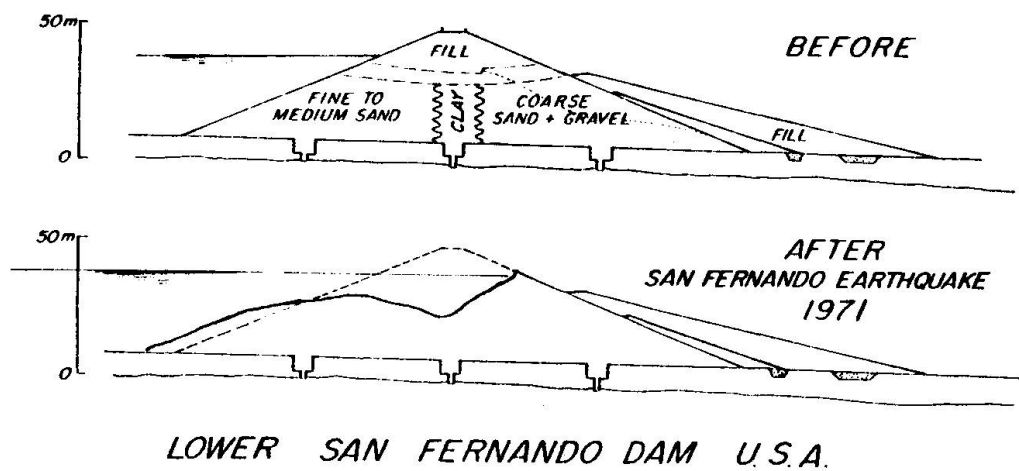


Fig. 5



3.3.2 An analysis of the Sheffield Dam failure has been given by Seed, Lee & Idris (ref. 9) which shows that the assumption that failure would occur on the arc-of-a-circle surface of minimum factor of safety gives a mode of failure very different from that which occurred. A dynamic response analysis using soil strength parameters based on cyclic loading simple shear tests and a finite element analysis, including a study of the liquefaction potential near the base of the embankment, give a mode of failure apparently in accord with the behaviour of the dam during the earthquake. It would, however, be interesting to study the alternative possibility that vertical cracks preceded the slide failure, as it is recorded that "After examination by several prominent engineers, the conclusion has been reached that the base of the dam had become saturated, and that the shock of the earthquake had opened vertical fissures from base to top; the water rushing through these fissures simply floated the dam out in sections".

3.3.3 It will be noted that the failures referred to have occurred in embankment dams constructed before the days of controlled compaction. Typical modern large dams have cores able to withstand limited tension, and shells which can take almost no tension, but compacted to a friction angle in the forties compared with the low thirties of an older dam. I have no knowledge of any modern embankment dam damaged by earthquake, but this does not mean that damage could not occur, as such dams may not yet have been subjected to strong shaking.

#### CHAPTER 4 - NEW STUDIES

4.1 Throughout the world engineers and experts in associated disciplines are engaged in study and research on the seismic aspects of dam design. A committee of the International Commission on Large Dams on this subject is supported by working groups in many countries. The time has come for a reappraisal of the "state of the art", and I put forward the following recommendations :-

4.2 Case histories and factual data should be assembled concerning the response of dams to earthquake. The record should include :-

- Seismicity
- Geological conditions
- Materials behaviour
- Structure behaviour.

4.3 Study the stress, strain and deformation of concrete dams when subjected to vertical and horizontal vibration, and the combination of these most detrimental to stability. Relate to case histories and establish optimum shapes and layout of structures; consider the use of post-stressed or other reinforcement where appropriate.

4.4 Consider embankment dams as part of the landscape and examine the effects (stress, strain and deformation) of vibration approaching from below or horizontally, and the combination most detrimental to stability. Relate mode of failure to case histories and establish optimum shapes and layout. Consider use of stainless steel strip or other reinforcement of the embankment where appropriate.

4.5 Continue research into behaviour of materials of construction subjected to rapid and reversal stresses as from earthquake. The risk of liquefaction can be avoided by appropriate specification for the materials and methods of placing embankments, but there may be a risk associated with in-situ materials.

#### REFERENCES

1. ICOLD, A review of earthquake resistant design of dams, Bulletin 27, March 1975.
2. An evaluation of a response spectrum approach to seismic design of buildings, U.S. Department of Commerce, Applied Technology Council, September 1974.
3. \*Recent concept of dynamic stability. Analysis of fill dams, Japanese National Committee on Large Dams, September 1977.
4. FOLQUE, J. et al., Seismic Study of Earth Dams, Proc. Third European Symposium on Earthquake Engineering. Sofia, September 1970.
5. Dynamic Analysis of Embankment Dams. U.S. Department of the Interior, USBR (preliminary)\*, March 1976).
6. SARMA, S.K., \*Response and Stability of Earth Dams during Strong Earthquakes Imperial College of Science and Technology, Nov. 1976.
7. AMBRASEYS, N.N., Long-period effects in the Romanian earthquake of March 1977. Nature, Vol 268, July 1977.
8. LANE, R.G.T., Seismicity at man-made reservoirs, Proc. ICE, Vol 50, September 1971.
9. SEED, H.B., LEE, K.L., and IDRIS, I.M., Analysis of Sheffield Dam Failure, Proc. ASCE, Soil Mechs. & Fdns. Div., Vol 95, SM6, November 1969.

\* Unpublished



Leere Seite  
Blank page  
Page vide

THE CONSEQUENCES OF PARTIALLY GROUTED JOINTS UPON  
THE ARCH DAM SEISMIC BEHAVIOUR

L'EFFET DE L'INJECTION PARTIELLE DES JOINTS SUR LE  
COMPOTEMENT SISMIQUE DES BARRAGES-VOUTES

DIE EINWIRKUNG DER TEILEINPRESSUNG VON BAUFUGEN  
AUF DAS ERDBEBENVERHALTEN DER BOGENSTAUMAUERN

Radu Prisca\*, Adrian Popovici\*\*, Constantin Stere\*\*\*

SUMMARY-RESUME-ZUSAMMENFASSUNG

By partially grouting some contraction joints, several favourable changes in arch dam seismic behaviour may occur. In this paper, a numerical study of the seismic behaviour of a large arch dam in Romania is being carried out, through the finite element method, following the hypotheses of a monolithic-continuous structure and, comparatively, of different dam joints grouting schemes. Some remarks related to the seismic behaviour of this large dam during the recent Vrancea Earthquake of March, the 4-th 1977 are also included.

L'injection partielle des joints entraîne des modifications favorables sur le comportement sismique des barrages-voutes. Dans l'ouvrage, tout en employant la technique des éléments finis, on analyse le comportement sismique d'un grand barrage en Roumanie à partir d'une hypothèse sur la structure monolithique et comparativement en différentes variantes d'injection des joints. On y fait également des remarques sur le comportement de ce grand barrage au récent tremblement de terre Vrancea, 4 mars, 1977.

Die Teileinpressung von Baufugen führt zu vorteilhaften Änderungen beim Erdbebenverhalten der Bogenstaumauern. Auf Grund der Methode der finiten Elemente, wird in der Arbeit das Erdbebenverhalten einer grossen Talsperre in Rumänien untersucht, unter der Voraussetzung einer einheitlichen Manerwirkung und vergleichend für verschiedene Einpressvarianten der Fugen. Gleichzeitig wird eine Diskussion über das Verhalten dieser grossen Talsperre bei dem kürzlich stattgefundenen Erdbeben (in Vrancea), vom 4 März 1977.

---

\* Dr.Doc.Eng., Professor, Department of Hydraulic Structures, Head, Civil Engineering Institute of Bucharest, Romania.

\*\* Dr.Eng., Reader, Department of Hydraulic Structures, Civil Engineering Institute of Bucharest, Romania.

\*\*\* Dr.Eng., Assistant Professor, Department of Hydraulic Structures, Civil Engineering Institute of Bucharest, Romania.

## THE CONSEQUENCES OF PARTIALLY GROUTED JOINTS UPON THE ARCH DAM SEISMIC BEHAVIOUR

R.Priscu, A.Popovici, C.Stere

One usually considers, through a current static and dynamic analysis, the arch dams as being monolithic structures with a linear-elastic behaviour [1], [2], [3]. However, the arch dam constructive make up of blocks separated by grouted joints leads to some peculiarities somehow differing from the current adopted model; thus, although grouted, the joints have a limited capacity of taking over the tensile and shear stresses. Therefore, when the state of stresses in the arch dam joints exceeds their tensile or shear strength, a reciprocal sliding of the joints or their opening may occur and, consequently, the dam structure is being deprived of its monolithic character.

Recently, several papers [4], [5] have dealt with the consequences of partially grouted joints upon the arch dam seismic behaviour. Following some model experimental research, they have put into evidence the antiseismic efficiency of a dam constructive system characterized by preserving about  $4 \div 5$  ungrouted joints over the upward one fourth of the dam height, the dam continuity at its crest being performed through a reinforced belt. The above system has shown some higher damping capacities against the dam structure with completely grouted joints (increasing  $2 \div 3$  times the fraction of critical damping) and a more favourable distribution of the dam response seismic stresses [4].

In this paper, the behaviour of a Romanian large arch dam is numerically simulated through the finite element method, by examining several dam constructive solutions with completely and partially grouted joints. Also, some interesting aspects related to this large dam seismic behaviour during the Romanian earthquake of Vrancea, 4 March 1977 are being commented upon.

### 1. THE COMPUTING MODEL

By the details of Figure 1 one presents the mapping plan and seve-



ral geometric elements of the Vidraru arch dam, taken up as a physical support for simulating the different constructive variants of our study. The Vidraru double curvature arch dam, built up on the Arges river and put into operation in 1965, is at present, the highest dam in Romania. It has the maximum height of 166m and the crest length of 292 m. The dam body has a slight geometrical skewness, being more developed at its upper part next to the left bank.

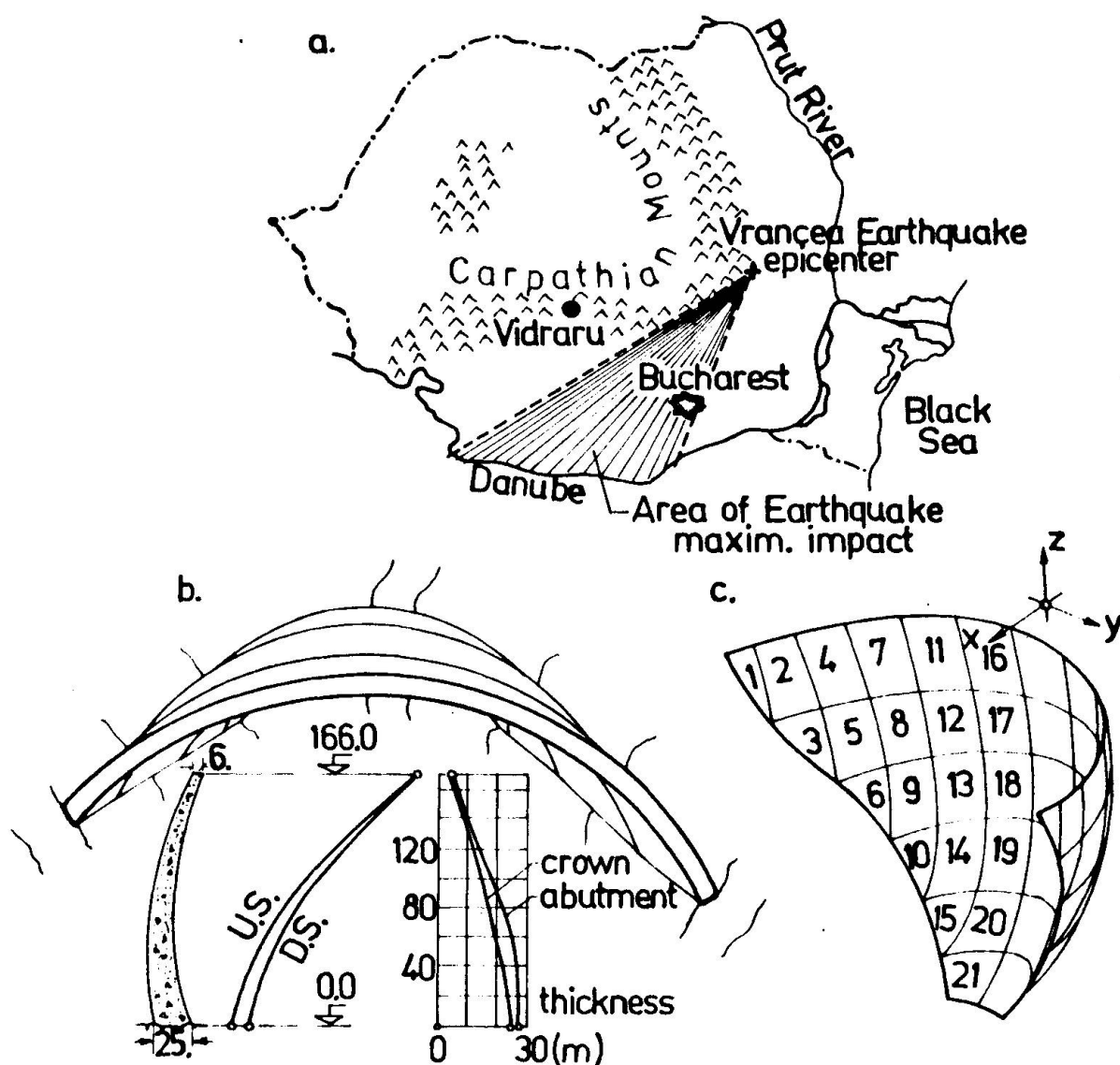
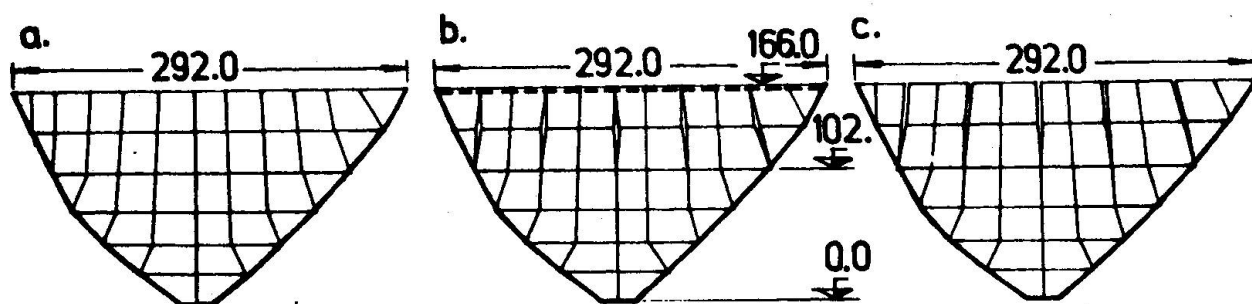


Fig. 1 Vidraru dam: a-the dam site related to the Vrancea earthquake epicenter, b- dam mapping plan and specific geometrical elements, c-thin shell-type finite element discretization network.

The discretizing of the structure has been carried out with finite elements of C.FELLIPA-R.W.CLOUGH thin shell type [6] which reproduce the dam mean surface (Fig.1,b). The quadrilateral element of an arbitrary geometry may be obtained by assembling four compatible triangles. Finally, the finite element used has 20 degrees of freedom, 5 degrees on each node, defined with respect to the element local coordinate system (one disregards the local torsion within the element).

The considered constructive variants of joints grouting and the corresponding discretization networks are presented in Figure 2. In fact, the following three cases have been accurately investigated: dam joints completely grouted, 5 ungrouted joints between the elevations 166 and 102 and reinforced belt at the dam crest, 5 ungrouted joints between the elevations 166 and 102. In nature, the considered structure has got complete grouted joints. The latter case has mainly served as testing model, by comparing its computed stresses and displacements with the Vidraru dam field measured ones; the relative changes which occur in the partially grouted structure have also been related to the monolithic dam case. The ungrouted joints have been reproduced by using double neighbouring nodes connected with beam-type elements of a reduced stiffness. Thus, the contiguous dam blocks work independently under tension loads and jointly concur in taking over compressions.



**Fig. 2** Dam joints grouting schemes:  
a-complete grouting, b-partial grouting and crest stiffening belt, c-partial grouting.

The reservoir water effect has been considered on the additional masses principle, by following the incompressible water hypothesis. Those additional masses ( $M_i$ ), perpendicularly applied on the dam surface, have directly been determined from the velocity potential function ( $\psi$ ):  $[M_i] = [\rho \int_{S_i} \psi \, ds]$ , where  $\rho$  is the water density and  $S_i$  is the  $i$ -node affected part of the dam upstream face.

The velocity potential function has numerically been determined through the finite elements method on a spatial elaborated network which reproduces the geometry of the reservoir-arch dam system. The dam upstream face is approximated with a cylindrical surface and the lake being with a prismatic shape. The  $\psi$  function is strongly dependent on the earthquake direction and dam-reservoir system geometry as well [7]. The velocity potential function variation is presented in Figure 3, for the Vidraru dam symmetrized halfstructure; the plotting is given for horizontal earthquakes both directed along and transverse the valley and for vertical earthquake as well.

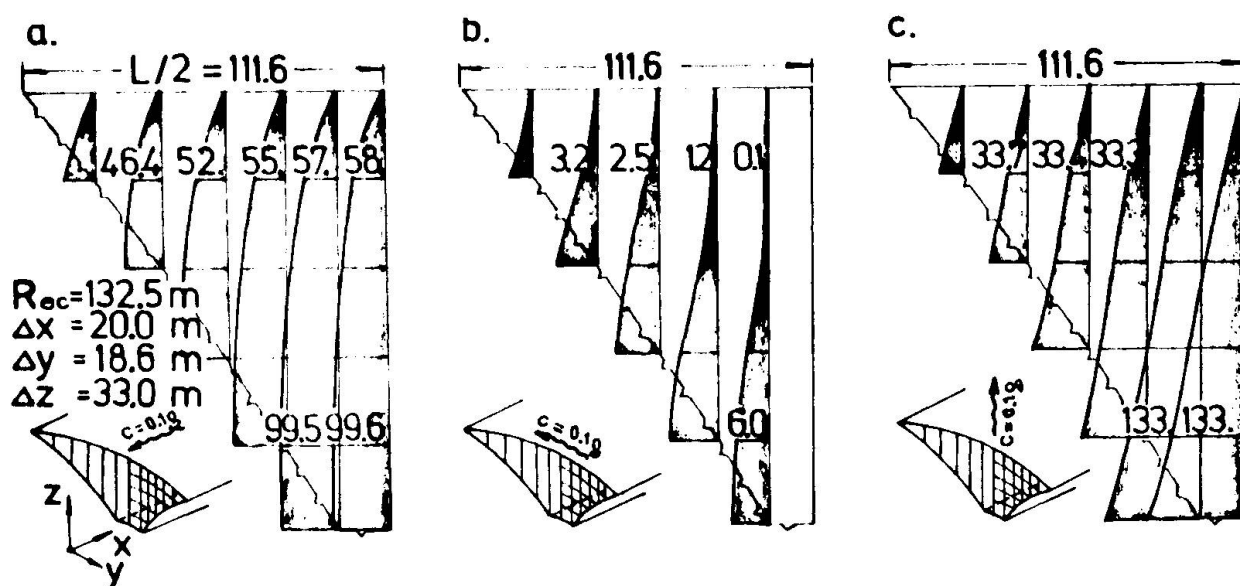


Fig. 3 Variation of velocity potential function  $\psi$  on the Vidraru dam halfstructure subjected to earthquakes on the directions: a-horizontal, along the valley, b-horizontal, transverse the valley, c-vertical.

The seismic analysis of the already mentioned variants has been carried out through the modal analysis with response spectra, by

following the structure linear - elastic behaviour hypothesis. In the dynamic analysis, the rotatory degrees of freedom are being eliminated by static condensation at the computing level of the total stiffness matrix; no translatory degrees of freedom on the vertical are being considered. The additional masses are computed for the direction of the dynamic degrees of freedom; the dam masses matrix and the additional masses matrix are both considered as being diagonal. The dam total response is computed through the Rosenblueth probabilistic relationship.

The excitation of the studied systems is being considered under the form of response seismic spectra, scaled up with a computing acceleration of 0.1 g according to the seismic standard in Romania. Comparatively, computations have been carried out with the response spectra set out on the basis of Bucharest recordings of the Romanian earthquake of Vrancea, March the 4-th 1977 (Figure 4). In conjunction with the Romanian above mentioned earthquake its slow oscillatory character should be noticed (seismic oscillatory periods of  $1.0 \div 1.5$  s). This aspect could be explained by the relatively weak ground (sands and clays, the groundwater table close to the surface) in the area where records were carried out.

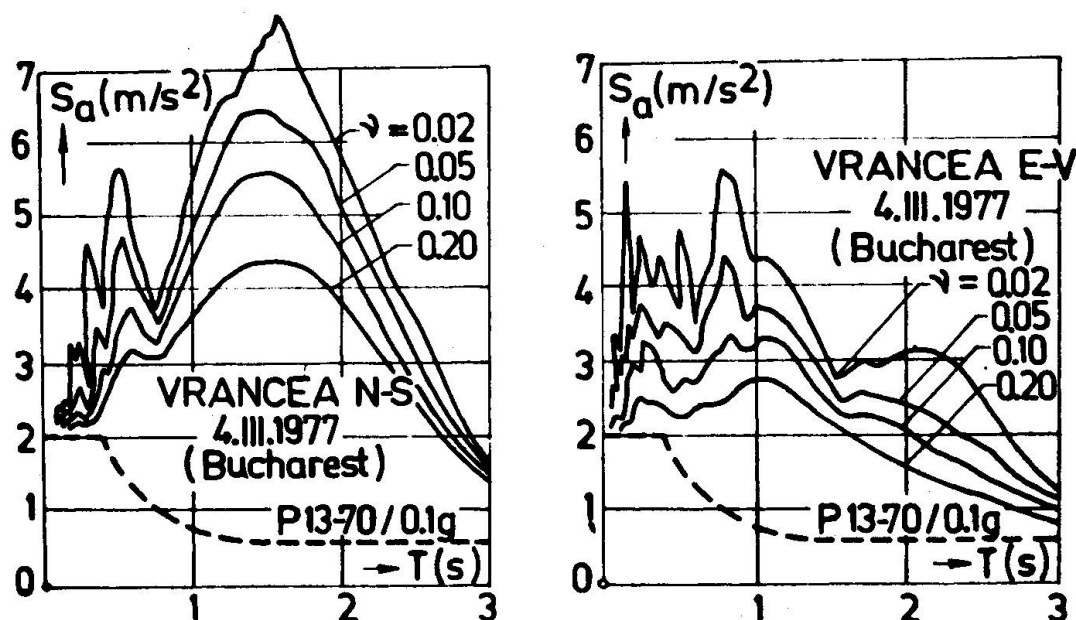
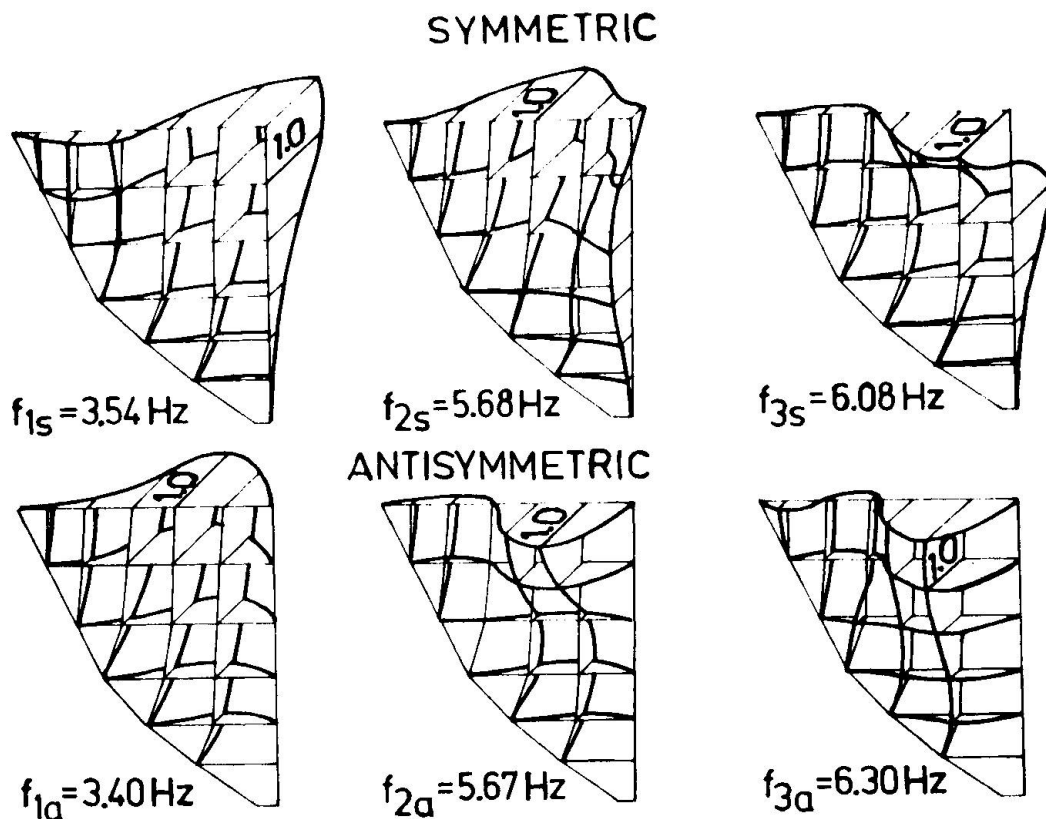


Fig. 4 The average spectra of the Bucharest recorded Vrancea earthquake of March, the 4-th 1977 (full line) and the Romanian in force standard response spectrum (dotted line).



## 2. THE SEISMIC ANALYSIS OF VIDRARU DAM

With the view to making the seismic analysis, the dam structure has been symmetrized and the analysis was carried out over the dam halfstructure with 40 horizontal dynamic degrees of freedom. Both cases of empty and full reservoirs have been considered each for the input ground acceleration directed along the valley and transverse to it.



**Fig. 5** Symmetric and antisymmetric eigenmodes of Vidraru dam for the empty reservoir condition ( $E_b = 370000 \text{ daN/cm}^2$ ,  $\mu = 0.15$ )

In figure 5, the first three symmetric and antisymmetric vibration modes are presented for the dam halfstructure and empty reservoir condition. When full reservoir condition is considered, the first eigenfrequencies have values of 1.95 Hz for the earthquake along the valley and of .21 Hz for the earthquake transverse the valley. However, the obtained eigenfrequencies and eigenmodes are within a range of values normally met with this type of structures;"in situ"

measurements have confirmed them out. The Vidraru dam first eigenfrequency, as measured out in situ for the reservoir water level situated at about one half of the dam height, was 2.63 Hz.

Some results with respect to the dam maximum seismic stresses are presented in Figure 6. Thus, for an input of the Romanian actual standard seismic response spectrum, scaled up to 0.1g and directed along the valley, the maximum seismic stresses are  $\sigma_h = 22 \text{ daN/cm}^2$ ,  $\sigma_v = 26 \text{ daN/cm}^2$  with the empty reservoir condition, and  $\sigma_h = 31 \text{ daN/cm}^2$ ,  $\sigma_v = 30 \text{ daN/cm}^2$  with the full reservoir condition. The same response seismic spectrum but transversally applied has given out more reduced unit stresses as  $\sigma_h = 6 \text{ daN/cm}^2$ ,  $\sigma_v = 5 \text{ daN/cm}^2$  with the full reservoir condition and  $\sigma_h = 4 \text{ daN/cm}^2$ ,  $\sigma_v = 5 \text{ daN/cm}^2$  with the empty reservoir condition.

Regarding the dynamic input of the Vrancea 4 March 1977 earthquake response spectrum, N-S component and  $\gamma = 5\%$ , as registered in Bucharest, maximum seismic unit stresses of magnitudes  $\sigma_h = 70 \text{ daN/cm}^2$  and  $\sigma_v = 51 \text{ daN/cm}^2$  have been computed for the earthquake applied along the valley. The Vrancea earthquake N-S component accelerogram, on the basis of which the response spectra have been set up, presents the maximum value of 0.24g. By normalizing the Vrancea N-S response spectrum up to a maximum acceleration of 0.1g, the maximum seismic unit stresses have come out to be  $\sigma_h = 29.2 \text{ daN/cm}^2$  and  $\sigma_v = 21.3 \text{ daN/cm}^2$ . The differences between the unit stresses which correspond to both input response seismic spectra, explain themselves through the quite important differences existing between the dam structure eigenfrequencies range and the Vrancea earthquake maximum spectral values range.

The examination committee which thoroughly inspected the Vidraru dam after the Vrancea earthquake of 4-th of March, 1977 estimated the ground motion intensity at the dam site in the range of VII-VIII M S K [8] ; this estimated seismic intensity would normally correspond to a maximum acceleration of about 0.1g. Therefore the seismic unit stresses, as computed through our study, have been about 25-30  $\text{daN/cm}^2$  for full reservoir. However, one should expect the dam real seismic stresses to be less than those computed, due to viscous-elastic-plastic actual behaviour of the concrete and to some structure dissipative capacities not taken

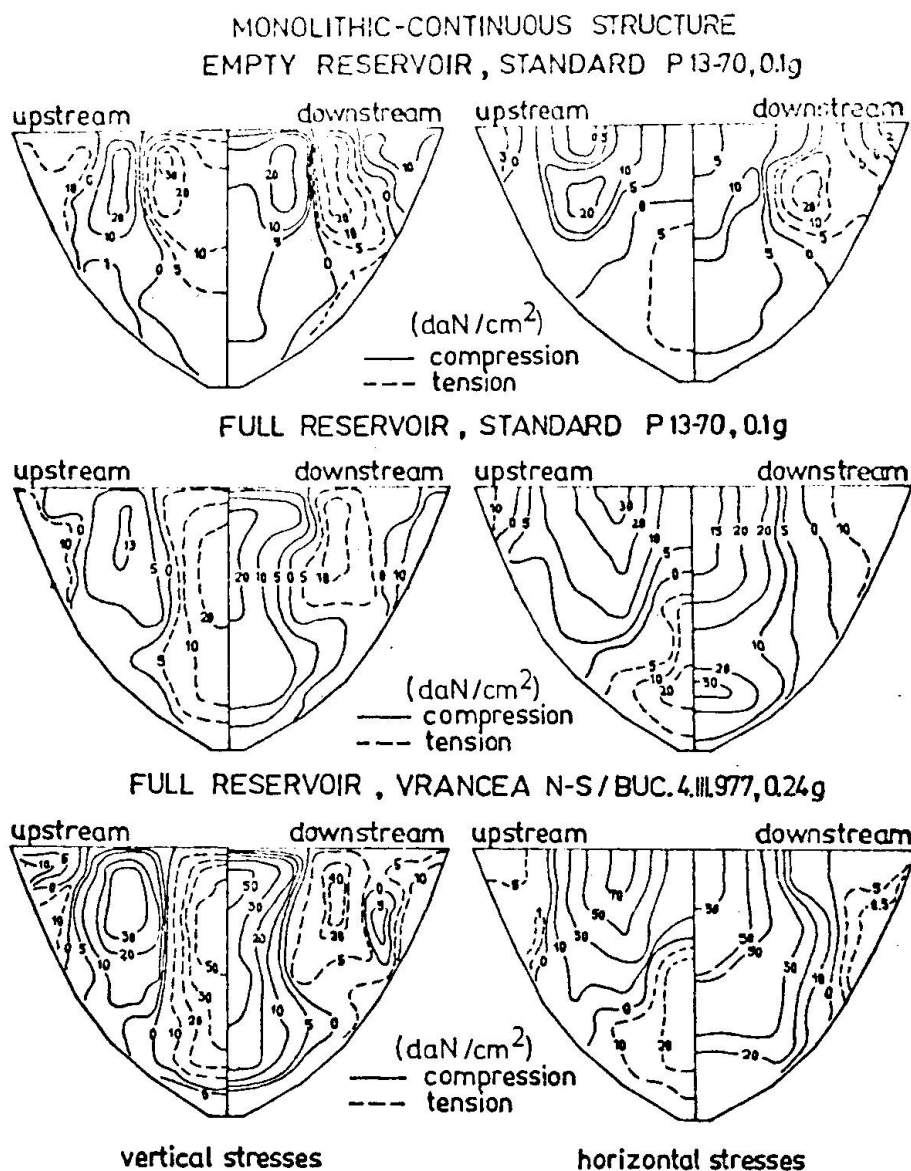


FIG. 6 Vidraru dam, the monolithic-continuous structure: Isolines of horizontal and vertical normal seismic stresses.

into consideration in our numerical model. Furthermore, at the Vidraru dam site, consisting of sound crystalline rocks, it would be less probable that the Vrancea earthquake accelerogram and, consequently, its response spectra should have oscillatory characteristics like those recorded in Bucharest. Unfortunately, excepting the Bucharest recorded accelerogram, there are no other recordings of the Vrancea earthquake of March, the 4-th 1977. Nevertheless, it has been remarkable that the Vidraru arch dam should withstand the Vrancea earthquake under best conditions, without any damages.

### 3. THE CONSEQUENCES OF PARTIALLY GROUTED JOINTS

The schemes of the dam with partially grouted joints which are to be investigated have been presented in Figure 2 b,c. In view of assessing the new state of stresses in the structure, due to constructive changes brought in by the proposed grouting schemes already given, a comparative study was carried out as a preliminary, referring to the dam main loadings of hydrostatic pressure and dead weight. In Figure 7, the diagrams of normal unit stresses  $\sigma_h$  and  $\sigma_v$  due to hydrostatic pressure are comparatively illustrated in the Vidraru dam central cross-section. The stresses in the dam monolithic - continuous structure do agree with those stresses computed by some other methods [9] and are confirmed by in nature recordings. By comparison with monolithic structure, both a reduction of catilever stresses and variations within broad limits of arch stresses over the dam ungrouted parts have been ascertained; however, the unit stresses present a unique grouping tendency over the dam lower and central parts, for all three variants. Following that previous static analysis, the case of partially grouted joints and without the upper monolithic belt has been ruled out because of the unacceptable stress distributions over the dam subjected to hydrostatic pressure; the arch compression stresses run up to  $110 \text{ daN/cm}^2$  over the dam ungrouted part as the tensile stresses reach  $45 \text{ daN/cm}^2$ .

The seismic analysis of the variant with five partially grouted joints and with a crest stiffening belt has shown up the dam structure become more flexible in comparison with the monolithic dam. In Table 1 one comparatively presents the first four eigenfrequencies of the monolithic continuous structure and the structure with partially grouted joints and crest belt as well. The computations have pointed out that no significant differences would appear in between the geometrical configurations assigned to first eigenmodes of the two above mentioned variants.

Table 1

Hypotesis	Variant	First four eigenfrequencies (Hz)			
Empty reservoir, symmetric	monolit	3.54	5.68	6.08	7.17
	partially grouted joints and crest belt	2.67	3.15	3.68	5.11
Full reservoir, symmetric	monolit	1.94	3.41	3.72	4.48
	partially grouted joints and crest belt	1.39	2.21	2.75	3.92



In figure 8 there are given out the seismic stresses which taking place in the structure with partially grouted joints and crest belt when subjected to a dynamic input of Romanian standard response spectrum, applied along the valley. An evident tendency of increasing the stresses towards the crest belt is steadily visible. At the dam lower part some generally small stress variations are found, by comparing with the similar case of the monolithic-continuous structure. For the full reservoir condition, the structure with partially grouted joints and crest belt has registered maximum seismic unit stresses  $\sigma_h = 44 \text{ daN/cm}^2$ ,  $\sigma_v = 34 \text{ daN/cm}^2$ , thus, increases of about  $1.1 \div 1.5$  confronted by the equivalent condition of the monolithic structure. For the empty reservoir condition, the maximum seismic stresses are  $\sigma_h = 43 \text{ daN/cm}^2$ ,  $\sigma_v = 47 \text{ daN/cm}^2$ , thus increases of about  $1.6 \div 2.0$  confronted by the similar condition of the monolithic structure. The stress increase is occurring mostly towards the crest belt and, therefore, the need of reinforcing that crest belt comes out to be most suitable

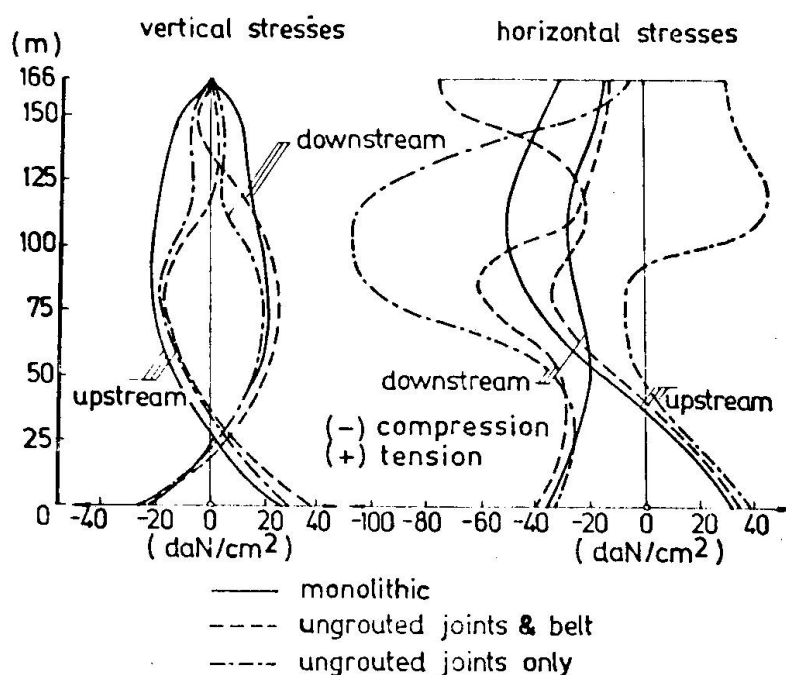
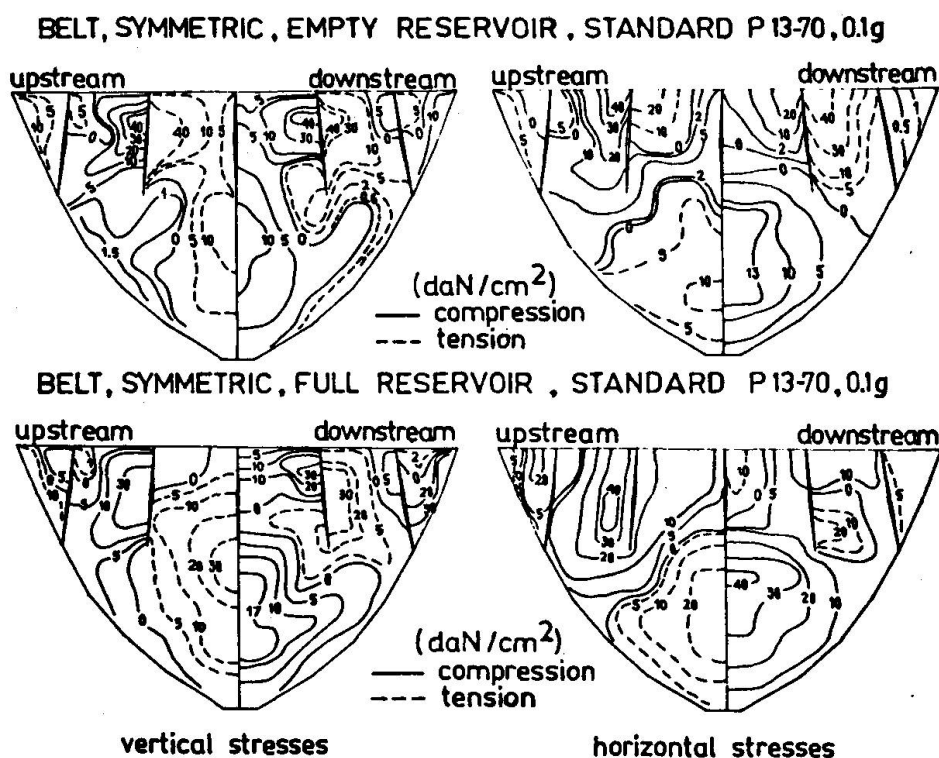


Fig. 7 Vidraru dam, different studied joints grouting schemes: horizontal and vertical normal stresses in the dam central cross-section, subjected to hydrostatic pressure.

Within this study, the influence of some additional dissipative capacities of the structure with partially grouted joints has not been considered. Model tests had previously put into evidence

some increases of the damping logarithmic decrement with respect to the first vibration eigenmodes ; thus, these increases did ranged from  $\delta = 0.12 \div 0.17$  for the monolithic structure to  $\delta = 0.30 \div 0.50$  for the structure with ungrouted joints over  $1/4$  of the arch dam height [4] . It seems these damping increasings may give some rather important reductions of seismic stresses without modifying yet their overall distribution.



**Fig. 8** Vidraru dam, the structure with partially grouted joints and crest belt: Isolines of horizontal and vertical normal seismic stresses.

#### 4. CONCLUSIONS

By taking into account the facts mentioned up to now, the following conclusions may be formulated:

. The constructive solution with 4-5 arch dam shrink joints being partially ungrouted over the upper  $1/4$  of the dam height offers some advantages with respect to dam seismic behaviour against the solution of the dam structure with complete grouted joints; that proposed solution permits securing some arch dam higher dissipative capacities and an improved dam flexibility.

. The constructive solution already mentioned should be associated with providing for a dam crest stiffening belt, which prevents the cantilever separate vibration; it will also prevent some unfavourable modifications of stresses within the dam structure subjected to permanent loads (hydrostatic pressure, dead weight) and seismic loadings as well.

. The dam crest stiffening belt seems to undertake some important pulsating stresses during seismic loadings; therefore, the belt adequate reinforcement should be necessary.

. The good behaviour of the Vidraru arch dam during the Vrancea earthquake of March, the 4-th 1977, do practically prove once more the arch dams outstanding capacity of accomodating themselves to earthquakes.

#### REFERENCES

1. OBERTI, G.: Effects of earthquakes on dams (lectures ISMES), Bergamo, 1968.
2. PRISCU, R., POPOVICI, A., ILIE, L.: Earthquake analysis of double curvature arch dams. Proc. International Symposium on Discrete Methods in Engineering, Milan, September, 1974.
3. CASTELLANI, A., CASTOLDI, A., IONITA, M.: Numerical analysis compared to model analysis for a dam subject to earthquakes. Proc. of the Fifth International Conference on Experimental Stress Analysis, Udine, 1974. Publication ISMES No.83.
4. BAHTIN, B.M., CERNIAVSKI, V.: About the importance of preserving some nonmonolithic parts in arch dams upon their dynamic behaviour (in russian), Buildings and Architecture, vol. 16, No.3, Moscow, 1973.
5. POPOVICI, A.: Contributions to the seismic analysis of arch dams (in Romanian), Ph.D. Thesis, Bucharest, 1975.
6. BATHE, J., WILSON, E.L., PETERSON, F.E.: SAP IV Structure Analysis Program for static and dynamic response of linear systems. EERC 73-11, University of California, Berkeley.
7. PRISCU, R., POPOVICI, A., ILIE, L., STEMATIU, D.: New aspects in the earthquake analysis of arch dams. Proc. International Symposium, Criteria and Assumptions for Numerical Analysis of Dams, Sept. 1975.
8. PRISCU, R.: The behaviour of Romanian dams during the Vrancea earthquake of March, the 4-th 1977 (in Romanian), Hidrotechnics, no.5, Bucharest, 1977.
9. PRISCU, R.: Some modern conceptions applied in constructing the arch dams in Romania (in Romanian), Hydrotechnics, no.8, Bucharest, 1964.

Leere Seite  
Blank page  
Page vide



## DUCTILITY OF REINFORCED CONCRETE COLUMNS

Gian Mario Bo

Associate Professor  
Istituto Tecnica delle  
Costruzioni  
Politecnico di Torino

Marco Capurro

Associate Professor  
Istituto Scienza delle  
Costruzioni  
Università di Genova

SUMMARY

A method is presented for calculating the rotation of the end plastic hinge in a reinforced concrete column subject to axial load, bending moment and shear. The method is based on the assumption that, in the regions adjacent to that to which ultimate bending moment is applied, the bond between tension metal reinforcement and concrete is completely inoperative. Besides, the plastic deformation of the tension steel is assumed to be linearly variable in the portion where slipping occurs from zero up to maximum value in the ultimate bending moment section.

The length of the plastic zone is then obtained on the basis of equilibrium considerations, while the overall rotation of the plasticization zone is calculated by taking the internal work to be equal to the external work.

## 1. INTRODUCTION

In a framed building structure subject to strong earthquakes, over stresses are generally produced in the members and particularly in the columns. The mode of failure of the structure under seismic loads and dead loads plus a fraction of vertical service loads depends on the capacity of deflection of the columns in the inelastic range. Hence, calculating the ultimate deflection of each single column, as permitted by the rotation of plastic hinges, is a fundamental step in the analysis and design of buildings exposed to seismic risk. A typical pattern for the ultimate behaviour of a simple oscillator subject to lateral load is shown in fig. 1.

The evaluation of the ultimate deflection  $\eta_u$  at the top of a column and more generally of any structural member subject to constant axial load and bending moment varying along the axis, requires the knowledge of the moment curvature diagram of the member and turns out to be rather complicated for R.C. columns. M- diagrams as available in the literature [1] may be usefully employed; in this case, however, the effects of confining of concrete due to transversal reinforcement are neglected, thus obtaining values of the deflection  $\eta_u$  significantly lower than the experimental ones [2] [3]. A different procedure consists of obtaining the ultimate curvature or the ratio of the ultimate to the perfectly elastic curvature at the clamped-end cross-section of the column [4].

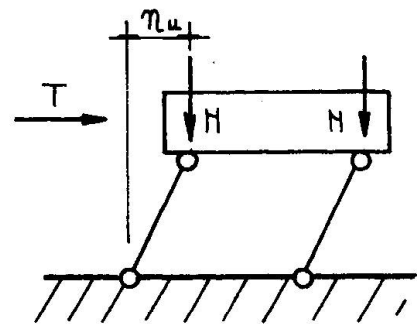


fig. n. 1

The structural member is assumed in this case to be divided into two sharply distinguished zones, in one of which the material behaves elastically, while in the other, close to the clamped end, plastic behaviour is widely predominant.

The length of the equivalent plastic zone is usually taken to be proportional to the depth and span of the column according to binomial relations [5].

According to [2] we have, for example:

$$\Delta_p = 0.50h + 0.2 \sqrt{h} \left( \frac{z}{h} \right) \quad (1)$$

From the knowledge of curvatures and the extension of the plastic hinge, values of the capacity of rotation  $\varphi$  may be easily calculated and hence the ultimate deflection is obtained. This method, however, applies only to a restricted range of dimensions of the rectangular cross-section and no extrapolation of the semiempirical relation (1) seems to be reliable to cover different shapes of cross-sections (such as cave or lamellar section and so on).

In the present work a theoretical approach is put forward allowing the designer to calculate the amount of rotation at the plastic hinge irrespectively of the hypothesis of plane cross-sections which has been commonly adopted so far in all R.C. calculations. In the regions adjacent to the clamped end, the bond between concrete and tension steel is assumed to have failed because of local **overstress** phenomena and cracking, so that slipping of longitudinal bars is permitted and consequently, over some fraction of the column length, the tensile stress in the reinforcement is, at a good estimate, constantly equal to the yield stress of steel.

The proposed method is more advantageous than the others described above insofar as it does not rely solely on experimental data and consequently it could lead to a further extension of its range of applicability.

## 2. BASIC ASSUMPTION

Let us consider a R.C. rectangular column with symmetrical single-layer reinforcement.

This column will be subjected to bending and axial force  $N$  lower than the balanced value  $N_b$ , with non-vanishing shear force  $T$  (fig. 2).

The problem is examined while the rotation of the plastic hinge is taking place.

At the clamped-end cross-section  $M=M_{ult}$  is assumed and the strains  $\epsilon'_{br}$ ,  $\epsilon_{au}$  are calculated according to the hypothesis of plane cross-sections. In the vicinity of the clamped end the tension steel will undergo yielding with  $\sigma_a = \sigma_{as} = \text{const}$  and will be strained plastically from zero plastic strain (at the top of the plastic region) to  $\epsilon_{au}$ , at a rate that, grossly estimated, may be assumed to be constant. Throughout the region affected

by the plastic hinge no assumptions concerning compatibility of strain for compression concrete and tensile reinforcement are made. The plastic region may be considered to extend up to the cross-section where, the tensile stress in steel altogether equalling  $\sigma_{as}$ , the amount of plastic strain  $\epsilon_a$  approaches zero.

In this cross-section the position of the neutral axis, on account of the hypothesis of free slipping of tensile steel in the plastic zone, may be assumed to coincide with the centroid of tensile reinforcement.

This would indeed be a drastic assumption, as some residual bonding effect is expected to work even in a widely cracked zone. More conservatively, the plastic region may be considered as ending below

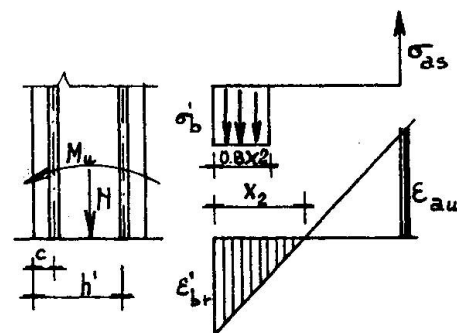


fig. n. 2

the cross-section where onset of yielding in the tensile steel takes place, the concrete still behaving elastically and in full bond with the tension bars; here the law of plane cross-sections is again held to apply.

Under all these assumptions the amount of rotation of the plastic hinge may be calculated and an estimate of its effective extension may be provided.

### 3. EVALUATION OF THE EXTENSION OF THE PLASTIC ZONE

Consider a column with rectangular cross-section as illustrated in fig. 3. Let:

$h$  = be the full depth of cross-section;

$h' = h - c$  = the reduced depth, with  $c$  = the distance of the reinforcement from the edge;

$b$  = the width of the cross-section;

$x$  = the position of the neutral axis with respect to the compression edge;  $\xi = x/h'$

$F_a = F'_a$  the area of both tension and compression reinforcement;

$\mu_a = \mu'_a = F_a / bh'$  the percentage of reinforcement;

$\bar{\mu}_a = \bar{\mu}'_a = \frac{\sigma_{as}}{\bar{\sigma}_b} \mu_a$  the mechanical percentage of reinforcement;

$\sigma_{as}$  being the yield stress of steel;  $\epsilon_{ae} \approx \frac{\sigma_{as}}{E_a}$  the first yielding strain in steel;

$\bar{\sigma}_b$  = the crushing stress of concrete;  $\bar{\epsilon}_{br}$  the ultimate strain of concrete;

$n = \frac{E_a}{E_b}$  the ratio of elastic moduli;

$n_d = \frac{N}{\sigma_{as} F_a}$  = the non dimensional axial load;

$T$  = the shear force

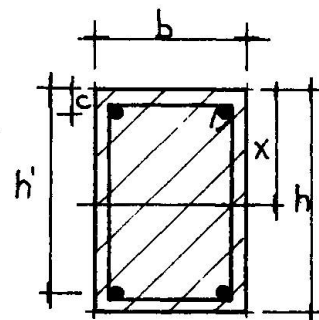


fig. n. 3

The assumptions discussed in the foregoing section lead to stress and strain distributions as illustrated in fig. 4.

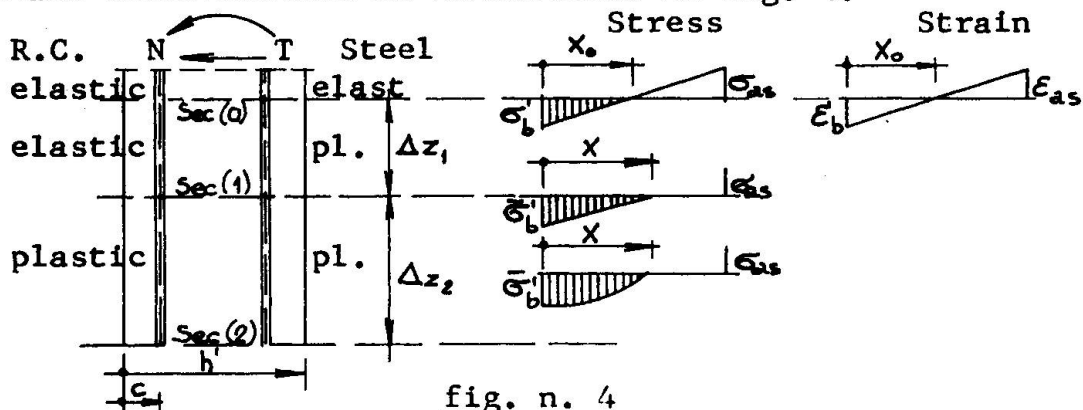


fig. n. 4

In the clamped-end cross-section, labelled (2) strain and stress distributions are assumed according to the usual assumptions of ultimate design. The compression region is supposed to be rectangular with effective depth  $0.8 x_{(2)}$ .

Between cross-section (2) and (1) the compression stress of concrete is assigned a curvilinear distribution over the depth  $x$ , but the compression resultant is always taken at a distance of approximately  $0.4x$  from the compressed edge. The total amount of compression may be expressed as

$$P_b = \bar{\sigma}'_b \cdot \alpha \cdot x \cdot b$$

$\alpha$  being a shape factor ranging between 0,5 (triangular elastic distribution) and 0,8 (ultimate distribution).

In cross-section (1) a triangular compression stress distribution is assumed with maximum value amounting to  $\bar{\sigma}'_b$ .

For cross-section (0) two alternative conditions are examined: both conditions (case a) stipulate that the steel is strained just at the yielding point with  $\epsilon_a = \epsilon_{ae}$  ( $\epsilon_{ae} \approx \sigma_{as}/E$ ) and  $\sigma_a = \sigma_{as}$ ; in the first case (case a) compatibility of strain between steel and concrete is introduced; in the other (case b)

$$x_{(0)} = h'$$

is assumed, disregarding compatibility of deformations on account of bond slip being allowed to take place below the cross-section (0).

From the equilibrium of the forces acting at cross-section (0) expressed by the equation

$$0.5 \bar{\sigma}'_b x_{(0)} b - N + \sigma'_a F'_a = \sigma_{as} F_a \quad (1)$$

and from compatibility of deformations, written as:

$$x_{(0)} = h' \frac{\epsilon'_b}{\epsilon'_b + \epsilon_{as}} \quad (2)$$

it is possible to obtain the position of the neutral axis  $\xi_0$  for case a, namely by solving the equation:

$$\xi_0^2 + 2n \xi_0 [\mu_a (1+n_d) + 0.8 \mu'_a] - 2 \mu_a n (1+n_d) = 0 \quad (3)$$

where  $\epsilon'_a \approx 0.8 \epsilon'_b$  has been introduced for the sake of simplicity. In the case b, we immediately have:

$$\xi_0 = 1 \quad (4)$$

In the region between the cross-sections (0) and (1) let us take into consideration the variations, with respect to a parameter



progressing along the column axis, of the equilibrium equations of both forces and moments. The quantities which may vary are, of course,  $\sigma'_b$  and the position of the neutral axis,  $x$ . The operator performing such variations is denoted by  $\delta$ . Then we obtain:

$$0.5 bx \delta \sigma'_b + 0.5 \sigma'_b b \delta x = -0.8 n F'_a \delta \sigma'_b \quad (5)$$

$$\delta M = 0.5 \sigma'_b b (h' - \frac{2}{3} x) \delta x + 0.5 bx (h' - \frac{1}{3} x) \delta \sigma'_b + 0.8 n F'_a (h' - c) \cdot \delta \sigma'_b \quad (6)$$

By eliminating  $\delta \sigma'_b$  between (5) and (6), the moment variation turns out to be:

$$\delta M = \frac{0.5}{3} \sigma'_b bx \delta x \quad (7)$$

hence, dividing by  $\delta z$ :

$$\frac{\delta M}{\delta z} = \frac{dM}{dz} = T = - \frac{0.5}{3} \sigma'_b bx \frac{dx}{dz} \quad (8)$$

This relation may be integrated between the cross-sections (0) ( $x = x_{(0)}$ ) and (1) ( $x = x_{(1)}$ ), after removal of  $\sigma'_b$  through the equilibrium of forces at a current coordinate  $z$

$$\frac{\Delta z_1}{h'} = \frac{\sigma_{as} F_a}{T} k_1 \quad (9)$$

where

$$k_1 = \frac{(1+n_d)}{3} \left[ \xi_0 - 2 \bar{\mu}_a (1+n_d) + 1.6 n \mu'_a (1 - \ln \frac{\xi_0 + 1.6 n \mu'_a}{\xi_1 + 1.6 n \mu'_a}) \right] \quad (10)$$

In the region between the cross-sections (1) to (2) with the assumption that the compression reinforcement remains elastic over the whole length  $\Delta z_2$ , and  $\sigma'_a \propto \alpha / 0.8 \cdot \sigma_{as} = 1.25 \alpha \sigma_{as}$ , the variations of the equilibrium equations are expressed as:

$$\bar{\sigma}'_b bx \delta \alpha + \bar{\sigma}'_b b \alpha \delta x = -1.25 \sigma_{as} F'_a \delta \alpha \quad (11)$$

$$\delta M = \bar{\sigma}'_b b h'^2 (0.4 \xi^2 + \xi \bar{\mu}_a + 1.25 \frac{c}{h'} \bar{\mu}'_a) \delta \alpha \quad (12)$$

By eliminating  $\xi$  between (12) and the equation of equilibrium of forces at a current coor.  $z$ ,  $\delta M$  as expressed by (12) may be integrated over the region between the cross-sections (1) ( $\alpha = 0.5$ ) and (2) ( $\alpha = 0.8$ ), thus giving:

$$\frac{\Delta z_2}{h'} = \frac{\sigma_{as} F_a}{T} k_2 \quad (13)$$

where

$$k_2 = 0.3 \left[ \bar{\mu}_a (1+n_d)^2 - 1.25 \frac{\bar{\mu}'_a}{\bar{\mu}_a} \left( 0.5 \bar{\mu}'_a - \frac{c}{h'} \right) \right] \quad (14)$$

Equation (14) may undergo further simplification by recalling that  $\mu_a = \mu'_a$ .

The total length of the plastic region is therefore:

$$\frac{\Delta z}{h'} = \frac{\Delta z_1 + \Delta z_2}{h'} = \frac{\sigma_{as} F_a}{T} (k_1 + k_2) \quad (15)$$

#### 4. EVALUATION OF THE PLASTIC-HINGE ROTATION

With the usual idealization of attributing the whole plastic rotation to a single point of the column axis, namely the idealized plastic hinge, the capacity of rotation  $\phi_u$  may be obtained from an energy balance between the inner plastic work made in the whole plastic region of length  $\Delta z$  by both concrete and steel while strained beyond the elastic limits, and the external work  $M_{ult} \cdot \phi_u$ .

In this manner, the problem is reduced to calculating the inner plastic work made both tension steel in the length  $\Delta z$  and by concrete in the inelastic range over the length  $\Delta z_2$ .

With the assumptions made in the foregoing the former is promptly calculated as:

$$\delta L_{pl(a)} = \frac{1}{2} \sigma_{as} F_a (\epsilon_{au} - \epsilon_{ae}) \Delta z \quad (16)$$

the stress in steel being constantly equal to  $\sigma_{as}$ .

The work of concrete in the region where this material is supposed to have abandoned the elastic range, may be expressed as:

$$\delta L_{pl(b)} = \int_0^{\Delta z_2} \int_{A'} \sigma'_b \delta \epsilon'_b dA' dz \quad (17)$$

$A'$  being the compression area as a function of  $z$ , namely  $A' = bx(z)$  and  $dA' = bdx$ . It is reasonable to assume a mean value for  $\sigma'_b$  over the compression area of each single cross-section, namely by putting

$$\sigma'_b \simeq \text{mean } \sigma'_b = \alpha(z) \bar{\sigma}'_b \quad (18)$$

in definition (17). Moreover, the strain  $\epsilon'_b(x')$  at any position in the compression area, may be expressed on account of compatibility of the deformation in the compression-concrete area, as

$$\epsilon'_b(x') = \frac{x'}{x} \epsilon'_b(z) \quad (19)$$

By introducing both (18) and (19) into the expression of plastic work, we have:

$$\delta L_{pl(b)} = \int_0^{\Delta z_2} \alpha \bar{\sigma}'_b \frac{\delta \epsilon'_b}{x} dz \int_0^x x' dx' \quad (20)$$

The inner integral may be calculated at once to yield  $x^2/2$ ; so that (20) is reduced to an integral over coordinate  $z$ :

$$\delta L_{pl(b)} = \frac{1}{2} \bar{\sigma}'_b \int_0^{\Delta z_2} \alpha x \delta \epsilon'_b dz \quad (21)$$

where  $\alpha$ ,  $x$ ,  $\delta \epsilon'_b$ , are all functions of  $z$ . On the basis of the equations of equilibrium both in finite and in varying form, and as the result of lengthy but plain calculations, we have succeeded in eliminating  $x$ , and [for  $\delta \epsilon'_b(z)$  we may accept a linear expression:  $\delta \epsilon'_b = z/\Delta z_2 (\bar{\epsilon}'_{br} - \epsilon'_{be})$ ] and in transforming (21) into an integral of a known function of  $\alpha$  over  $\alpha$  itself. This can be solved through direct integration, yielding the final result:

$$\delta L_{pl(b)} = \frac{\sigma_{as}^2 F_a^2 h'}{T} (\bar{\epsilon}'_{br} - \epsilon'_{be}) \cdot k_3 \quad (22)$$

being

$$k_3 = 0.25 k_2 \left[ 1 + n_d - 0.389 \frac{\bar{\mu}_a}{\mu_a} \right] \quad (23)$$

The plastic work of the compression concrete is however small (amounting to no more than a certain percentage of steel work) and sometimes it is not totally wrong to think of neglecting it in comparison with the work of steel. It may be useful to notice that, in any case, the amount of plastic work of concrete is not affected by the situation at cross-section(1), whether compatibility is assumed according to case a or free slipping of steel reinforcement is supposed (case b). In the latter case, the only modification to be brought into the foregoing results, involves, as previously pointed out, the length  $\Delta z_1$  which in turn, enters into the expression of  $\delta L_{pl(a)}$ . As a consequence of this modification,  $\delta L_{pl(a)}$  is expected, and has been actually calculated, to increase significantly (up to several times), probably overemphasizing the ductility of the column (\*). Finally, the total

(\*) A more general approach would be that of finding  $\xi_0$  from a condition of partial compatibility imposed on the deformations at cross-section (0). The concrete strain  $\epsilon'_b$  would be compatible, in this case, not with the total steel strain  $\epsilon_{ae}$ , but with a fraction of it obtained by subtracting from  $\epsilon_{ae}$  the amount of slip rate  $(du/dz)_0 \approx (f/\Delta_f)$  due to cracking, where  $f$  is the crack width and  $\Delta_f$  the spacing .../...

ultimate rotation of the plastic hinge is calculated as:

$$\varphi_u = \frac{L_{pl(a)} + L_{pl(b)}}{M_{ult}} \quad (24)$$

$M_{ult}$  being the ultimate moment of the column to be obtained from the equilibrium of cross-section (2). The deflection at the top of the column permitted by the rotation of the plastic hinge may be estimated as approximately

$$\eta_{pl} \cong \varphi_u \left(1 - \frac{\Delta z}{2}\right) \quad (25)$$

$l$  being the span of the column and supposing the plastic hinge reduced to a point located at the centre of the plastic zone.

In the diagrams of fig. 6 the ratios

$$\frac{\Delta z}{h'} / \frac{\sigma_{as}^F a}{T} \quad \text{and} \quad \varphi_u / \frac{\sigma_{as}^F a}{T}$$

are plotted versus the non-dimensional axial force  $n_d$  for three different reinforcement percentages. The capacity of rotation of the column decrease rapidly with increasing axial force, in spite of a not negligible spreading out of the plastic region.

In fig. 7 the effect of increasing the column depth can be followed, leading to decrements both of  $\Delta z/h'$  and of  $\varphi_u$ , although with a clear tendency to asymptotes for very deep cross-sections. The effects of varying  $\bar{\epsilon}'_{br}$  and  $\bar{\sigma}'_b$  have also been considered with the conclusions that  $\varphi_u$  increases nearly proportionally with  $\bar{\epsilon}'_{br}$  and even more decisively with the strength of concrete.

.../...

of cracks, both calculated at cross section (0). The details of a procedure of this type at present are still to be worked out.

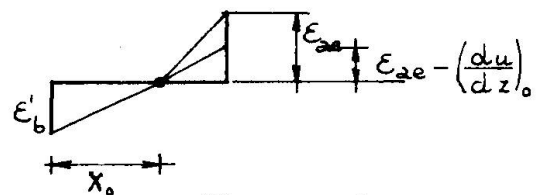
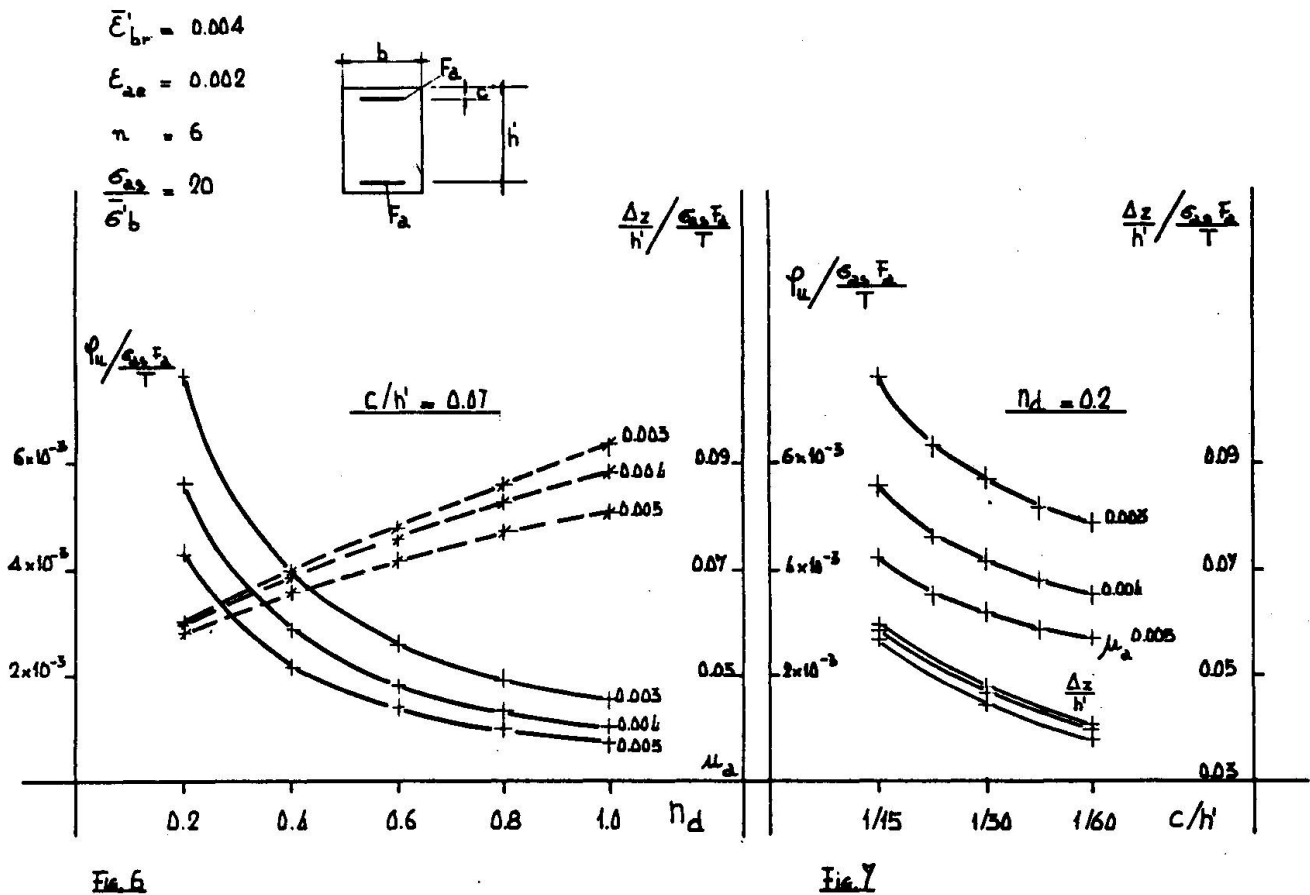


fig. n. 5



## REFERENCES

- [1] Macchi G. and E. Siviero  
"Deformability of prismatic R.C. members with rectangular cross-section under combined bending and axial load"  
Comité Européen du Béton - Bulletin d'Information n. 101 - Paris - 1974 - pagg. 191 and following.
- [2] Corley G.W.  
"Rotational capacity of reinforced concrete beams" -  
Journal of the Structural Division - ASCE - October 1966
- [3] Jirsa J.O.  
"Factors influencing the hinging behavior of reinforced concrete members under cyclic overloads"  
Fifth World Congress of Earthquake Engineering - Roma - 1972 - pagg. 1193 and following
- [4] Blume J.A., Newmark N.M. and L.H. Corning  
"Design of Multistory Reinforced Concrete Buildings for Earthquake Motions"  
Chicago - 1961 - Portland Cement Association - pagg. 113 and following
- [5] Park R. and T. Paulay  
"Reinforced Concrete Structures" - New York - 1975 - John Wiley and Sons - pagg. 248 and following



SEISMIC DESIGN AND VERIFICATION OF SEISMIC EFFICIENCY  
OF A HIGHRISE REINFORCED CONCRETE BUILDING

Kiyoshi Muto <sup>1)</sup>  
Tadashi Sugano <sup>2)</sup>

### Summary

The authors designed a successful construction of the first highrise reinforced concrete building to be built in Japan after obtaining a special approval from the Minister of Construction. The structural design was carried out based on structural experiments and nonlinear dynamic analysis. After completion of the building, earthquake observations have been continued at the basement, 9th and 19th floors. The two largest earthquake motions were simulated. The computed accelerations showed good agreement with the observed ones. This proves that our dynamic analysis is sufficiently accurate.

### Resume

Les auteurs ont étudié la construction du premier grand immeuble en béton armé, erigé au Japon, après avoir obtenu l'approbation spéciale par le Ministre de Construction. L'étude structurale a été effectuée suivant les bases de l'essai de structure ainsi que de l'analyse dynamique non-linéaire. Après l'achèvement de l'immeuble, les observations sismiques ont été continuées au sous-sol, à 9<sup>e</sup> étage, et à 19<sup>e</sup> étage. Les deux plus grands mouvements sismiques ont été simulés. Les accélérations calculées se montraient bonne concordance avec celles observées. Ceci prouve que notre analyse dynamique est suffisamment exacte.

### Zusammenfassung

Die Verfasser projektierten ein in Japan erst ausgeführtes Stahlbetonhochgebäude mit der Sondergenehmigung vom Minister des Aufbaus. Die Konstruktionsprojektierung wurde durch die konstruktiven Versuche und unliniarte dynamische Analysis gemacht. Nach der Baufertigstellung ist die Erdbemessung im KG., 9. OG. u. 19. OG. durchgeführt. Die mit Komputern ausgerechneten Beschleunigungen hatten gute Stimmung mit den Messungsergebnissen bei zwei größten Erdbeben. Das zeigt, daß unsere dynamische Analysis genügende Genauigkeit hat.

---

1) Professor Emeritus, University of Tokyo, President, Muto Institute of Structural Mechanics Inc. Tokyo, Japan

2) Dr. Eng. Senior Research Engineer, Muto Institute of Structural Mechanics Inc. Tokyo, Japan

## 1. INTRODUCTION

It was believed that the construction of highrise buildings using reinforced concrete would be difficult in Japan due to the problems of earthquakes. As a common practice, reinforced concrete (RC) structures have traditionally been forbidden for buildings of 7 stories (20m) or more. Taller buildings than 31 meters were composed of either combined structural steel and reinforced concrete, or of structural steel.

The year following the Tokachioki Earthquake of 1968, the authors began to perform experiments for the improvement of the aseismic properties of reinforced concrete members. And it was found that, with adequate arrangement of reinforcing bars, brittle failure of the member is completely prevented and sufficient deformability and ductility are secured.

With the support of these experimental findings and dynamic computer analysis, the authors succeeded in designing an 18-story RC apartment building. It was confirmed that stresses in all of the building members remained in allowable values during the severe earthquake (maximum acceleration 0.3g) and the maximum ductility factor remained at 1.66 against worst earthquake (maximum acceleration 0.5g). Since this building was unconventional in terms of both height and structure, Article 38 of the Japanese Building Standard Law required that special approval be obtained from the Minister of Construction.

In September 1972, soon after applying and receiving of a special permit, construction work of the building was started, and in January 1974 it was brought to a successful completion. This paper describes the preliminary studies, the earthquake resistant design and post construction studies of dynamic behavior of this building.

The second highrise building (Makomanai Apartment, 11 stories) was designed by the same method and now under construction at Sapporo. Building G which is to be 25 stories apartment is now being designed.

## 2. PRELIMINARY STUDIES

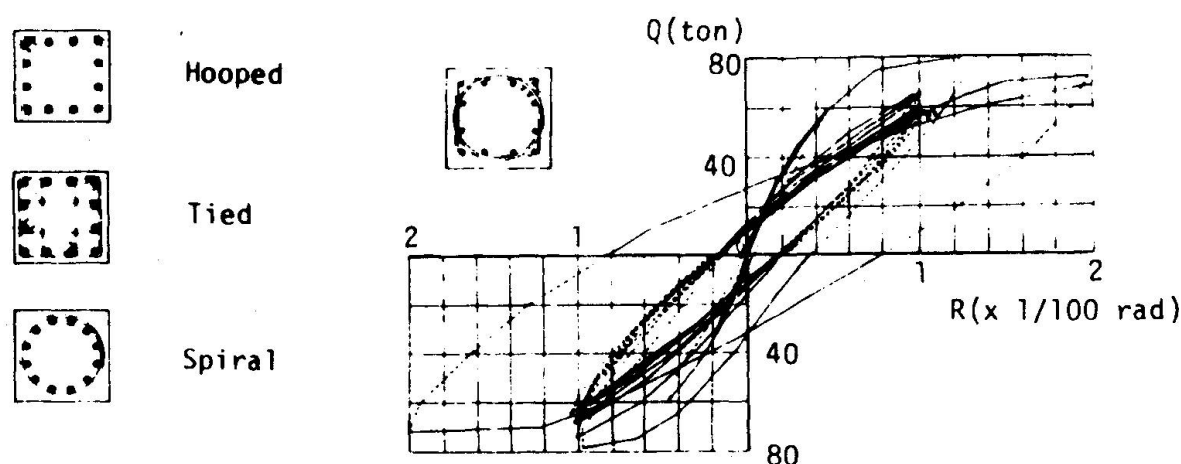
Various experiments were carried out to confirm the practicability of each of new construction methods. Among them the following three series of tests contributed much to the realization of the highrise RC buildings.

### 2.1 Studies of shear reinforcement of columns

Many RC columns reinforced by poor hoops suffered from brittle shear failures by the Tokachioki earthquake of 1968. The main reinforcing bars had buckled and concrete burst out. This illustrated an important role of confinement of concrete. Immediately after the earthquake, the authors performed column tests with three different types of transverse reinforcements, as shown in Fig. 1. The effects of transverse reinforcing bars of respective hoop, tie and spiral type were examined under identical condition. Then it was recognized that the hoop column lost its load bearing capacity soon after repeated loading at a deflection angle of 1/100. By contrast, the tied and spiral columns with proper amount of reinforcements were capable of deforming up to large deflection without any decrease of load bearing capacity.

While seeking an arrangement of longitudinal bars which would allow the beam reinforcing bars to pass easily through the column and also searching for method of prefabricating the column and beam bars on the ground for lifting into place, a new arrangement of the reinforcing bars for columns was developed. The shear reinforcement of the column was combination of spiral and square hoop, which was named Kajima Spiral.

It was also ascertained by testing that the deformability and ductility of this column were as same as those of the spiral column or tied column as shown in Fig. 1.



a. Three Types of Reinforcement

b. P- $\delta$  Curves of Kajima Spiral Column

Fig. 1 Experiments of Columns

## 2.2 New anchorage system

The newly developed anchoring method for the beam reinforcement was subjected to the Construction Minister's approval. In the U Anchor Method, the ends of the main reinforcing bars in beam are anchored by form of the letter U at the beam-column joint of exterior frame as shown in Fig. 4. By developing the U Anchor Method and Plate Anchor Method, it became possible to prefabricate the reinforcement and to place the concrete for columns separately from that for beams and floor slabs.

The experiments on the effects of new anchoring methods were performed. From the load-deflection curve of the transverse framing with continuous anchorage as shown in Fig. 2, it is obvious that the test specimen is found to be stable enough even after 10 cycle repetition of loading with story drift of 1.5/100 up to 5/100. Conventional type of anchorage with the embedded reinforcing bars in the column was also tested under the same condition, and it was found that there were no significant differences between them.

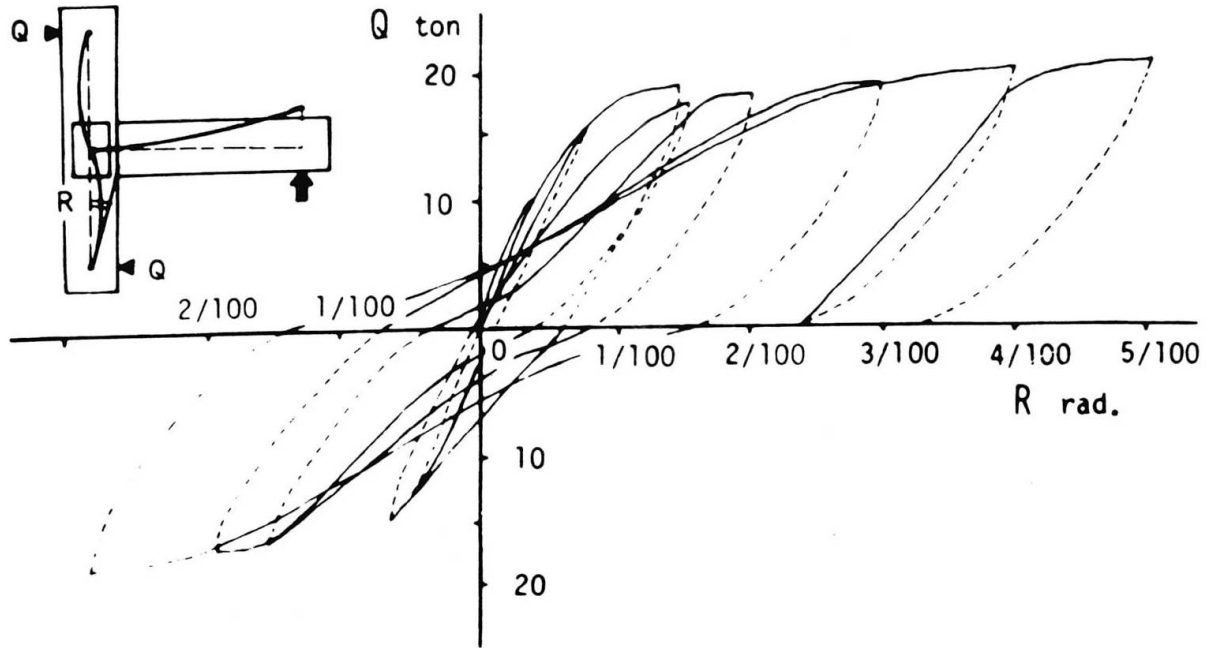


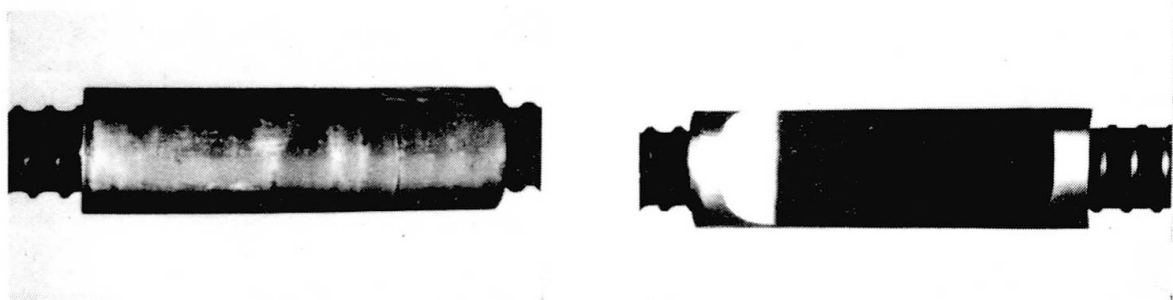
Fig. 2 Load-Deflection Curve of Exterior Framing including U Anchor Method

### 2.3 Joints of large-size reinforcing bars

When the stress in columns and beams increases in tall buildings, it becomes necessary to use large-size reinforcing bars. In such cases it is desirable to use a welded butt joint or sleeve joint rather than a lap joint. A welded butt joint is effective for the size of D32(#10) or less.

Various types of sleeve joints for heavy (D35 or more) bars were tested. Among them the Cadweld joint, mortar joint and squeeze joint was found to be highly reliable, satisfying all of the requirements for reinforced concrete specifications. In case of Cadweld or mortar sleeve joints, special moltend metal or strong mortar is used as joiner or connector between steel bar and sleeve. Regarding the squeeze type, the inside surface of the sleeve interlock with ribs of a specially developed reinforcing bar such as Rivercon as shown in Fig. 3.

For the building described herein, Cadweld joints were used but for the second tall building the squeezed joints were used after making cost studies of both joints.



a. Squeezed Joint

b. Cut off Section

Fig. 3 Squeezed Sleeve Joint

### 3. SEISMIC DESIGN

#### 3.1 Seismic design criteria

The author has established a basic criteria of earthquake resistant design. It is classifying earthquake intensities into three classes, and regulating the response of the building or degree of damages as follows:

Class I	Moderate earthquake (Max Acc. 0.1g)	No structural damages
Class II	Severe earthquake (Max Acc. 0.3g)	The stress in all members should be within allowable stress
Class III	Worst earthquake (Max Acc. 0.5g)	Building suffers some damages but never collapses

Maximum accelerations of the earthquakes were increased appreciably, in consideration of the fact that this building was to be the first highrise reinforced concrete structure in Japan exceeding the prior legal height limit.

#### 3.2 Outline of the building

The building herein has 18 stories with one story basement and is 48.9 meters tall. The outline of the building structure is shown in Fig. 4 together with typical structural details.

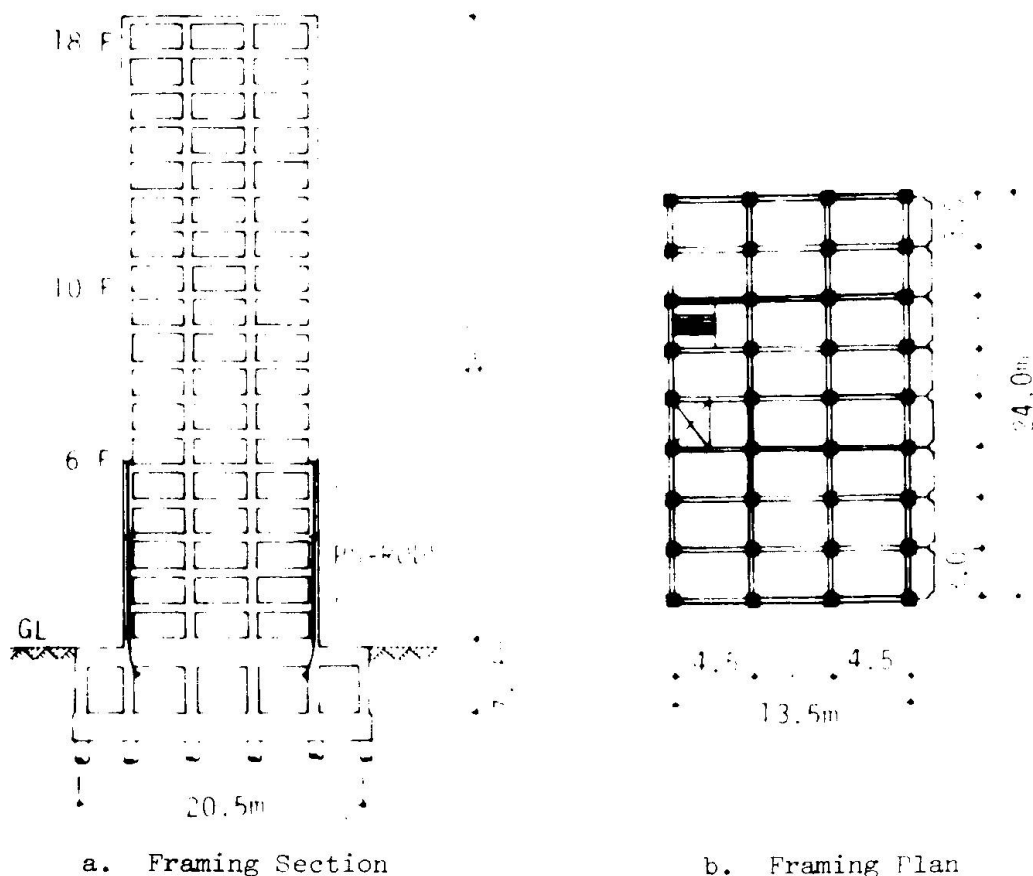


Fig. 4 Outline of Structure



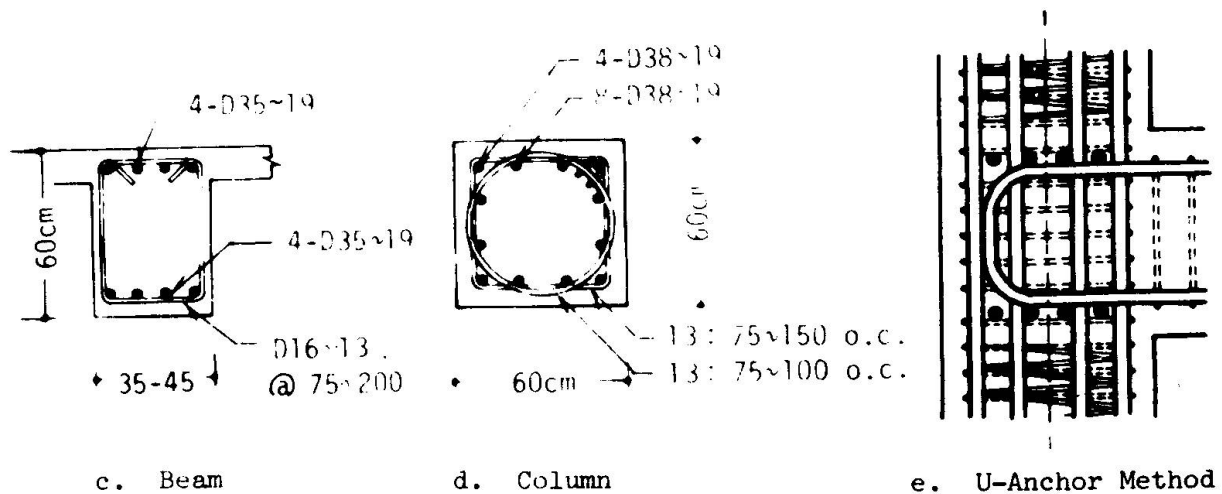


Fig. 4 Outline of Structure

Columns are all 60cm square which shear reinforcements consist of Kajima Spiral. Shear reinforcement ratios are 0.75 - 1.20% which was determined after various experiments. Beams are all 60cm in depth and 35, 40 or 45cm in width. The reinforcing bars of beams have newly developed U-shaped anchorage, thereby simplifying the task of prefabricating the reinforcement as mentioned before.

Moreover, the exterior columns from the first to the sixth floor are prestressed with PS steel rods as a protection from the tensile forces which may be induced by overturning moments. This step exceeded the required safety standards and furthermore registered an important advancement in the design of still higher buildings.

### 3.3 Dynamic analysis

#### a. Vibration model

In order to analyze dynamic behavior of the building accompanied by cracking and yielding, an idealized vibration model with 18 lumped mass is established. As shown in Fig. 5, the vibration model is assumed to have two kinds of stiffness. One is shearing stiffness which is derived from bending and shear deformation of beams and columns and shear deformation of beam-column joints, while the other is bending stiffness due to axial deformation of columns. Shear stiffness is assumed to have nonlinear degrading property and bending stiffness remains linear.

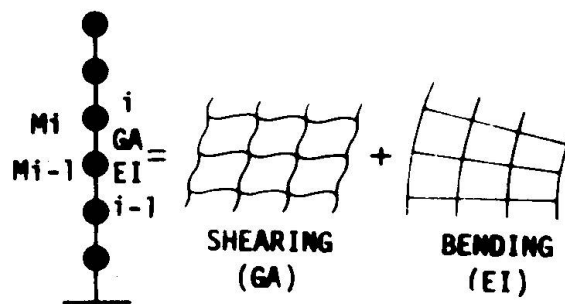


Fig. 5 Modeling

#### b. Shear stiffness and idealization of hysteresis loop

Static nonlinear frame analysis against the gradually increased lateral forces is carried out. Then the relations between story shears and shearing drifts are idealized by three straight lines (skeleton curve) in consideration of cracking and yielding of the members. In the nonlinear dynamic analysis shear stiffness property is defined by the skeleton curve and idealized hysteresis rule. Hysteresis loop with degrading stiffness property is idealized as shown in Fig. 6.

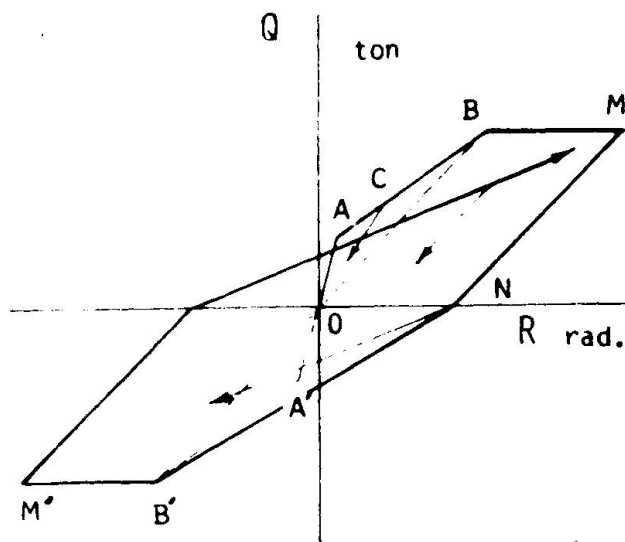


Fig. 6 Idealized Hysteresis Loop of Shear Stiffness

Point A in the figure indicates the first tensile crack. Up to this point, the structure is completely elastic. In the region between points A and B the curve tends to return to the origin (O) when unloading occurs. Point B means that yielding has occurred in the beam. In case where the load is decreasing at point M, the rigidity is the same as the gradient OB until the load becomes zero. Once zero is achieved, the curve points towards the opposite maximum deflection ever experienced.

#### c. Analytical conditions

Assuming that the building is fixed on the 1st floor, four types of input earthquake waves, El Centro 1940 NS, Taft 1952 EW, Tokyo 1956 NS and Sendai 1962 NS are adopted. Maximum acceleration of ground motion are selected 0.1g, 0.3g and 0.5g corresponding to the design criteria. Viscous damping is assumed and 3% of critical damping for the elastic 1st mode is adopted.

#### d. Results of dynamic analysis and seismic safety

The 1st vibration periods in the elastic range are 0.81 sec. in longitudinal direction, and 0.95 sec. in transverse. Responses of the dynamic analyses show similar results for longitudinal and transverse directions. Hence the results of longitudinal direction only will be described. Fig. 7 shows the maximum story shear and story drift resulting from severe earthquake (0.3g). It is noticed that stresses in all members remain in allowable values and maximum story drift is only 1.22cm at 11th story, which correspond to 0.45/100 deflection angle (see Table 1). Under the worst earthquake of 0.5g, yielding occurs but the maximum ductility factor remains at 1.66 at 12th story. These response values satisfy entirely the seismic design criteria established at the outset.

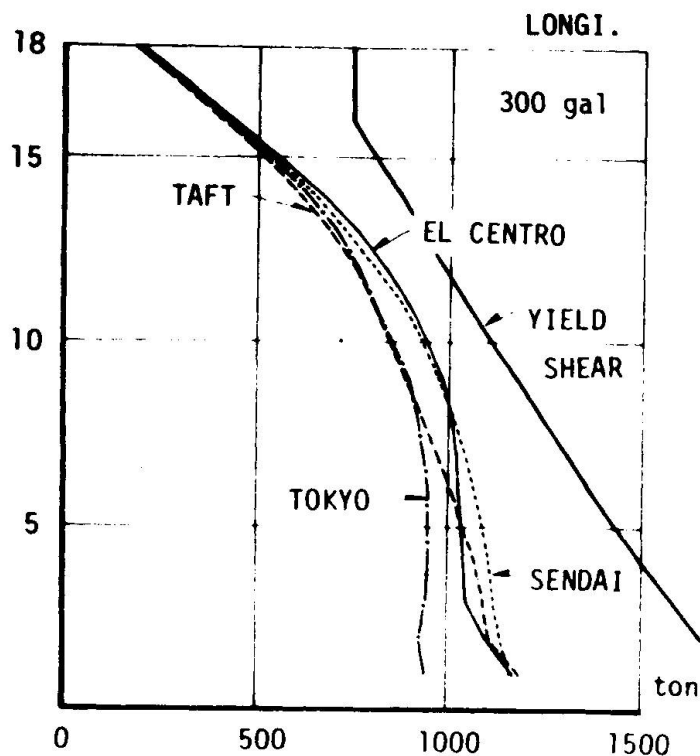


Fig. 7 Maximum Story Shear (0.3g)

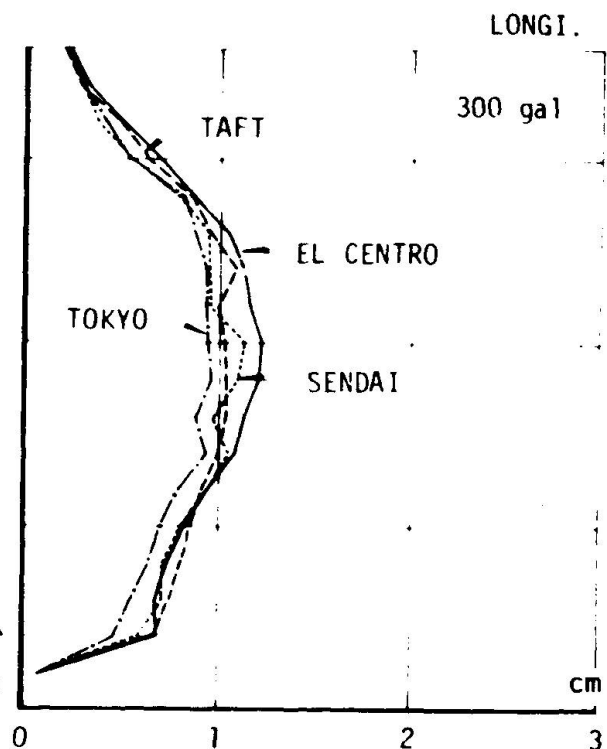


Fig. 8 Maximum Story Drift (0.3g)

Table 1. Damage Evaluation due to Earthquake Response

Intensity of earthquake	Base shear (B.S. coefficient)	Story drift	Yield (Steel)		Ductility factor
			Column	Beam	
Class I (100 gal)	950 ton (0.17)	0.4cm (at 11th story)	None	None	-
Class II (100 gal)	1180 ton (0.21)	1.22cm (at 11th story)	"	"	-
Class III (500 gal)	1910 ton (0.34)	(at 12th story)	"	2-16th Floor	1.66 (at 12th Floor)

#### 4. POST CONSTRUCTION STUDIES

##### 4.1 Forced vibration test

Immediately before the completion of the building, vibration tests were carried out. Vibration exciter was installed at the 19th (roof) floor. The periods and damping factor in transverse direction were obtained as shown in Table 2. The periods obtained by the test were about 20% shorter than those estimated in designing due to the difference of stress level (1st mode 4 - 5 gal, 2nd mode 10 gal in test) and the absence of live loads. It is noteworthy that the displacement at the top in the 1st vibration mode includes 1.4% of sway and 7.6% of rocking due to the deformation of soil and piling.

Table 2 Periods and Damping in Transverse Direction

	1st	2nd	3rd
Period	0.83 (sec)	0.27	0.15
Damping factor	1.5 (%)	3.1	6.5

#### 4.2 Earthquake observation

Earthquake observations are being taken by servo-type accelerographs installed at the underground, basement, 9th and 19th floors. Among many observed records, the following two earthquakes are noteworthy.

	A Earthquake (Izu Peninsula Coast)	B Earthquake (Eastern Saitama)
Occurred	: May 9, 1974	: August 4, 1974
Magnitude	: 6.9	: 5.8
Location of Focus	: 138°48'E 34°34'N	: 139°55'E 36°01'N
Focal Depth	: 20 kilometers	: 20 kilometers
Epicentral Distance	: 150 kilometers	: 40 kilometers

The local intensities of the site are both III in Japan meteorological intensity scale, which corresponds to IV or V in modified Mercalli scale. Acceleration time histories observed in the transverse direction at the basement are shown in Fig. 9. Acceleration response spectra are also shown in Fig. 10.

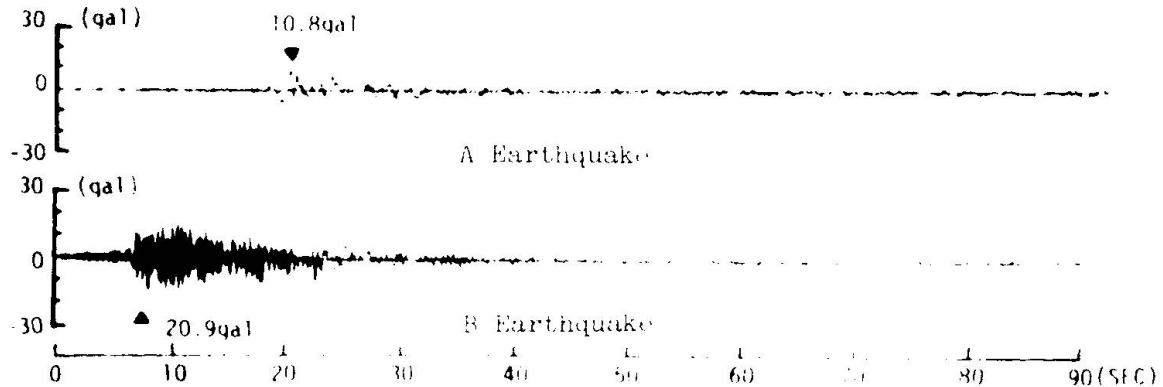


Fig. 9 Observed Acceleration at Basement (Transverse)

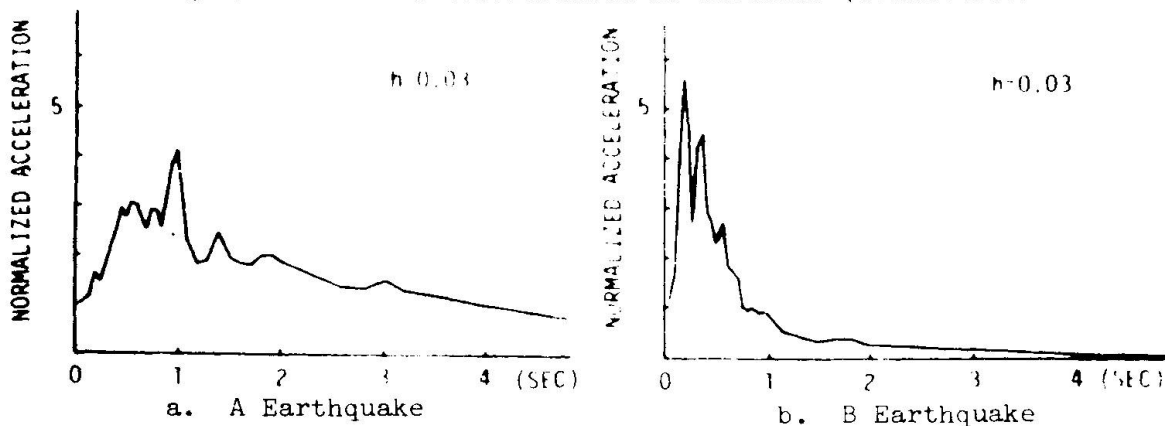


Fig. 10 Acceleration Spectra of Observed Earthquake (Transverse)

The frequency components of the two earthquakes were quite different that the motions of the building varied correspondingly. In the A earthquake, the first vibration modes of 0.8 seconds in the longitudinal direction and 1.0 second in the transverse were prominent. For both directions the amplifications of the accelerations were six times at the top floor relative to the basement. By contrast in the B earthquake, the second modes of 0.3 seconds were the most prominent in both directions and the amplification factors were only two.

### 4.3 Simulation of earthquake motions

#### a. Vibration model

Essentially same model as that was adopted in the seismic design was used for the simulation of the earthquakes. Some modifications have been incorporated in reference to studies on forced vibration test. For instance, a freedom of base rotational motion is additionally considered in this model. Rotational stiffness is assumed considering the reactions of soil and piling. Therefore, the 1st and 2nd vibration periods of the model in transverse direction are to be estimated 1.02 seconds and 0.32 seconds. It was decided that, damping for reinforced concrete should differ from that for soil. Therefore, 2% of critical damping ratio in the fundamental mode is applied to the upper-structure while 10% is to base foundation. Equivalent damping factor for the 1st mode of this model is also computed to be 2.4%.

#### b. Simulated results

##### Case of A Earthquake

Computed acceleration time history due to the A earthquake at the 19th floor is compared with the observed earthquake waves as shown in Fig. 11. A major motion in the input acceleration has a principal component of 1 second, which makes the upper floor accelerations extraordinarily amplified. For instance, the 19th floor acceleration is 6 times larger than that of the basement. Computed acceleration time histories coincide with the observed ones. The response spectra in Fig. 12 also show that both accelerations are quite identical.

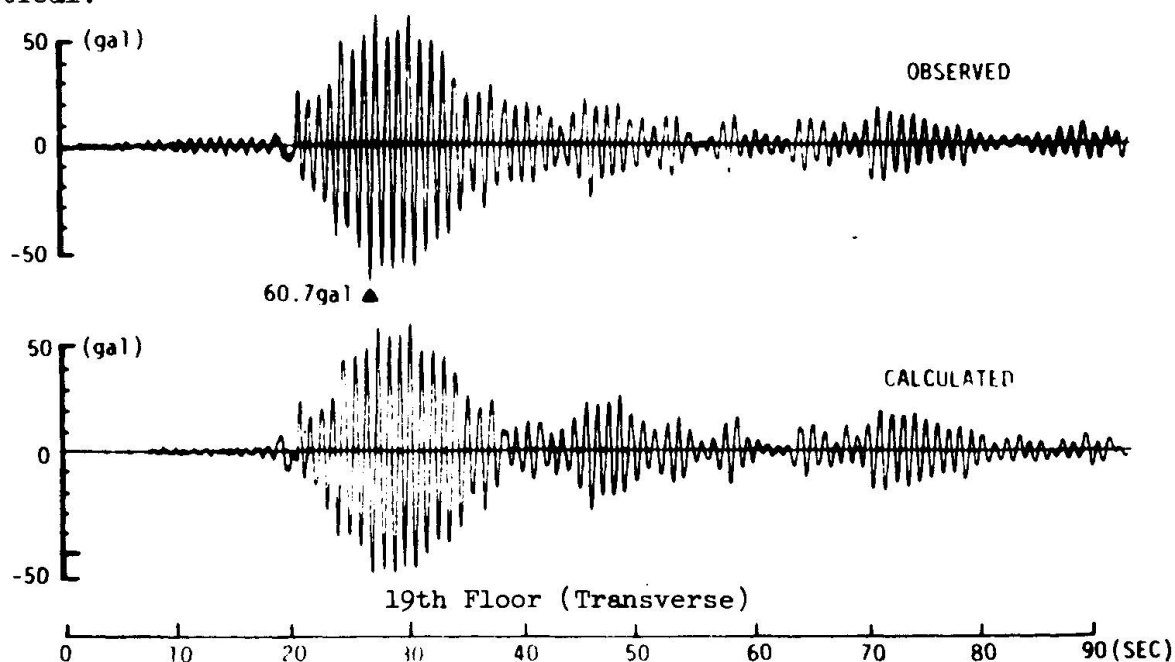


Fig. 11 Acceleration Time History (A)



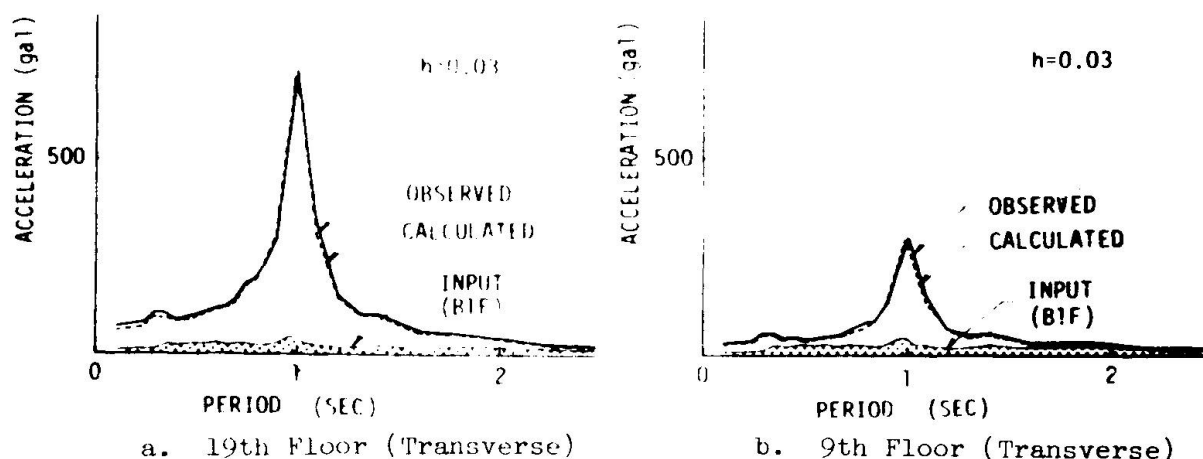


Fig. 12 Comparison of Acceleration Spectra (A)

### Case of B Earthquake

Fig. 13 shows the comparison of the observed and computed accelerations due to the B earthquake. Reflecting the fact that the basement record has prominent periods of 0.3 and 0.2 seconds at the time of major motion, the building is sharply excited at the fore part of the duration, then gradually changed to an oscillation with a longer fundamental period. Amplification ratios of acceleration both at the 9th and 19th floors are about twice as that of basement acceleration. These tendencies are clarified by Fig. 14 showing the response spectra. It is also concluded that dynamic behaviors of the building are precisely reproduced by analytical simulations throughout lengthy duration of the earthquake.

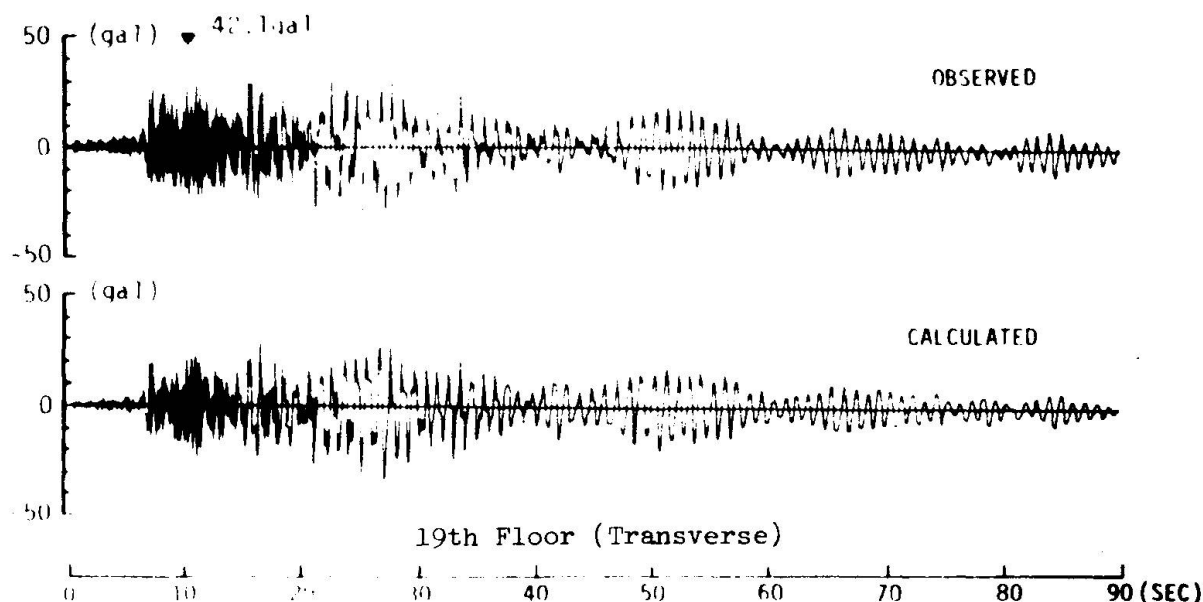


Fig. 13 Acceleration Time History (B)

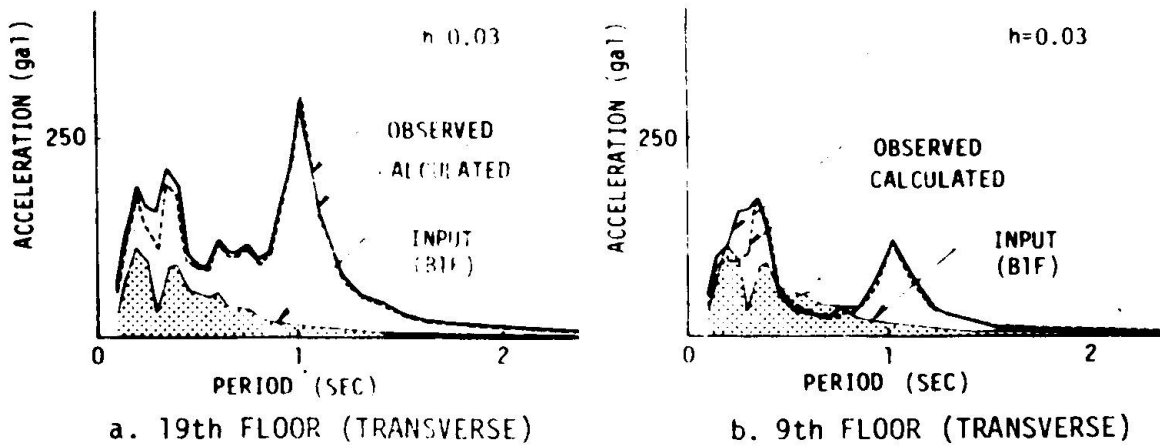


Fig. 14 Comparison of Acceleration Spectra (B)

#### REFERENCES

1. Kiyoshi Muto; "Earthquake Resistant Design of Tall Building in Japan" Lecture Note for Life Long Learning for the Earthquake Resistant Design of Engineering Structures in University Extension, June 1972. University of California, Berkeley.
2. Toshihiko Hisada, Nobutsugu Ohmori and Satoshi Bessho; "Earthquake Resistant Considerations on Reinforced Concrete Columns with Transverse Reinforcement", Earthquake Engineering & Structural Dynamics, The Journal of the International Association for Earthquake Engineering, Vol. 1, No. 1, 1972, John Wiley & Sons, London.
3. Ray W. Clough and Sterling B. Johnston "Effect of Stiffness Degradation on Earthquake Ductility Requirements", Proceedings of Japan Earthquake Engineering Symposium, Oct. 1966, Tokyo.
4. Kiyoshi Muto, Tsunehisa Tsugawa, Masanori Niwa, Hiromichi Shimizu "Simulation Analysis of a Highrise Reinforced Concrete Building in Two Different Earthquakes" Proceedings of the 6th World Conference on Earthquake Engineering, Jan. 1977, New Delhi

PROBLEMS FOUND DURING THE SEISMIC DESIGN OF STRUCTURES AND  
EQUIPMENTS OF A NUCLEAR POWER PLANT

L. LAZZERI, F. BOZZO, G. FILIPPI  
(SAIGE SpA , GENOA- ITALY)

ABSTRACT

The aim of this paper is a review of the main points found during the analysis of a nuclear power plant from the seismic point of view .

The main points are :

- soil structure interaction
- modelling of structures
- static equivalent models
- floor response spectra
- piping analysis
- electrical cableways
- heavy components

## 1. INTRODUCTION

The seismic analysis of nuclear power stations structures and components is one of the main problems, the designer has to solve in order to assess the safety of the populations even in the case of extreme earthquakes events. The aim of this paper is a brief analysis of the different problems one has to face, from the soil-structure interaction to sample analysis of different equipments in a nuclear power station.

## 2. SOIL-STRUCTURE INTERACTION

As it is well known (see, as an example ref [1] ) the soil structure interaction problem is of paramount importance in determining the response of the structures to the seismic excitation. The usual and simplest way of considering the soil-structure problem is by means of a set of springs, which model the stiffness of the ground surrounding the structure. This method, largely based on a method proposed by Whitman [2], [3], has been widely used in the past and it is quite satisfactory when the soil is relatively uniform and no large embedment is present. Different methods [4], [5], [6], [7] dealing with modifications and corrections of the original half space method have been proposed, however finite element methods (based on the use of the computer code FLUSH and subsequent modifications [8], [9], [10]) are available for an efficient evaluation of the soil-structure interaction phenomenon. A lot of papers was written to compare the different advantages of the two methods, however in this paper, the authors have simply decided to report their particular experience in this field.

The usual spring methods has large advantages in terms of cost and simplicity, so that many parametric analyses can be performed considering even a large spread of data regarding the soil characteristics [11] and is generally satisfactory. However, many cases exist where a good assessment of the phenomenon can be obtained by the use of the FLUSH code, as an example with relatively complicated soil profiles, with large embedment phenomena or when the so called building-soil-building phenomena may have importance. As far as this last aspect is concerned some runs have been performed in the case of neighbouring buildings on a relatively hard but comparatively not uniform soil (the modulus of elasticity ranging from 20000 to more than 100000 Kg/cmq). The first example is shown in fig.1, where two building of relatively similar weight and size have shown a coupled behaviour quite similar to the uncoupled one. The coupling phenomenon is definitively more easily discerned in the example in fig.2a, the response spectrum in fig.2b in one building clearly presents a peak corresponding to the eigenfrequency of the other building. However in this case too, while significative effects can be anticipated in terms of the response spectra, no large influence in the building accelerations was detected. Again this is quite possibly due to the relative resemblance of the two buildings, while the building-building interaction phenomenon should quite possibly be more important for small buildings near much heavier ones.

### 3. MODELLING OF STRUCTURES

A discussion of the techniques used in analyzing and modelling the civil structures of a nuclear power stations is given in reference [1]. In many cases, particularly for stiff buildings on very soft soils, a very simple model of the building (stick model) is adequate to predict the behaviour of the building [12]; a lumped masses model is used, the masses are generally placed at the floors levels with beam connections, representing the stiffness of the walls connecting subsequent floors. However for panels buildings (box type buildings) the stick model may be not quite adequate and for relatively stiff soil, where influence of the building stiffness may be important, finite elements model may be necessary. In fig.3a an example of a finite elements model is shown and the results of the dynamic analysis is shown in fig.3b; obviously enough the coupling of the panels vibrations with the over all building vibration, which is visible in the eigen frequency pattern in fig.3b, is not detectable with a stick model. On the other end box type buildings can be quite complicated and an efficient model can be very expensive due to its size, so that substructuring and condensing techniques are to be used.

### 4. STATIC EQUIVALENT MODELS

For obvious economical reasons the dynamic models are relatively of small size and their use can be not quite adequate to compute the inertial forces for the subsequent stresses evaluation. Again huge (thousands degrees of freedom) finite elements models have been used [12], but their use is very expensive so that simplificative assumptions have to be used. To test different methods some runs have been made by the authors and their colleagues in SAIGE [13][14]. In fig.4a a simplified model is shown; it has been loaded by constant inertial forces in the horizontal plane and by vertical forces on the floor simulating a rotation effect. The displacements pattern is shown in fig.4b,c. While the simplifications in the model may be relatively important (only the lower portion of the building has been modelled, while the influence of the stiffness of the upper portion may have some importance) some general conclusions may be drawn:

- the shear is absorbed only by the walls parallel to the direction of the seismic excitation and it is relatively constant in them
- the bending moment is not absorbed by the structure as a whole, rather the normal stresses are concentrated mainly in the corners or where two normal walls are present
- the floors are not rigid as regards the out of plane bending and are not consequently adequate to transfer the stresses from one end of the building to the other one
- some deformations take place even due to in plane forces, however this effect is much more limited than the previous ones, so that a relatively uniform shear stress distribution takes place

- the vertical forces consequent to rotational accelerations are taken directly by the floors where they are applied and transferred locally to the vertical frames.

Particularly for low and wide buildings the shears seem to be absolutely predominant and the floors are generally adequate to act as rigid frames so that the seismic shears are taken by the vertical walls between subsequent floors independently from the distributions over and under the connected floors. The behaviour is quite opposed to the one usually known as typical of 'shear type buildings' and represents consequently the other extreme.

However there are buildings where both bending and shears may play an important role so that finite elements models only can be used for a relatively exact evaluation of the seismic stresses.

## 5. FLOOR RESPONSE SPECTRA

As it is well known, the modelling of the structures is limited to the main components, while the minor ones are neglected. However there are many components (piping, valves, pumps, electrical components, etc.) which are important for the safety of the plant and whose seismic analysis has to be performed. For relatively light components it is comparatively accurate to assume that no feedback action takes place from the component, so that the seismic time history due to the earthquake and filtered by the building can be directly assumed by it. This procedure is generally known as 'calculating a floor response spectrum' and it is used even for relatively heavy components even if in this case the procedure may be relatively pessimistic [15]. Many techniques have been proposed using both stochastic [16] or semistochastic methods [17], [18]; the use of these methods has large advantages in terms of cost and time as they are based on the use of the response spectrum analyses for the buildings. On the other end time histories analyses have been proposed and used even if they are relatively expensive. The first problem to be solved is the generation of a time history compatible with the given ground response spectrum; starting with a paper by Nih Chien Tsai [19] techniques have been proposed [21] and an earthquake time history representation by means of a Fourier series. Both the SIMQKE program [20] and a home-made program THAMS [22], [23] based on reference [21]. In fig.5 the time history compatible with the standard USA Regulatory Guide 1.60 is shown as generated by THAMS program is shown.

Much discussion has been made about the relative merits of the simplification and time history methods, it is the authors' opinion that the use of the time history methods are quite necessary in many cases (as an example whenever non linear techniques are necessary or when time histories are necessary as an example for tests on heavy machinery or electric components), however defects in the methods (lack in uniqueness in the solution, costs) may make the simplification ones preferable. As an example, in many cases, it is not quite necessary to know exactly the floor response spectrum rather it is important to know for which frequencies there is the so called peaks region (large amplifications



in the accelerations) and which is the minimum frequency for which the floor response spectrum is flat. In this cases the advantages of the simplified methods are obvious.

## 6. PIPING ANALYSIS

The seismic analysis of piping runs is one of the main tasks for the designer of a nuclear power system, due to the large numbers of components to be analyzed. It should be further mentioned that ASME 3 NB pipes generally have some problems concerning the thermal analysis and consequent fatigue evaluation, so that it is convenient to have pipings as flexible as possible; obviously enough this necessity is contrary to the seismic one, as it is customary to have eigen frequencies higher than the peak zone ones in order to minimize the accelerations in the pipe [24]. Then the use of viscous or inertial snubbers has been found particularly useful in solving this problem. However the costs of these equipments is comparatively large so that there is a strong necessity for the limitation of their number, besides the dynamic analyses themselves are relatively expensive and time consuming so that some predesign criterion is very useful indeed [25].

Some simple predesign criteria (based on a hypothetic independent behaviour of each span of pipe between successive supports) are used for the sizing of the snubbers and a preliminary evaluation of their collocation. Then a final dynamic analysis is performed for a final appraisal of the solution; an example is given in ref. 5.

It should further mentioned that a huge number of piping in a nuclear power station do not have dilatation problems and their minor importance does not require particular dynamic analysis, hence the simplified analysis are particularly interesting. Two criteria are generally considered,

- each span is considered in an independent way so that the fundamental eigen frequency is larger than the one corresponding to the beginning of the flat region in the FRS,
- the maximum stresses are very low so that the seismic excitation does not contribute to a substantial increase in the stresses.

## 7. ANALYSIS OF ELECTRICAL CABLEWAYS

Most of the safety related components are electromechanical, whose energy comes via electric wiring; then they must be analyzed from a seismic point of view. The problem does not present substantial difficulty from a theoretical point of view, however the huge number of components to be analyzed represents a difficulty in itself. Normalization and the use of computerized procedures is then absolutely necessary in order to perform these analyses within reasonable time and costs. ASDIC [26] is an answer to these necessities; the code is capable of analyzing the support structures of cableways and electric wirings,

determining the maximum loads (dead load and seismic loads specified under the form of support structures) compatible with each geometric configuration (as an example see fig.6) Then the use of ASDIC together with a normalization makes these analyses quite easy.

#### 8. ANALYSIS OF HEAVY COMPONENTS

The analysis of heavy components is a necessary step in assessing the safety of the plant from the seismic point of view . While many analyses have been performed for important mechanical components such as pressure vessels, pumps etc., few analyses have been reported about electrical equipments such as motors, alternators etc. From a theoretical point of view many problems seem to exist as relative displacements between the stators and rotors could cause heavy consequences on the normal service of the machinery. For this reason some analyses have been performed (see fig.7) on typical machinery by means of finite elements models (approximately 1000 degrees of freedom). The results have been quite good showing that the normal working necessities claim for heavy rigidity necessities, so that the machines are generally rigid . Partial vibrations of some panels might take place, without any loss of functionality of the machine itself. Besides no large relative displacements among the different parts of the structure take place as due to the seismic excitation, so that no large electrical problems are anticipated.

#### 9. ACKNOWLEDGMENTS

The authors are greatly indebted with their colleagues in the Special Calculations Group of SAIGE without whose help all the described calculations could not have been performed.

#### REFERENCES

1. IAEA Standard on Seismic Analysis
2. Whitman Richart "Design procedures for dynamically loaded foundations J Soil Mechanics and Foundation division of ASME, Nov. 1967 SM6 Nov.1967
3. Biggs Whitman "Soils structure interaction in nuclear power plants 1 SMIRT Conference , Berlin 1971
4. Hall Morrone Soil structure interaction parameters for a nuclear containment vessel 2 SMIRT Conf. paper K2/6, Berlin 1973
5. Hadijan Luco Two - dimensional approximations to the three - dimensional soil - structure interaction problem. Nuclear Engineering and Design 31/2 1974
6. Luco Westmann "Dynamic response of circular footings - J. Engineering Mechanics Division of SAIGE EM-5 , 1971
7. Kausel Roesset "Soil structure interaction problems for nuclear containment structures ASCE - Power Division Specialty Conf. 1974 Denver

8. Lysmer Udaka Tsae Seed "FLUSH a computer program for approximate 3D analysis of soil-structure interaction problems" Rep. EERC 75-30, Nov.1975
9. Seed Lysmer "Soil structure interaction analysis by finite element methods State of the art" 4th SMIRT Conference St.Francisco paper K2/1 , 1977
10. Romo Organista, Lysmer , Seed "Finite Elements Random Vibration method for soil-structure interaction analysis" 4 SMIRT Conf. St.Francisco 1977, paper K2/3
11. Lazzeri Sano " Seismic analysis of the primary building of a BW reactor "V WCEE Conference , paper , Rome 1973
12. Bergeretto Giuliano Lazzeri "A complete analysis of a nuclear building to nuclear safety standards" paper J2/2, 3 SMIRT Conference , London 1975
13. Bozzo Lazzeri Internal SAIGE Report
14. Porfido Personal communications (Internal SAIGE Report)
15. Castellani "On design criteria for equipment mounted on a massive structure" V WCEE Conference , Rome 1973
16. Sing Ang "Stochastic predation of maximum seismic response of light secondary systems" paper K6/1 2 SMIRT Conference Berlin 1973
17. Biggs Roesset Seismic Analysis of Equipment mounted on massive structures" Seismic design for Nuclear Power Plants Edited by Massive
18. Lazzeri "Floor response spectra by the use of a modified white noise technique " paper K4/2, 2 SMIRT Conf., Berlin 1973
19. Nih Chien Tsai "Spectrum compatible motions for design purposes" ASCE J. Engineering Mechanics Division Vol. 98, EM2, April 1972
20. Gasparini Van Marke "Simulated Earthquake motions compatible with prescribed response spectra" MIT Pipl. N.R 76-4
21. Sachs Scanlan "Earthquake time histories and response spectra " J. Engineering Mechanics Division EM4, Aug 1974
22. Cecconi Bettocchi PhD Thesis in Civil Engineering -Univerity of Genoa 1976
23. Laguzzi e Cabella - PhD Thesis in Civil Engineerin-Univ.of Genoa 1977
24. Bisconti Lazzeri Strona "Analysis of piping for nuclear reactor Applications" Chapter 7 of Developments in stress Analysis for Press.Components
25. Stevenson Bergman "Determination of support spacing tables used in the design of safety class Nuclear plant Piping" 4 SMIRT Conf. St.Francisco 1977, K6/19
26. Lazzeri Strona "ASDIC theoretical manual " SAIGE Rep. 0226Z.

FIG. 1

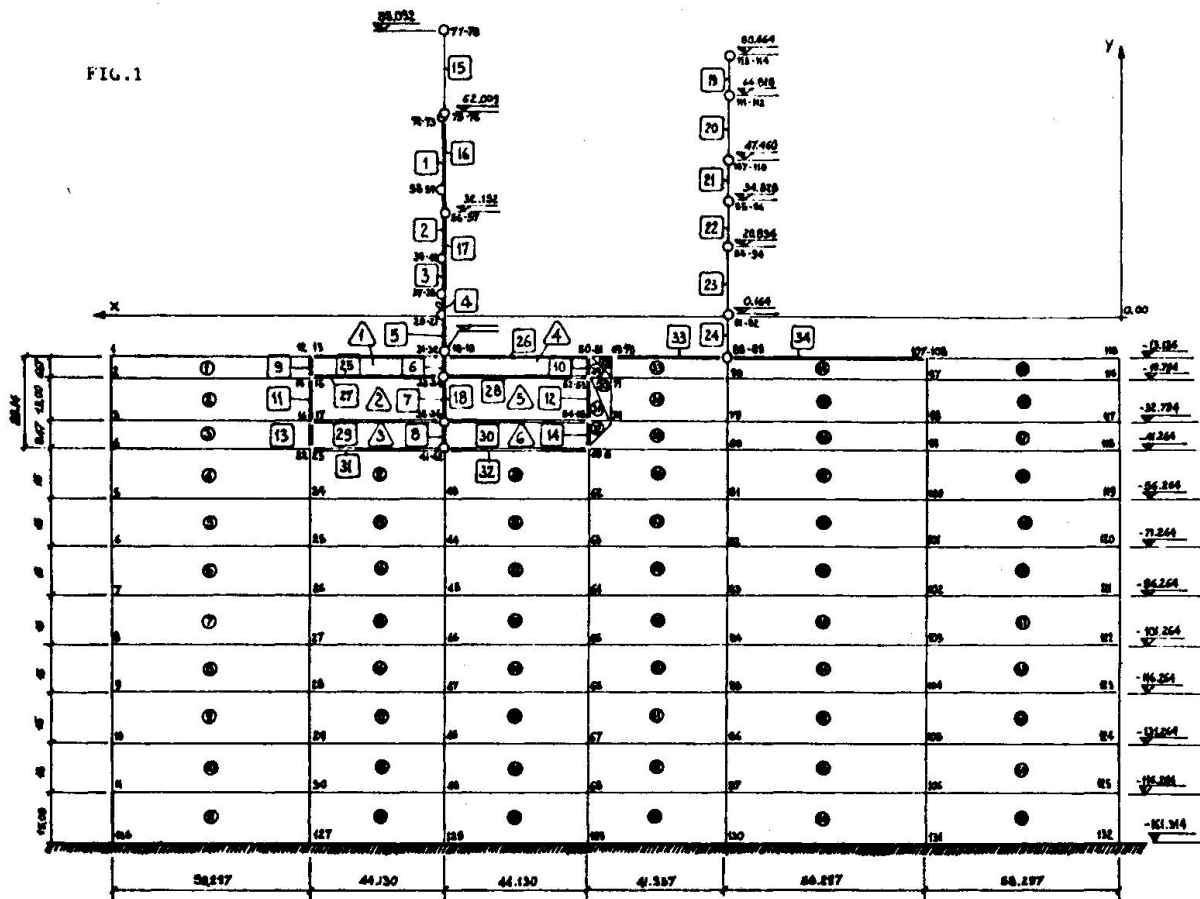
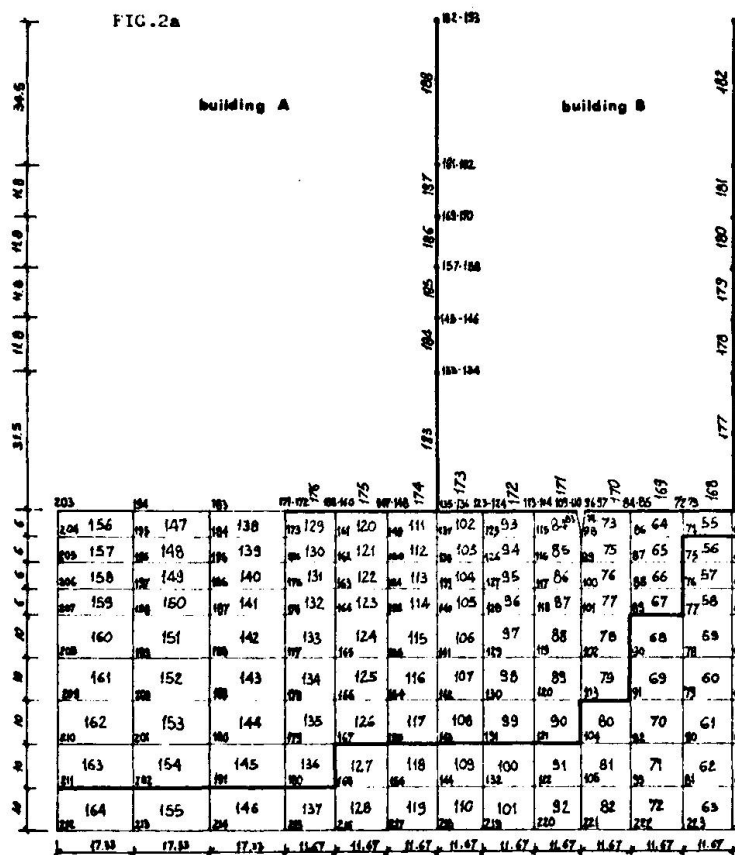
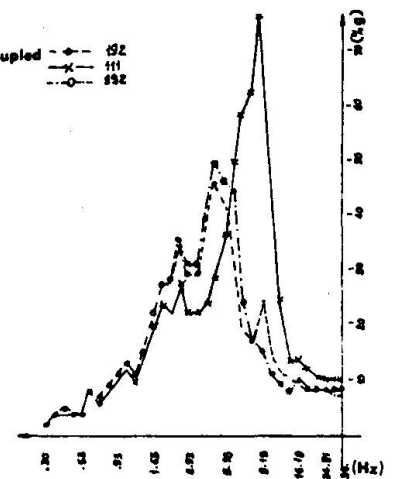


FIG. 2a



building A) coupled  
 B) coupled  
 A) coupled

FIG. 2b



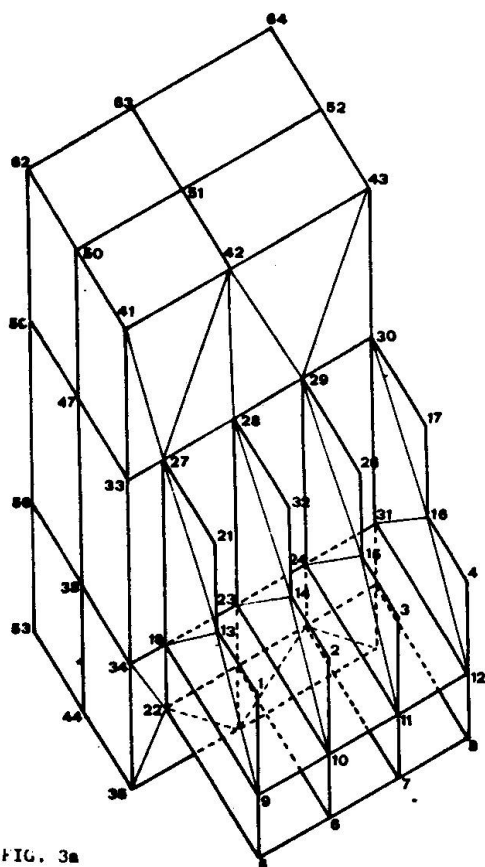


FIG. 3a

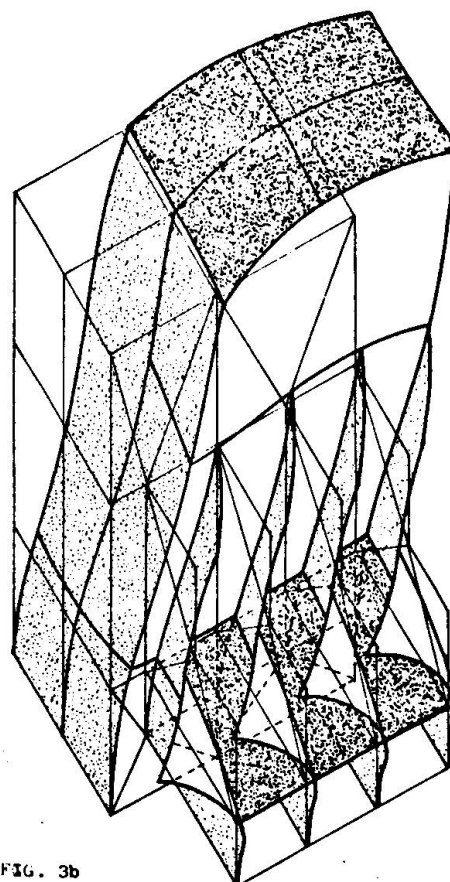


FIG. 3b

MODEL

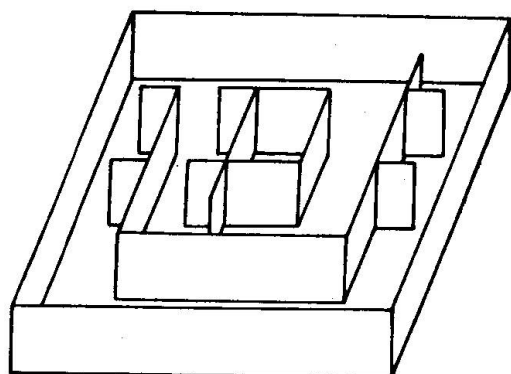


Fig. 4a

HORIZONTAL DISPLACEMENTS

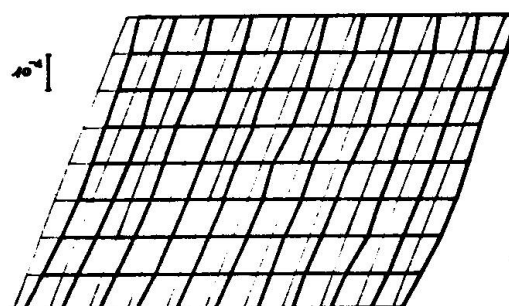


Fig. 4b

SHEAR STRESS

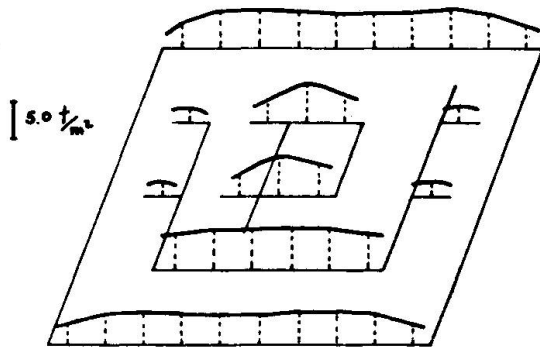


Fig. 4c

VERTICAL STRESS

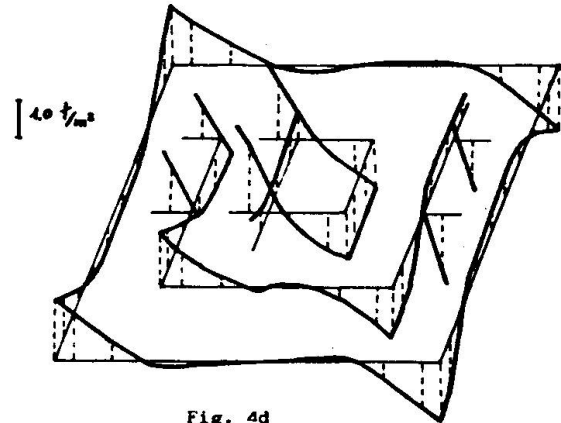


Fig. 4d

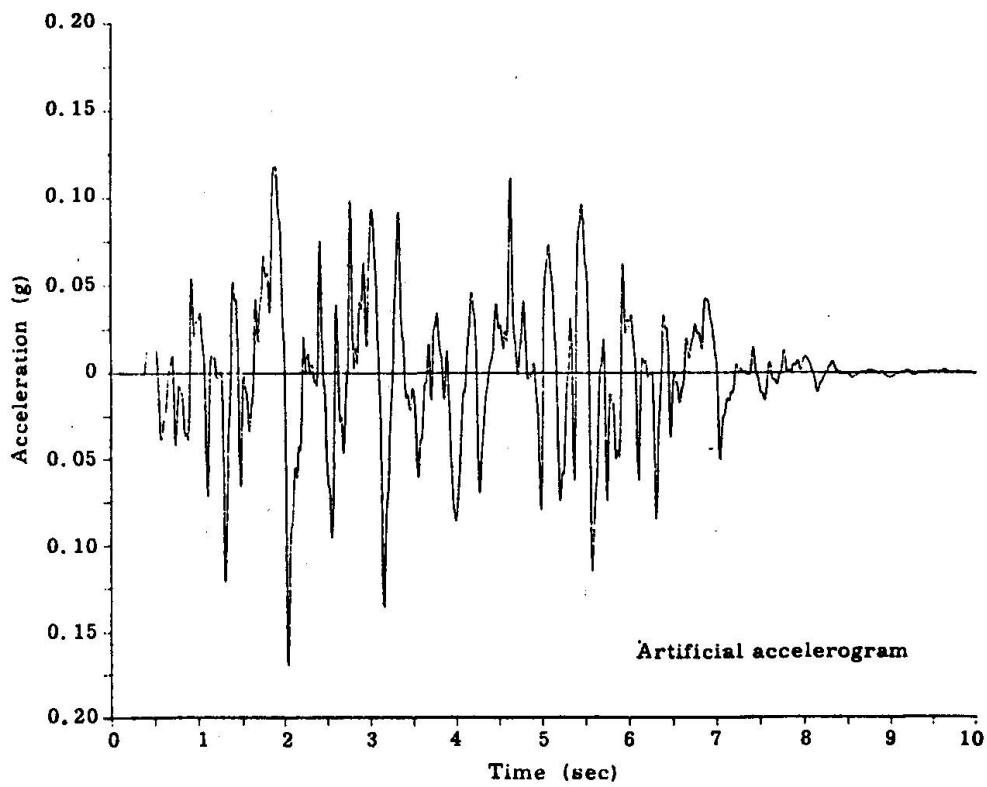


FIG. 5



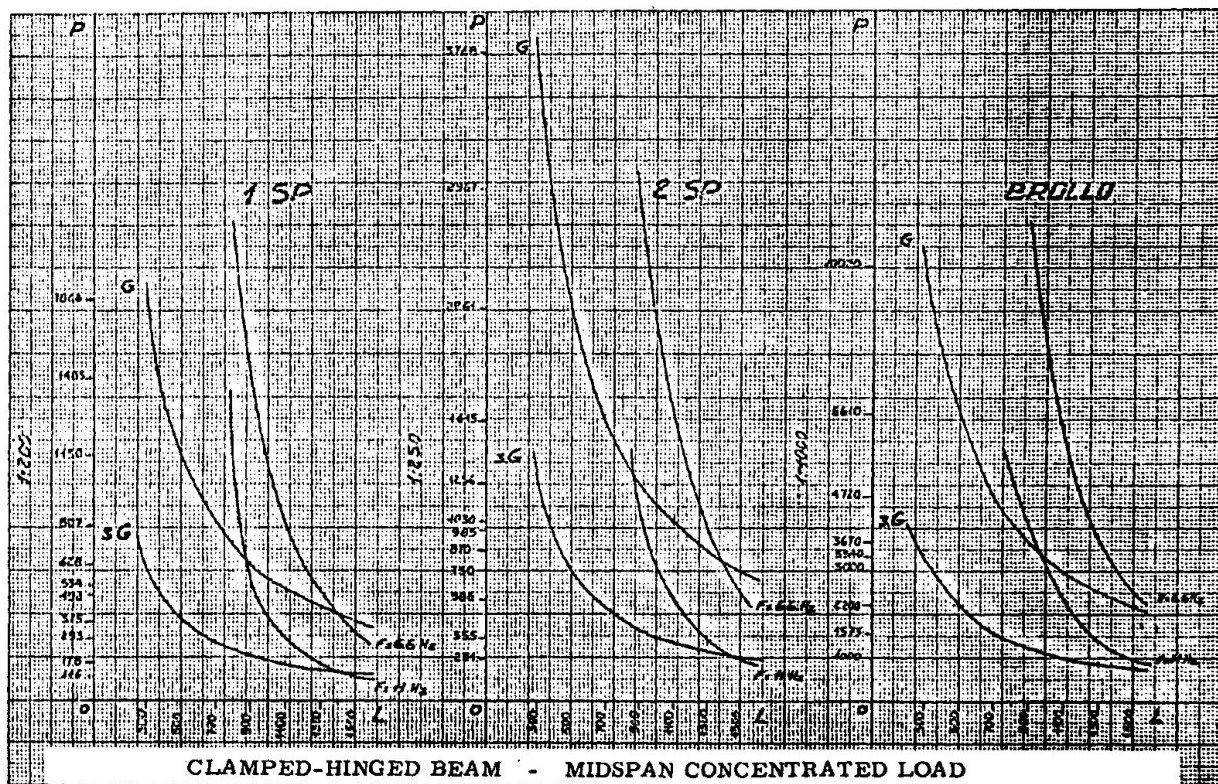


FIG. 6

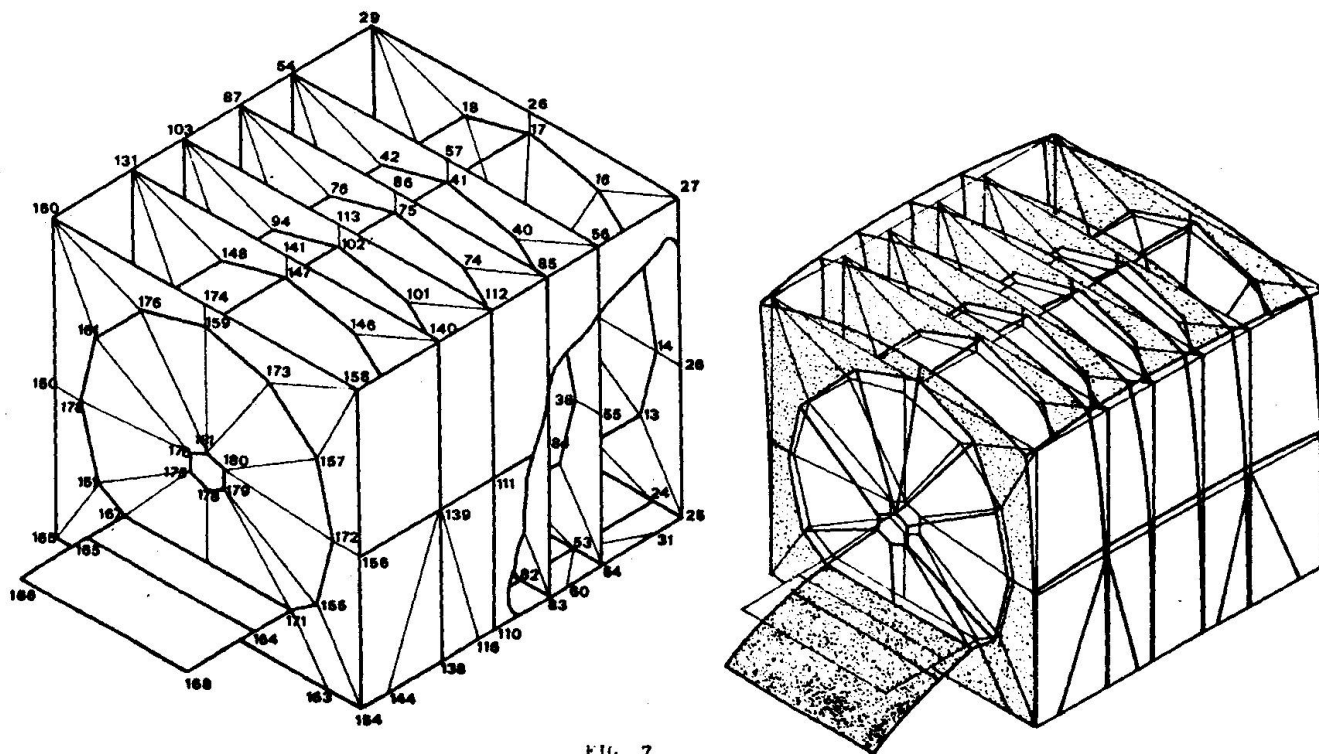


FIG. 7

Leere Seite  
Blank page  
Page vide

## SEISMIC BEHAVIOUR OF GUYED MASTS

Ondřej F i s c h e r , Ing. C.Sc.

CS Academy of Sciences, Prague, Czechoslovakia

## SUMMARY

The method for computation of natural vibrations of guyed masts with respect to the mass of guys is described and the possibility of solving the amplitudes excited by the motion of the ground using modal analysis is demonstrated. At last the check of stresses caused by the permanent change of the distance between shaft and guy foundation blocks is given.

## RÉSUMÉ

On a développé dans cette article une méthode de la résolution des vibrations propres du pylône en prenant compte la masse répartie des haubans. On y présente aussi une méthode de la résolution des amplitudes des vibrations, qui prennent naissance dans le mouvement des appuis, par la décomposition d'après les formes propres, aussi que la méthode de la résolution d'influence du changement permanent de distance parmi des foundations du pylône et des haubans.

## ZUSAMMENFASSUNG

Im Artikel wird gezeigt die Berechnung von Eigenschwingungen des abgespannten Mastes mit Berücksichtigung der Masse von Pardunen, und die Lösung von seismisch erregten Schwingungen nach dem Verfahren der Zerlegung in Eigenschwingungsformen. Zum Schluss wird die Schätzung von Spannungen gegeben, die durch die nachhaltige Veränderung des Abstandes zwischen Schaft und Pardunen Fundament verursacht sind.

## 1. INTRODUCTION

Guyed masts are structures enabling the attainment of great heights at relatively low costs and are, therefore, the tallest structures in the world in general. Their static as well as dynamic behaviour, on the other hand, is very complicated: a considerable source of difficulties in the static analysis are the non-linearity of supports and the great deformations of the shaft. In dynamic analysis the assumption of linearity may be preserved in the majority of the cases, but great difficulties are due to a large number of natural frequencies and modes, and to their mutual proximity. Particularly if the computation considers the mass of guy cables the frequency spectrum is very dense. E.g. for a television mast with 4 guy levels and the height of 320 m altogether 14 natural frequencies were found within the limits of 0 - 1.0 Hz. This number is even higher if the mast is guyed by different cables in each level /e.g. oscillating about the equilibrium position at a certain deflection due to static wind/. A radio mast with heavy cables carrying heavy insulators will also have a major number of natural frequencies. On the other hand, in the case of a mast with light cables of man-made fibres the mass of these cables will practically play no role at all.

The seismic excitation of the mast may be due to either the motion of the shaft foundation /horizontal displacement or rotation, if the mast is clamped at its foot/, or to the horizontal movement of the cable anchorage foundation. Vertical movement is not dangerous for the shaft, it could endanger the galleries or cabins located on the mast; in the case of guy cables it would come into consideration in exceptional cases only, since it does not produce simultaneous oscillations of the shaft. The frequencies of natural seismicity /2 - 5 - 10 Hz/ are comparable with higher natural frequencies of the mast. These, however, similarly as the higher modes, cannot be estimated approximately; it is therefore very difficult to find some quasistatic solution. Intuitively it is possible to say that these modes, in which the higher vibrations of the cables prevail, do not manifest themselves, since the damping of the cables is in general higher.

On the other hand the shaft, usually of allwelded design or connected by means of friction bolts, has an extremely low damping, so that the modes in which the shaft vibrations prevail, can be excited even in high frequencies.

Simultaneous, but probably very little synchronous excitation of the shaft and guy-anchorage foundations should reduce the resulting excitation of the mast as a whole. Nevertheless, at higher frequencies the excitation transferred by the cables can be absorbed and the vibrations of the shaft itself may ensue.

Another danger to a guyed mast during earthquake is due to the fact that a permanent change of the distance between the foundation of the shaft and the foundation of the guy cable may occur. A suitable location and foundation of the mast in uniform geological conditions should eliminate this undesirable effect; however, if it is not possible, it is necessary to foresee a certain change of these distances and estimate it in the design. The stresses due to this effect may be considered as temporary; after the earthquake the cable length may be rectified and the shaft stresses annuled.

During stochastic excitation of the limited white noise type the response of the mast consists of the vibrations in natural modes, whose frequencies are very near one to the other. In this way beats occur and the case may arise in which the top of the mast is suddenly displaced by a considerable amount in a certain moment. As a rule this effect will not be dangerous for the mast; however, if it has been provided at the top with a pendulum vibration absorber of a considerably lower frequency than the frequency of the afore mentioned lurch, the absorber may break away. In such a case the absorber should be therefore provided with buffers limiting its displacements.

## 2. DETERMINATION OF NATURAL VIBRATIONS OF A GUYED MAST

For the solution of natural vibrations of a guyed mast a computer

programme has been in use in our institute for a number of years, modelling the mast as a continuous beam on elastic supports with constant normal force and bending stiffness in every span, and solving it by the slope-deflection method [1]. /This programme was written by J.Náprstek/. Recently it was completed by the introduction of the mass of guy cables, using Koloušek's solution [2], further elaborated and experimentally verified by Davenport [3].

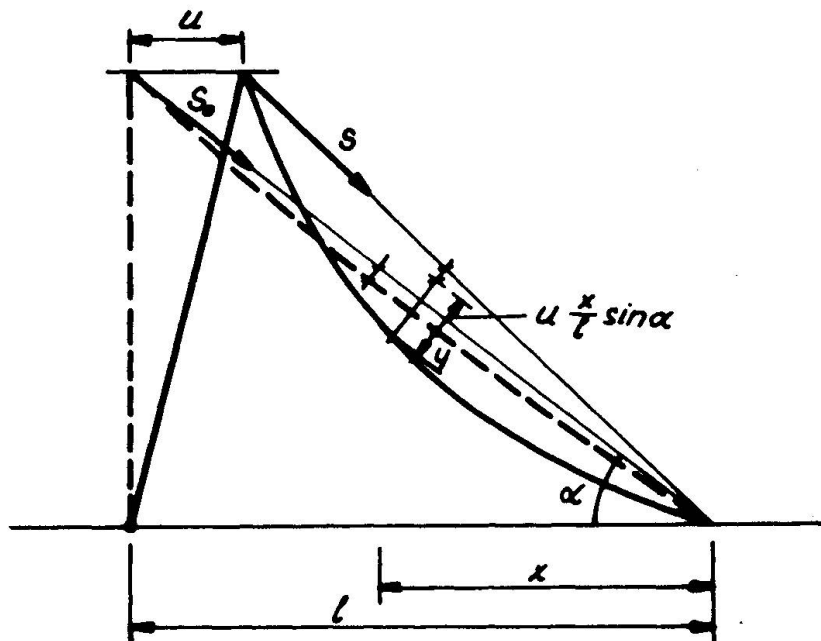


**Fig. 1** Displacement of one guy of the support

According to these for the cable amplitude can be written /Fig.1/

$$y(x) = u \frac{x}{l} \sin \alpha + u L \left[ \frac{1}{1 - \Omega^2} \sin \frac{\pi x}{l} + \frac{1}{3(9 - \Omega^2)} \sin \frac{3\pi x}{l} + \frac{1}{5(25 - \Omega^2)} \sin \frac{5\pi x}{l} + \dots \right]$$

$$L = - \frac{4}{\pi} \cos \alpha \frac{1 - \frac{\pi^2 S_0^2 \operatorname{tg} \alpha}{2EA\mu g l} \Omega^2}{\frac{\pi^2 S_0^2}{EA\mu g l} - \frac{\mu g l}{S_0} \eta(\Omega)} \quad /1/$$

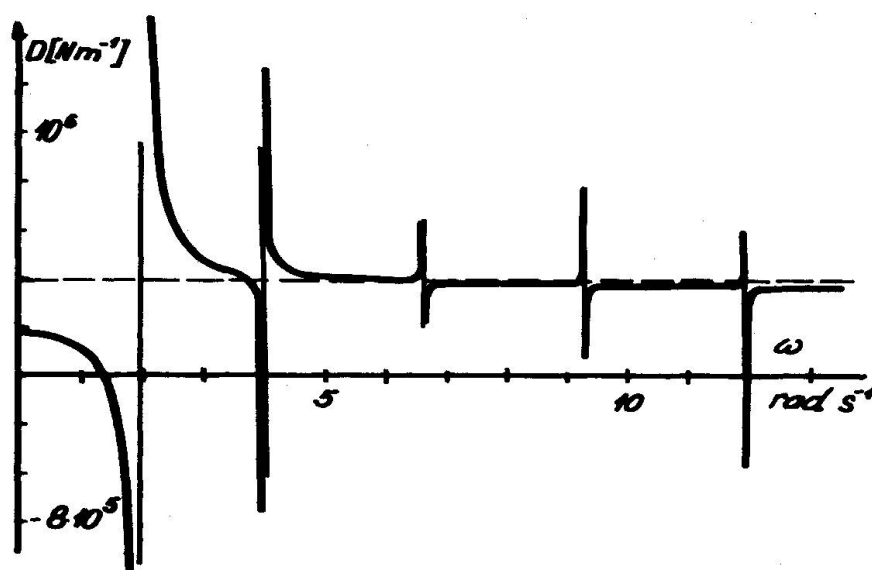
$$\Omega = \frac{l}{\pi \cos \alpha} \sqrt{\frac{\mu}{S_0}} \omega \quad ; \quad \eta(\Omega) = \left[ 1 - \frac{2}{\pi \Omega} \operatorname{tg} \left( \frac{\pi \Omega}{2} \right) \right] : \Omega^2$$

and for the horizontal force in the upper end of the cable



$$R = -u \frac{S_0 \cos^3 \alpha}{l} \frac{1 - \mu g l \Omega^2 \operatorname{tg} \alpha \eta(\Omega) : 2S_0}{\frac{S_0}{EA} - \left( \frac{\mu g l}{\pi S_0} \right)^2 \eta(\Omega)} \quad /2/$$

The reaction of a cable support depends on the frequency of motion. For 3 cables in one level it equals 1.5 times the force per one cable /2/, for 4 cables double the force. If the cables in one support are different, their forces must be composed generally in the resultant reaction. An example of the "spring constant"  $D = R : u$  of such a reaction is shown in Fig.2. With the excep-



band and in computation can be lost even with a very small step  $/\Delta\omega = 0.01 \text{ rad.s}^{-1}/$ . In such a case the zero point approaches the asymptote, i.e. the natural frequency of the mast is very near to the natural frequency of the cable; it is therefore of some importance only for this one cable and with reference to the mast as a whole they play no practical role. In most cases it will be sufficient to consider the stiffness of supports /2/ only until the 2nd natural frequency of the support and further on the constant stiffness /3/ can be used. To the natural frequencies determined in this way the natural frequencies of the isolated cables should be added assuming that in these vibrations the mast remains at rest. After the determination of natural frequencies also the ratio of node displacements and rotations is obtained, from which the natural mode of the shaft and that of the cables /1/ is determined, and the generalised mass

$$m_{(j)} = \int \mu v_{(j)}^2(x) dx \quad /4/$$

where the integral includes the whole mast and all guys.

### 3. SOLUTION OF RESPONSE OF A GUYED MAST TO SEISMIC EXCITATION

For the solution of the response of the structure to random as well as deterministic stationary excitation the modal analysis is most suitable, as a rule. Particularly in the case of little-damped structures it is always possible to consider one natural mode only whose frequency is near to the excitation frequency. By a suitable procedure it is possible to get over the fact that the amplitude of a structure with a moving support cannot be expressed by means of the base system of natural modes.

Starting from the general equation of motion of a prismatic beam

$$\mu \frac{\partial^2 v(x,t)}{\partial t^2} + 2\mu \omega_b \frac{\partial v(x,t)}{\partial t} + EJ \frac{\partial^4 v(x,t)}{\partial x^4} = 0 \quad /5/$$

let us expand the solution according to the modes of natural vibrations and supplement it with zero term corresponding with the given excitation of zero frequency and unit displacement, thus having the meaning of the static deflection of the structure caused by unit displacement of the given support. Then it is

$$v(x, t) = v_0(x) q_0(t) + \sum_j q_{(j)}(t) v_{(j)}(x) \quad /6/$$

Substituting the solution /6/ into /7/, multiplying the whole equation by  $v_{(k)}(x)$  and integrating over the whole member we obtain

$$\ddot{q}_{(k)}(t) + 2\beta\omega_{(k)}\dot{q}_{(k)}(t) + \omega_{(k)}^2 q_{(k)}(t) = -[\ddot{q}_0(t) + 2\beta\omega_{(k)}\dot{q}_0(t)] \quad /7/$$

where it has been introduced

$$v_{(k)}^{\overline{W}}(x) = \frac{\mu \omega_{(k)}^2}{EJ} v_{(k)}(x) \quad ; \quad v_0^{\overline{W}}(x) = 0 \quad ; \quad \omega_b = \beta \omega_{(k)}$$

$$P_{(k)} = \frac{\int v_0(x) v_{(k)}(x) dx}{\int v_{(k)}^2(x) dx}$$

In /7/  $q_0(t)$  - time function of the support movement

$\beta$  - relative damping

$v_0(x)$  - deflection line caused by unit displacement of the support .

Supposing harmonic excitation  $q_0(t) = q_0 \exp(i\omega t)$ , /7/ will change into

$$\ddot{q}_{(k)}(t) + 2\beta\omega_{(k)}\dot{q}_{(k)}(t) + \omega_{(k)}^2 q_{(k)}(t) = q_0\omega^2 P_{(k)} - 2q_0\beta\omega_{(k)}\omega P_{(k)} i \quad /8/$$

The second term on the right hand side can be neglected for little damped structures. From /8/ the generalised coordinates are

$$q_{(k)} = \frac{q_0\omega^2 P_{(k)}}{\sqrt{(\omega_{(k)}^2 - \omega^2)^2 + 4\beta^2\omega_{(k)}^2\omega^2}} \doteq \frac{q_0 P_{(k)}}{\left(\frac{\omega_{(k)}}{\omega}\right)^2 - 1} \quad /9/$$

in the near vicinity of resonance

$$q_{(k)} = \frac{q_0 P_{(k)}}{2\beta} \quad /10/$$

This result means that the effect of the movement of the support on the structure can be replaced by the effect of loading, proportionate with the static deflection curve due to the given displacement. The solution itself can be effected using modal analysis, and the resulting amplitude is superimposed to the original static deflection line. For little damped structures in /6/ one term prevails and for the resulting amplitude can be written

$$v(x) = v_0(x) + q_0 p_{(j)} : 2 \beta \quad /11/$$

### Numerical example

Let us determine the amplitude of vibrations of a beam clamped on both ends, whose lower end moves harmonically  $v_a(t) = 1 \sin \omega t$ . Natural frequencies of a clamped beam are

$$\omega_{(j)} = \lambda_{(j)}^2 \sqrt{EJ : \mu l^2}$$

where  $\lambda_{(j)} = 4.730, 7.853, 10.996, 14.137, \dots$

The corresponding natural modes are

$$v_{(j)}(x) = (\operatorname{sh} \lambda - \sin \lambda)(\operatorname{ch} \lambda x : l - \cos \lambda x : l) - (\operatorname{ch} \lambda - \cos \lambda)(\operatorname{sh} \lambda x : l - \sin \lambda x : l)$$

The static bending line for  $v_a = 1$  is

$$v_0(x) = 2 x^3 : l^3 - 3 x^2 : l^2 + 1, \quad q_0 = 1$$

The amplitude of the beam at the frequency  $\omega = 4.50^2 \sqrt{EJ : \mu l^2}$  is described by generalised coordinates determined according to /9/, in this particular case neglecting the damping, viz.

$$q_{(j)} = 2.989, 0.0464, 0.00791, 0.00222, 0.000803, \dots$$

The excitation frequency  $7.60^2 \sqrt{EJ : \mu l^2}$  gives the coordinates

$$q_{(j)} = -0.7762, 2.739, 0.0811, 0.0195, \dots$$

An exact solution of the same example, obtained from a general equation

$$v(x) = C_1 \operatorname{ch} \lambda x : l + C_2 \operatorname{sh} \lambda x : l + C_3 \cos \lambda x : l + C_4 \sin \lambda x : l$$

with boundary conditions

$$x = 0 : v = 1, v' = 0 \quad x = l : v = 0, v' = 0$$

yields the results whose graphic representation does not differ.

## 4. EFFECT OF THE CHANGE OF SUPPORT DISTANCE

A change of the distance between the foundation of the shaft and that of the cable can occur either by gradual displacing of the equilibrium position during seismic vibrations, or suddenly with a geological disturbance between both foundations. Further on the time-history of this displacement is not considered. It is only

assumed that this change is not so sudden as to produce impact phenomena in the cable. The method of solution used is analogous with that used in [4].

Let us consider one support of a mast, consisting of a windward and leeward cables /see scheme on Fig.3, notation according to Fig.1/. The foundation of the leeward guy has been moved from the shaft by  $\Delta l$ : the leeward guy is stretched, its sag is reduced and the support will displace in the same direction. This displacement reduces again the force in the leeward guy and increases the force in the windward one. If the mast is statically determined, this displacement will continue untill both forces are equal which will occur obviously with the displacement  $u = \Delta l : 2$ .

If the mast is statically indeterminate, the displacement of the support causes the deformation of the shaft and consequently the plastic or elastoplastic reaction depending on the magnitude of the displacement. The new equilibrium position is determined by the condition that the force in the windward guy and the reaction of the deformed shaft may equalize the force in leeward cable. If the displacement of the guy foundation proceeds in a non-negligible velocity, the displacement of the support will continue by inertia beyond the equilibrium position so far, until the kinetic energy in this equilibrium position is annuled by a further deformation of guys and shaft. The process is then repeated giving rise to vibrations, which will be obviously soon damped. The mast with 3 guys in one level can be solved similarly: instead of 2 windward guys one identical guy can be considered, its end displacement is, however, only  $1/2$  of the displacement of the support. The shortening of the distance  $l$  will manifest itself by the reduction of the force in leeward guy and the support will be drawn towards the windward guy. This effect will probably be less dangerous, the solution would be similar.

The displacement of the support  $u$  brings about in the windward and leeward cables the forces related as follows

$$u = \frac{l}{\cos^2 \alpha} \left[ \frac{(\mu g l)^2}{24} \left( \frac{1}{S_{ow}^2} - \frac{1}{S_w^2} \right) + \frac{S_w - S_{ow}}{EA} \right] \quad /12/$$

$$u = \frac{l}{\cos^2 \alpha} \left[ \frac{(\mu g l)^2}{24} \left( \frac{1}{S_l^2} - \frac{1}{S_{ol}^2} \right) + \frac{S_{ol} - S_l}{EA} \right] \quad /13/$$

where  $\mu g$  - weight of unit length of the guy

$EA$  - tensile stiffness of the guy

$S_{ow}$ ,  $S_{ol}$  - initial forces in windward, leeward guys

$S_w$ ,  $S_l$  - forces in the guys at the displacement  $u$

In original equilibrium position  $S_{ow} = S_{ol} = S_o$ .

Owing to the displacement of the foundation of the leeward guy in leeward guy  $S_o$  changes into  $S_{ol}$ , for which holds /13/ with

$$u = -\Delta l, \quad S_{ol} = S_o, \quad S_l = S_{ol}$$

Using dimensionless expression

$$\psi = \frac{\mu g l}{S_o} \quad ; \quad \varphi = \frac{EA}{S_o} \quad ; \quad x = \frac{S_{ol}}{S_o} \quad ; \quad \lambda = \frac{\Delta l}{l} \cos^2 \alpha$$

/13/ can be rewritten

$$x^3 + x^2 \left( \frac{\psi^2 \varphi}{24} - 1 - \varphi \lambda \right) - \frac{\psi^2 \varphi}{24} = 0 \quad /14/$$

and consequently

$$x_l^3 + x_l^2 \left( \varphi \varepsilon + \frac{\psi^2 \varphi}{24 x^2} - x \right) - \frac{\psi^2 \varphi}{24} = 0 \quad /15/$$

Similarly for the force in windward cable from /12/ holds

$$x_w^3 + x_w^2 \left( \frac{\psi^2 \varphi}{24} - \varphi \varepsilon - 1 \right) - \frac{\psi^2 \varphi}{24} = 0 \quad /16/$$

In these expressions has been further introduced

$$x_l = \frac{S_l}{S_{ol}} = \frac{S_l}{x S_o} \quad ; \quad x_w = \frac{S_w}{S_{ow}} = \frac{S_w}{S_o} \quad ; \quad \varepsilon = \frac{u \cos^2 \alpha}{l}$$

Solving /15/ and /16/ the reaction of the support can be obtained

$$R = (S_l - S_w) \cos \alpha$$

or

$$S = x_l - x_w \quad ; \quad S = \frac{R}{S_o \cos \alpha} \quad /17/$$

An example of the calculated relation between the reaction  $R$  and displacement  $u$  of the support for various initial foundation shift  $\Delta l$  is shown in Fig.3.

For the analysis of stresses in the mast it is necessary to determine, apart from the force of the support  $R(u)$ , also the reaction of the shaft to the displacement of the support under consideration  $P(u)$ . It means to solve the mast without this support, loaded in this place by a horizontal force of various magnitudes. Obviously, this relation will have to be solved even beyond the yield limit considering the formation of plastic hin-



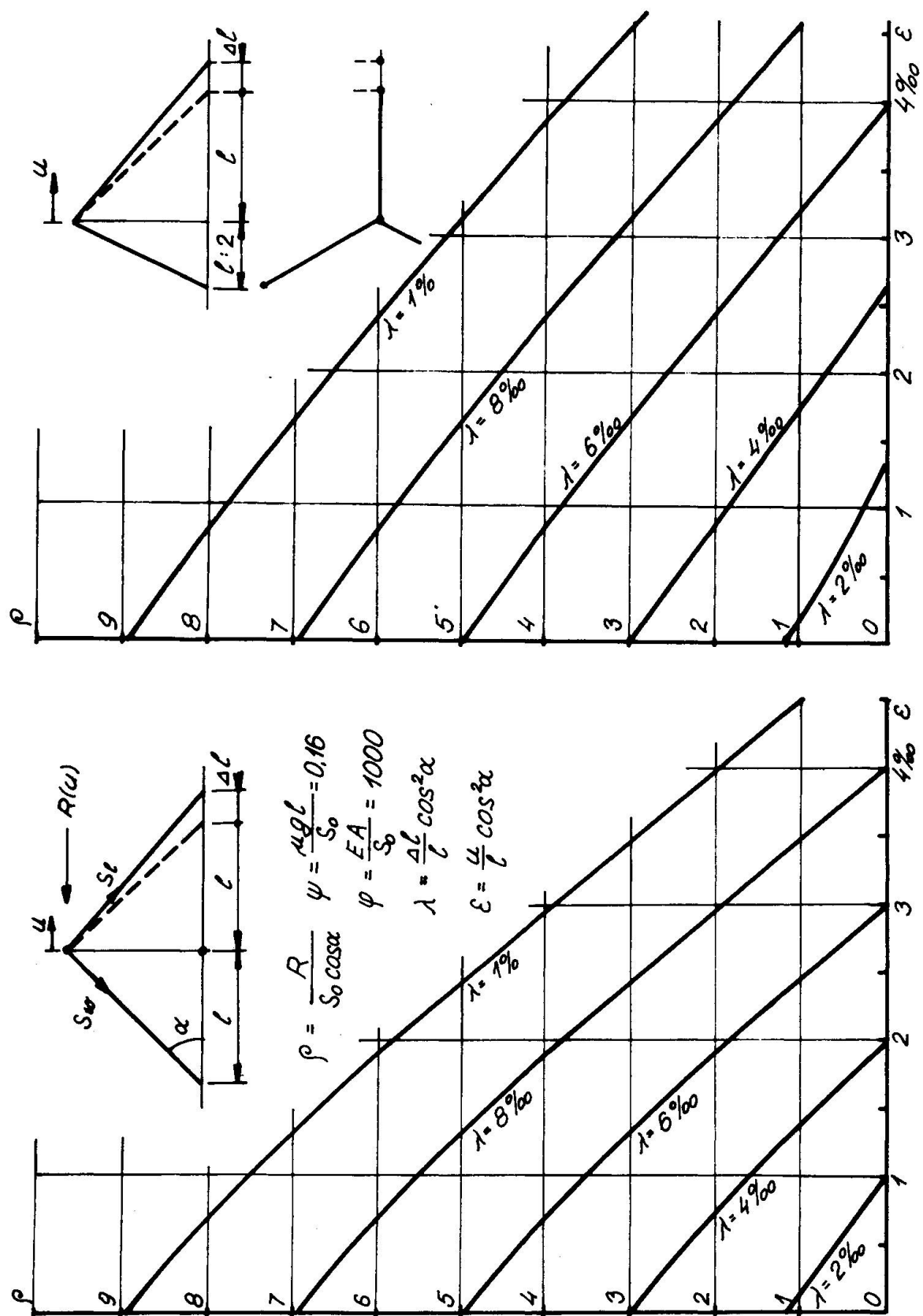


**Fig. 3** Support reaction and displacement for different shifts of the guy foundation block

ges and the possibilities of mast failure. Both these relations will be plotted in one diagram /Fig.4/. At the point of intersection of both lines there lies the new equilibrium position of the support. The extreme displacement of the support is given by the condition of equal aereas between both lines before and beyond the equilibrium position. From the position of these points on the curve  $P(u)$  the danger of failure or the extent of damage can be judged.

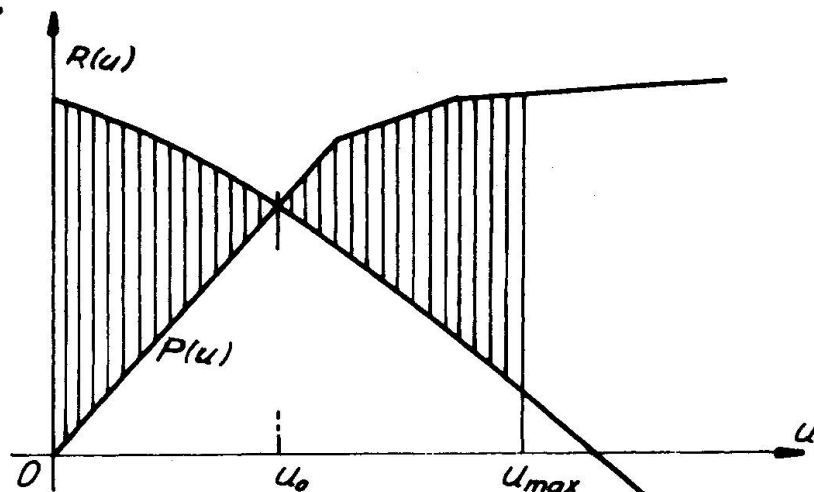


Fig. 4 Guy support force and restoring force of the mast

## 5. CONCLUSION

Generally small seismic effect can be expected from guyed masts, nevertheless vibrations of the shaft in some higher mode can occur. The solution of such a case must be carried out exactly, since a simplified approach can hardly find higher modes. In bad geological conditions the effect of the change of mutual position of foundations should be assessed.

## REFERENCES

1. Koloušek, V.: Dynamics in Engineering Structures. Butterwords London, Academia Praha, 1973
2. Koloušek, V.: Solution statique et dynamique de pylones d'antenne. Mémoires AIPC V, Zurich 1947
3. Davenport, A.G, Steels, G.N.: Dynamic behaviour of massive guy cables. Proc. ASCE, ST 2, April 1965, p. 44 - 70.
4. Fischer, O.: Effect of rope failure on a guyed mast. Proc. conf. IASS-Cable structures, Bratislava 1975, p.282 -288.

## EARTHQUAKE-RESISTANT DESIGN OF SUBMERGED TUNNELS

## L'ÉTUDE ANTI-SISMIQUE D'UN TUNNEL IMMERGÉ

## DIE ERDBEBENBESTÄNDIGKEIT ABGESENKTER TUNNEL

by

S. Okamoto

President, University of Saitama

Professor Emeritus, University of Tokyo

Japan

C. Tamura

Professor, Institute of Industrial Science

University of Tokyo

Japan

## SUMMARY

It is shown from the results of earthquake observations and model vibration tests of submerged tunnels that deformations of such tunnels during earthquakes are governed by the deformation of ground. The features of earthquake resistance of submerged tunnels are described and the concept serving as the basis for earthquake-resistant design, points to be kept in mind in designing, and examples are given.

## RÉSUMÉ

D'après les résultats de l'observation de tremblements de terre et d'essais de modèles de vibrations sur des tunnels immergés, il est apparu clairement que le comportement d'un tunnel de ce type pendant les tremblements de terre est principalement fondé sur la déformation du terrain selon l'axe du tunnel. Les caractéristiques de la résistance de tels tunnels aux tremblements de terre, le concept fondamental d'une structure résistante aux tremblements de terre pour de tels tunnels, et les considérations faites au sujet de leur structure sont décrites.

## ZUSAMMENFASSUNG

Auf der Grundlage von Erdbebenbeobachtungen und Vibrationsmodellversuchen an abgesenkten Tunneln wurde festgestellt, daß das Verhalten eines solchen Tunnels im Verlauf von Erdbeben hauptsächlich durch eine Verformung des Bodens entlang der Tunnelachse bestimmt wird. Der Inhalt befaßt sich weiterhin mit der Charakteristik abgesenkter Tunnel in Bezug auf Erdbebenbeständigkeit, dem Grundkonzept einer erdbebenbeständigen Konstruktion für solche Tunnel und Punkte, die bei deren Konstruktion berücksichtigt werden müssen.

## 1. INTRODUCTION

Due to the earthquake situation of Japan there has been much concern regarding earthquake resistance of submerged tunnels and studies of this matter have been continued and earthquake-resistant design standards have been established. Recently, submerged tunnels as listed in Table 1 including those under construction have come to be built, mainly as major traffic facilities. In this paper, the behaviors of submerged tunnels during earthquake, their structural features, and methods of response analysis will be described.

## 2. FEATURES OF SUBMERGED TUNNELS SEEN FROM ASPECT OF EARTHQUAKE RESISTANCE

Seen from a structural standpoint a submerged tunnel is comprised of the so-called submerged tunnel, approaches, shafts and ventilation towers. These sections, respectively, have the characteristics described below.

2.1 Submerged Tunnel This is a tubular structure of large cross section usually buried in soft ground at the bottom of water or below the ground water line. Therefore, the stability of the ground during earthquake is an essential condition for earthquake resistance of the tunnel, and the interaction of the ground and the tunnel becomes a fundamental matter. It may be anticipated that there will be portions produced in the tunnel walls which are in stress conditions of more or less pure compression or pure tension. Since concrete is generally used as the principal material, it will be necessary for these stress conditions to be watched.

2.2 Approach This is a section from the submerged tunnel section to the surface which usually is of tunnel or open channel structure, or a combination of both. Examinations of these structures are normally by the seismic coefficient method.

2.3 Shaft, Ventilation Tower These are vertical structures provided at the tunnel portion with the main purposes of construction of the tunnel and ventilation, with some towers rising as high as 40 m above the ground surface. In connection with the tunnel, these structures frequently comprise a part of the tunnel. The behaviors are considered to be similar to those of buildings in general and earthquake-resistant design is being done by the seismic coefficient method.

Tunnels of this type are structures connecting parts such as the above which have differing dynamic properties. Consequently, the manner in which these structural parts which indicate divergent behaviors during earthquake are connected is an important problem of earthquake resistance of the structure. In order to solve this problem, it is necessary not only for the behaviors of the ground and the various structural parts during earthquake, but also behaviors during normal times such as uneven settlement of the ground to be known.

Evaluation of earthquake resistance is carried out not only from the viewpoint of structural dynamics, but also based on various factors such as type, function, importance, scale, etc. of the structure. When cases of these long structures built at the bottom of water and moreover in the ground being used as major traffic routes are visualized, it is necessary for special considerations to be given to functioning of safety facilities such as fire extinguishing and water drainage in case of emergencies, and securing of sureness of action during emergencies. Since this will also influence the structure itself, investigations and examinations will be necessary from the planning stage.

The above indicates features regarding the earthquake resistance of submerged tunnels.

### 3. BEHAVIORS OF SUBMERGED TUNNELS DURING EARTHQUAKE

3.1 Earthquake Damage to Tunnel Submerged tunnels have not yet experienced major earthquakes, and thus, there is an important significance with respect to determining earthquake resistance in knowing the behaviors and the kinds of damage suffered when similar structures are subjected to strong earthquake motions.

In general, earthquake damage to mountain tunnels is restricted to limited portions at epicentral areas with damage conditions being comparatively constant, and with most of the damage occurring at portals or their vicinities, while at middle portions of tunnels where the geology is generally good, damage is small. When there has been damage at the middle portions of tunnels, that this was due to the poor conditions of the ground at the location of the damage can be pointed out from cases during the Kanto Earthquake, Kitamino Earthquake and the Niigata Earthquake. This indicates that the conditions of the ground around the tunnel exert a great influence on the tunnel. It has been reported that the conditions of the natural grounds of damaged tunnels at relatively long distances from epicenters were all poor.

Komine Tunnel on the Atami Line (present Tokaido Main Line) is an example of damage of a tunnel in soft ground. At this tunnel, the portion 184 ft from one of the portals had retaining walls built on excavating ground consisting of red clay by open cut, with reinforced concrete girders crossed over to provide a cover for a backfilled structure, a structure extremely different from the case of an ordinary mountain tunnel. This open-cut section crumbled, but going in further toward the Atami side, the geology became better and there was almost no damage. This damage is considered to have been caused due to the structure having been in soft ground with little coverage so that structurally the earth pressure during earthquake could not be resisted.

At the time of the Niigata Earthquake ( $M = 7.5$ ), the city of Niigata at a distance approximately 40 km from the epicenter suffered extreme damage with liquefaction of the ground as the main cause. Near Niigata Station there was jetting of soil at the surface of the ground. An underground passageway at this station was a reinforced concrete structure of a box cross section supported by foundation piles and the cross section itself was not damaged at the time of the earthquake, but misalignment and rotation occurred at joints in the longitudinal direction so that the surface of the bottom slab became uneven and ground water entered the tunnel from the joints.

The examples of damage described above indicate that for tunnels in soft ground both earthquake resistance of the transverse cross section and earthquake resistance in the longitudinal direction must be considered in structural design.

Since submerged tunnels are buried near the surface of soft ground, these examples of damage serve as valuable references, but because water pressure comprises a great part of the load, the transverse cross section is made strong in design in any event, and the structure and strength in the axial direction will consequently become subjected to serious consideration.

3.2 Earthquake Observations The behaviors of submerged tunnels buried in soft ground will be described based on the results of several earthquake

observations. As far as the authors know, earthquake observations are being carried out at the submerged tunnels of Haneda, Kinuura Port, Tokyo Port and Ohgishima. The items of measurement do not necessarily coincide, but acceleration, strains and displacements of tunnel walls are main, besides which there are reinforcing bar stress transducers and joint meters installed. There are also cases of accelerometers installed at the ground surface and in the ground in connection with the behaviors of the structures. The following discussion is centered around earthquake observations on Haneda Submerged Tunnel (Japanese National Railways) which have been going on since 1970.

3.2.1 Haneda Submerged Tunnel This tunnel extends from a point at the left bank of the Tama River somewhat upstream from the entrance to Haneda Airport, crossing the river in a slight arc convex in the upstream direction to reach the Kawasaki side, and the length of the submerged tube part is 480 m. The tube is composed of 6 reinforced concrete elements of oval-shaped cross section each having a length of 80 m, height of approximately 8 m, and width of approximately 13 m with corrosion-proofed steel plates 6 mm in thickness forming an outer shell. These elements will be tentatively numbered herein as 1, 2, ..., 6 in order from the Kawasaki side.

With respect to the ground, a soft alluvial layer of about 40 m at the middle of the river and 10 and several meters at the Kawasaki side cover the well-compacted so-called Tokyo Sand-Gravel Stratum. The predominant frequencies of the ground obtained from microtremor observations were 0.23 to 0.33 Hz, 0.5 to 0.79 Hz, and 0.9 to 1.1 Hz. As observation instruments two accelerometers each were installed at Element No. 2 and No. 4, while four strain meters each were provided to measure strains of side walls in the axial direction.

From April 1970 until the present it has been possible to record more than 30 earthquakes where strains and accelerations were of extents considered to be significant for analyses. Fig. 1 shows a portion of the record for an earthquake of  $M = 7.3$  which occurred east of Hachijo Island on December 4, 1972 in which the maximum strain for all earthquakes up to the present was recorded. In this figure, No. 4 TSA is the horizontal acceleration in the direction orthogonal to the tunnel axis observed at Element No. 4, while Nos. 5 to 8 are strains in the direction of the tunnel axis recorded at the tunnel walls. Although measurements of strain were made at two points 50 m apart, that the strain waveforms are very closely similar, and moreover, that there is practically no phase differential, that the predominant frequency of the strain waveform agrees well with the low-order predominant frequency, and that predominant vibrations of approximately 7 sec are seen at the end of the record, are prominent features.

Fig. 2 is the record of an earthquake of  $M = 4.9$  and epicentral distance of 17 km which occurred at the northern part of Tokyo Bay on March 27, 1973. Compared with Fig. 1, vibration components of short periods are predominant in the acceleration waveforms indicated by TAA and TSA from which it is seen that strains in the direction of the tunnel axis are extremely small for the degree of acceleration.

Fig. 3 illustrates maximum acceleration and maximum strain by earthquake. The greater part of the measurement results are contained between two roughly parallel straight lines and the two lines are surmised to represent the upper and lower limits. The points in the vicinity of the lower limit line are for cases of earthquakes in which the magnitudes were small (5.1 and under) and the epicentral distances were short, and vibration components of relatively short periods of 2 to 3 Hz or more are predominant. The points near the upper limit line are for cases with practically no vibration components of relatively



short periods as mentioned above, and vibration components of periods of 1 to 2 sec or longer are predominant where large strains are produced considering the degree of acceleration. It is important that for the same maximum acceleration sizes of strains varied as much as 15 to 20 times, and this can be considered as representative of the frequency response properties of tunnel strains against acceleration. At the upper limit line the strains were  $1.5$  to  $2.0 \times 10^{-6}$  per gal, while at the lower limit line they were about  $0.1$  to  $0.15 \times 10^{-6}$ .

Fig. 4 indicates the relation between maximum strain and epicentral distance with magnitude as the parameter. When magnitude is at a constant level, it is seen that the degree of reduction in maximum strain with increase in epicentral distance is extremely small compared with the maximum acceleration of earthquake motion, and that there is not very much reduction according to distance. It is thought this is because the low-order predominant period of the ground is long and earthquake motion components having this period are not decreased very much by the increase in distance. Also, it may be considered that in the range of short epicentral distances, vibration components of short periods become relatively large in number. Based on the figure, for the range of around  $M = 5-7$ , the following experimental formula holds between maximum strain  $\epsilon_m(\mu)$  produced at this tunnel during earthquake, and magnitude  $M$  and epicentral distance  $\Delta$  (km):

$$\log_{10} \epsilon_m = 0.7M - \frac{\Delta}{450} - 3.2$$

Figs. 5 and 6 are power spectra of strain waveforms and acceleration waveforms for 107.8 sec of the initial part (indicated by (a) in the figure) and the part between 56 and 80 sec (indicated by (b) in the figure) of maximums in the earthquake record of Fig. 1. Although the relative size of the extreme maximum value for each frequency varies, it may be seen that both are predominant at roughly identical frequency portions. In cases of earthquakes of around  $M = 6-7$ , vibrations of about 0.3 Hz do not appear very prominently, and vibrations of about 0.5 to 1 Hz are predominant.

When taking into account also that the frequencies of predominant vibrations at this observation site determined from microtremor observations are at relatively low levels such as 0.23 to 0.33 Hz, 0.5 to 0.79 Hz, 0.9 to 1.1 Hz, and 1.3 to 1.4 Hz as previously mentioned, it may be considered that the vibrations predominant in the acceleration record and the strain waveforms during earthquake are vibrations of the ground. When strain records and acceleration records are compared, that the sizes of strain and acceleration are not directly related can be seen from the records of the two in Fig. 1, and rather, the spectrum of strain is similar to the form of the spectrum of displacement converted from the spectrum of acceleration. Also, it may be seen that when strain records are viewed from an overall standpoint there is geometrically great similarity. This is especially distinct in cases of earthquakes of comparatively large magnitudes (indicating magnitudes of about 6 or higher).

Fig. 7 indicates the strains produced in the tunnel in the axial direction and due to bending deformation calculated from strain records of the right and left walls. The strains due to axial-direction deformation had vibration components of long periods, and those due to bending deformation were vibrations of relatively equal periods. Power spectra regarding these are also given in the figure. As for the sizes of strains due to axial-direction deformations, they were approximately quadruple the strains due to bending deformation, and it is necessary to pay attention to the fact that the width of the tunnel is 13 m. Further, regarding the phase differentials between recorded waveforms for measurement points 205 m apart, there were practically no cases of axial-



direction deformations, with only slight amounts seen to occur in cases of bending deformation.

3.2.2 Kinuura Port Tunnel Kinuura Port Underwater Tunnel which was opened in 1973 has a submerged tunnel section of a length of 480 m comprised of 6 elements of reinforced concrete box cross sections of height of 7.13 m and width of 15.6 m. The soil conditions differ somewhat for the two sides, with down to -5 m from the ground surface being considerably soft fill, and below -18 m consisting of diluvial sand-gravel and sand layers, but at the intermediate silty clay, the negative side was a hard clay layer of N-value 9 to 13 and the other side a soft clay layer. Observations are being made by the Port and Harbor Research Institute of the Ministry of Transport, and the instruments used for observations are 19 accelerometers at vertical shafts and submerged elements, one displacement meter at the middle of the submerged tunnel, and strain meters in couples right and left at three cross sections for a total of six, and four reinforcing bars stress transducers each at the submerged elements and vertical shafts.

Fig. 8 gives the acceleration records in the direction perpendicular to the tunnel axis obtained at the ground surface and the land tunnel parts in case of an earthquake of epicentral distance of 185 km, depth of 60 km and  $M = 5.8$ . Further, from the records of accelerometers and reinforcing bar stress transducers, it was judged that the submerged tunnel does not behave uniformly as a whole, but shows complex behaviors in connection with the vibration properties of the surrounding ground.

For earthquakes of magnitudes of 5.3 and 4.9 and epicentral distances of 30 km and 50 km, respectively, short-period components were predominant and it was found that the ground and the submerged tunnel did not show behavior as one.

3.3 Vibration Model Experiments In investigating the behavior during earthquake of this type of tunnel the authors conducted model experiments with the objectives of grasping principle-wise the behaviors of the ground and the tunnel which are basic and the interactions thereof.

The experiment generally carried out consists of making a three-dimensional model of a fairly broad area on a shaking table using a material of low Young's modulus in which the tunnel model is buried, and applying vibrations. It appears there is no other way of showing in an experimentally measurable range that self-vibrations of surface layer ground are predominant in a strong earthquake. As for experiments in the elastic range, it is easier by this method to improve reproducibility and accuracy of the experiments, and this method is rather of advantage for the objective.

Fig. 9 shows the case of a model vibration experiment conducted by the authors, the model being 2.2 m in length and 0.8 m in width. The material for the ground was gelatin, while the tunnel was made of silicone rubber. The so-called bedrock was made horizontal, and of the length of 2.2 m, the two end portions had surface layer ground which was thick and after passing sloped sections the middle had a uniformly thin surface layer ground. This model, because of the limitations in performance of the shaking table, was subjected to sinusoidal vibrations in the one direction of horizontal (either axial direction or direction orthogonal to axis). Since the model tunnel was made of silicone rubber and there is no suitable gage for dynamically measuring strains of the model tunnel available at present, measurement of displacement was substituted.

The fundamental matters clarified by the model experiments may be summarized

as follows:

- When grounds having differing self-vibrations are adjacent, the range in which there is interaction is comparatively small and effect is limited to the adjoining area and its vicinity. However, in case of high-order vibrations the influence is seen over a relatively wide area.
- The tunnel vibrates at the frequency of the vibrations of the ground and deforms in correspondence with deformation of the ground. Consequently, the tunnel may be considered as a massless beam connected to the ground.
- A submerged tunnel shows bending deformation and expansion deformation.
- Shaft and ventilation tower portions show rocking motions.

Considered together with phenomena observed in similar experiments carried out separately, the following were also clarified:

- When subjected to vibrations at waveforms of real earthquakes low-order natural vibrations are seen to be extremely predominant in vibrations of the surface layer ground.
- When two kinds of ground having greatly differing natural frequencies adjoin each other through a sloped section, each ground vibrates with its own natural vibration, the vibrating states vary at the slope, and a large section force is produced in the tunnel at this part.
- In relation to the gradient of the slope, intermediate vibrations between the natural vibrations of the grounds at the two sides are seen to be predominant, and there are cases when phases become divergent along the axial line.
- Since displacement of ground directly related to displacement of the tunnel is displacement of the ground at the tunnel location, the distribution of displacement of the ground in the direction of depth must also be considered.
- Since the stiffness of the tunnel against deformation in the axial direction of the tunnel is extremely great compared with that of the ground in which it is buried, when the wave length of the displacement of the ground measured along the axial line is relatively short, it is difficult for the tunnel to deform in accordance with deformation of the ground. Consequently, the behavior of the tunnel is determined by the distribution of dynamic characteristics of the ground on the axial line of the tunnel for a relatively long section. Accordingly, when there are local variations in the state of vibration of the ground, the movement of the tunnel will not necessarily be the same as for the ground in some cases.
- With respect to a direction perpendicular to the tunnel axis, since the tunnel is more easily deformed than in the above case, the deformation of the ground is more easily followed.
- Since shaft and ventilation tower portions generally have great rigidities against bending deformation, they vibrate in accordance with the distribution of displacement of the ground in the direction of depth and rocking vibrations are produced.
- By adopting a joining method allowing movement at the joints of shafts and ventilation towers with the tunnel it will be possible to alleviate large

local stresses produced at the joints,

Besides experiments of this type, the authors have conducted vibration experiments burying tubular bodies in actual ground. These experiments, when seen from the standpoint of similarity, may be said to comprise vibration tests of the actual tubular bodies buried. In these experiments, long steel pipes or vinyl pipes of relatively large diameters were buried near the ground surface, and vibrations were produced by a special S-wave generating apparatus or by explosions and impact, and displacements of the pipes and ground, accelerations, and strains were measured. As a result, it was learned that the tubular bodies often vibrated in the same manner as the ground. In these experiments, there were cases when vibrations of the tubular bodies were induced, although very slightly, by impact.

#### 4. INTERACTION OF GROUND AND TUNNEL

Regarding the interaction between the ground and tunnel, it was learned from earthquake observations and experimental studies that the behavior of a tunnel during earthquake can be considered as that of a beam (or a pipe) of which mass can be neglected connected to the ground by a spring — not necessarily a linear spring. When the shear deformation of the tunnel is ignored the following equations hold true for deformations of the beam,

##### Deformation in Axial Direction of Tunnel

$$EA \frac{d^2 u}{dx^2} - K_x u = -K_x u_G$$

##### Deformation in Direction Orthogonal to Tunnel Axis

$$EI \frac{d^4 v}{dx^4} + K_y v = K_y v_G$$

where

- $A$  : cross-sectional area of tunnel
- $E$  : Young's modulus of tunnel material
- $I$  : geometrical moment of inertia of tunnel cross section
- $K_x, K_y$  : spring constants of springs connecting tunnel and ground for displacements in axial direction and direction orthogonal to axis of tunnel.
- $u, u_G$  : displacements in axial direction of tunnel of tunnel and ground, respectively.
- $v, v_G$  : displacements in direction orthogonal to tunnel axis of tunnel and ground, respectively.

In order to investigate the response of the tunnel to deformation of the ground, letting  $u_G$  and  $v_G$  be

$$a \cos \frac{2\pi x}{\lambda}$$

and obtaining the solutions to the above equations, they will respectively be

$$u = \frac{\beta_x^2}{\left(\frac{2\pi}{\lambda}\right)^2 + \beta_x^2} a \cos \frac{2\pi x}{\lambda}$$

$$v = \frac{\beta_x^4}{\left(\frac{2\pi}{\lambda}\right)^4 + \beta_x^2} a \cos \frac{2\pi x}{\lambda}$$

and the axial strains ( $\epsilon_x$ ) or fiber strains ( $\epsilon_y$ ) of the tunnel against  $u$  and  $v$  may be expressed by the following equations, respectively:

$$\epsilon_x = \frac{du}{dx} = - \frac{\beta_x^2 \cdot \frac{2\pi}{\lambda}}{\left(\frac{2\pi}{\lambda}\right)^2 + \beta_x^2} a \sin \frac{2\pi}{\lambda} x$$

$$\epsilon_y = r_0 \frac{d^2 v}{dx^2} = - \frac{\beta_y^4 \left(\frac{2\pi}{\lambda}\right)^2}{\left(\frac{2\pi}{\lambda}\right)^4 + \beta_y^4} \cdot \gamma \cdot a \cos \frac{2\pi}{\lambda} x$$

However,

$$\beta_x^2 = \frac{K_x}{EA}, \quad \beta_y^4 = \frac{K_y}{EI}$$

$r, r_0$  : distance measured from neutral axis of tunnel and edge distance

The value of  $|\epsilon_x|$  is a maximum at  $\lambda = 2\pi/\beta_x$  and

$$|\epsilon_x|_{\max} = \beta_x/2$$

The value of  $|\epsilon_y|$  indicates a maximum at  $\lambda = 2\pi/\beta_y$ , and with  $r = r_0$ , becomes

$$|\epsilon_y|_{\max} = r_0 \beta_y^2/2$$

Fig. 10 indicates the relation between strain in the axial direction of the tunnel and the wave length of the ground for  $\beta_x$  and  $\beta_y$ .

In general, since  $\beta_x < \beta_y$ , the wave length which indicates the maximum value of strain due to axial-direction deformation is several times the wave length for bending deformation, and therefore, it is seen to be preeminent at the portion where wave length is long compared with the case of bending deformation, and moreover, preeminent at a wave length realm of fairly wide range. From this, in case of vibration having an amplitude spectrum which is constant, the spectrum of strain produced at the side wall of the tunnel will have a realm of wave length predominant for the direction of bending deformation which differs from the realm of wave length predominant for axial deformation.

## 5. BASIC THINKING IN EARTHQUAKE-RESISTANT DESIGN

As previously stated, since a submerged tunnel is a structure of a new type which shows behavior during earthquake which differs from that of a structure on land, in order for rational earthquake-resistant design to be made, it is necessary to establish the manner of thinking and method of design based on the behavior. For this purpose, the Japan Society of Civil Engineers organized a committee to study earthquake resistance of submerged tunnels with deliberations commenced in 1971, and in 1975 completed "Specifications for Earthquake Resistant Design of Submerged Tunnels" (hereinafter to be called

"Specifications"). In this, the thinking with regard to design is described from a new viewpoint. A discussion follows below.

5.1 Earthquake for Design It has been clarified that the earthquake resistance of a submerged tunnel is closely related to the ground in which it is buried.

In major earthquakes of the past failures and damage have occurred over wide areas at alluvial ground, and even in medium-scale earthquakes, as seen in the case of the Fukui Earthquake, there was failure of the ground at the epicentral area. And as previously described, it was learned that when the period of the low-order predominant vibration of the ground is 1 sec or longer, strains in the axial direction produced in the tunnel walls during earthquake will not be reduced as much even when epicentral distance is increased, and that rather, it is the magnitude of the earthquake which greatly influences strains. For these reasons, it is necessary to consider earthquakes occurring in a comparatively wide area as earthquakes to be considered for earthquake-resistant design. In the Specifications, it is proposed to estimate the frequency of earthquake occurrence in an area with a radius of 200 km with the construction site as the center based on earthquake records from the beginning of history and using the formula of ISHIMOTO-IIDA. The scales of earthquakes and their number occurring during a given period in the future is to be estimated by this means. The earthquakes and their scales which are frequently used for dynamic analyses of submerged tunnels in the vicinity of Tokyo are great earthquakes of magnitudes of around 8 belonging to the Outer Seismic Zone and earthquakes of magnitudes about 7 occurring at close distances. Further, it is stipulated in the Specifications that earthquake observations are to be carried out in order to know beforehand the natures of ground motions at the tunnel site as a safety measure for the submerged tunnel.

5.2 Stability of Ground The examinations of stability of ground during earthquake presently being made may be broadly divided into examinations of the stability of slopes and examinations of liquefaction of sandy ground. In both cases, the problems are difficult ones where earthquake motion, topography, geology and ground structure are inter-related and many investigations and research works are now in progress in this regard. For a submerged tunnel, even in case of a cohesive soil which does not easily liquefy, the displacement of the ground during earthquake must not be so large that damage is inflicted on the tunnel, and care must be exercised that reduction in bearing power will not be extreme to produce trouble with respect to earthquake resistance.

This problem may be split along the lines of stability of ground in a comparatively wide area at the tunnel site and stability of ground in the immediate surroundings of the tunnel. Care will be required since there will be cases of the measures against earthquake differing according to the above.

In order to examine the earthquake resistance of the structure and stability of ground in relation with the ground and soil properties, it is necessary besides various static and dynamic laboratory tests using samples, for various measurements to be made with boreholes such as speed of seismic waves and velocity of seismic waves, and seismic prospecting to be carried out. The Specifications cite the following as investigations and tests to be implemented:

- Boring and sounding (standard penetration tests)
- Sampling and laboratory tests of samples
- Measurement of seismic wave velocities with boreholes
- Measurement of density of soils



#### - Microtremor observation

There are times when the values obtained from a plural number of such tests and investigations on the same dynamical quantity will not coincide. This is because differences are produced depending on strain level, method of testing and process of testing. This is especially so with the results of dynamic testing, and in case of evaluation in relation to earthquake resistance there are numerous difficult problems. Although it cannot be said that under the present circumstances a method of evaluation has been firmly established, the information will be of importance when making an engineering judgment of stability.

With regard to stability of ground the sliding plane method is customarily used for slopes. In the Specifications, it is stipulated that even for horizontal ground a horizontal sliding plane is to be assumed in the ground and sliding of the plane evaluated through application of the seismic coefficient method. It is proposed that in certain cases the surface layer should be made equivalent to a shear vibration model having one-degree-of-freedom plastic spring characteristics to make earthquake response calculations for examination of displacement of ground.

Concerning liquefaction, ground consisting mainly of sand of uniform grain size which is not well compacted is considered as being a problem. As methods of examining stability, there are methods from the aspect of stress such as the one in which stress conditions during earthquake are assumed and testing is done reproducing the stress conditions in the sample, and the one in which loads of stationary waveforms and real earthquake waveforms are applied, while there are also methods from the aspects mainly of condition of ground and material such as N-value and grain-size distribution. Studies related to liquefaction are now in active progress and the phenomenon is gradually coming to be clarified, but there is still necessity for examination, and the Specifications take the stand that stability of the ground is to be judged from grain-size distribution, N-value, and maximum acceleration of ground carrying out dynamic tests on soil and grasping the properties of the soil during earthquakes. Depending on the results it may become necessary for foundation improvement, rerouting and structural changes to be made.

The stability during earthquake of soil backfilled around the tunnel is also of importance. Complex stress conditions are produced in the surrounding ground of the tunnel during earthquake. Care must be exercised since large plastic deformation and liquefaction of the surrounding ground will be the causes of instability, uneven settlement and upheaval of the tunnel.

5.3 Basic Concept of Earthquake-Resistant Design As previously mentioned, since a submerged tunnel possesses a number of distinct features, there are areas in the method of earthquake-resistant design which differ from those for structures of other types. The essentials of the basic principles given in the Specifications will therefore be listed below.

- Consideration is given for earthquake resistance of the total structural system including the topography and geology of the construction site.

- In carrying out earthquake-resistant design for the various parts of the tunnel, the displacement of ground during earthquake or the design seismic coefficient is to be used as the basis, while for the total structural system, design and examination based on dynamic analyses are to be performed.

- For design of joints and other parts where variation in rigidity will be

prominent, the influences and effects thereof are to be examined.

- For safety measures during earthquake, considerations are to be given that control and operation of various facilities for the safety measures will be carried out with sureness.

Regarding the first point it has already be explained in outline. What should be noted with respect to the second point is that designing is to be done based on displacement of the ground, and that dynamic analyses are to be made for the total structural system. In the past, in earthquake-resistant design of ordinary structures, the basic factors had been the inertia forces of the various structural parts during earthquake, but in the case of a submerged tunnel, the displacement of the ground during earthquake is the basic factor, according to which the concept of design becomes different. Since the measure of design seismic coefficient which considers earthquake force is changed to displacement, it becomes necessary for examinations to be made of the data required and of the relation between acceleration and displacement. Further, as described previously, since a submerged tunnel comprises a structural system where structures of different properties in earthquake response are connected and made continuous, even if each of the structural parts is designed by an established method, a necessity arises for matters concerning connections and behavior as a whole to be studied. The third point has a relation to the second. Not only will the methods of connecting the various structural parts, and types and methods of joining elements greatly influence stress levels produced, but also they will have a relation with functioning of the tunnel, and therefore, it has been stipulated that examinations are to be made with special care. According to an example of analysis, for a submerged tunnel section of length of approximately 1 km, in case free displacement was permitted between the submerged tube part and a vertical shaft, relative displacement of several cm was computed to occur. In regard to the fourth point, it is directed that measures for safety during earthquake are to be implemented in addition to structural design, and that considerations are to be given to planning, structure, equipment and materials so that the safety measures will be actuated without fail during earthquake.

The above signifies that earthquake-resistant design which had been made separately for the various parts due to the characteristics of this structure is to be carried out in unified form.

5.4 Dynamic Analysis Next, an outline will be given with respect to dynamic analysis. Ventilation towers and retaining walls of approaches are designed for earthquake resistance by the conventional seismic coefficient method or the modified seismic coefficient method, and there is much experience regarding their earthquake resistances, whereas tunnels of this type have not experienced major earthquakes. Accordingly, it was decided that dynamic analyses should be made to more accurately grasp dynamic behavior of the structural system including the ground. It is proposed in the Specifications that as dynamic analyses, experimental analyses based on model vibration experiments in the laboratory be carried out in addition to earthquake response calculations. The objective is to grasp in detail and with accuracy, through organic combination of the two analyses, the behaviors during earthquake of the ground and tunnel under three-dimensional and complex ground conditions. For earthquake response analysis there are the method of determining response by a three-dimensional finite element method and the method described below which utilizes models for dynamic analysis, with the latter being generally used.

5.4.1 Models for Dynamic Analysis The authors, with the basic information as described above concerning behaviors of ground and tunnel during earthquake



obtained from earthquake observations and model experiments, have proposed dynamic analysis models which are of theoretical nature yet aim for practicality. These models, as indicated in Fig. 11, are divided into numerous segments cut by the surrounding ground of the tunnel and planes perpendicular to the tunnel axis, with each segment replaced by a one-masspoint-spring system equivalent to primary shearing vibration and with these masspoints further connected in the axial direction of the tunnel by springs, for calculating the planar displacement waveform of the ground during earthquake spring-connecting this and the tunnel to determine the deformation of the tunnel. Since the correspondence of this model with high-order vibrations is not adequate, there have been cases where response accelerations have been calculated to be fairly small, but for strains in the axial direction of the tunnel, sufficient accuracy has been obtained as there is little effect of high-order vibrations of the ground. Regarding the effect of high-order vibrations on strain, it is possible for approximate calculations to be made through improvisations of the application method of the model. However, when the state of the ground is extremely complex three-dimensionally, there may be cases arising where this model will not be adequate. On analysis by this model for the previously described vibration model experiments, results which agreed well with those of the experiments were obtained.

5.4.2 Model Vibration Experiments Gelatin and soil stabilizer of the acrylamide type were used as materials for ground in model experiments, while silicone rubber was used as the material for tunnels.

It is difficult under present circumstances to numerically analyze the earthquake response of a submerged tunnel when it is constructed at ground where topography, soil and ground composition are complex. Model vibration experiments are very effective in such cases. Models used are whole models covering wide areas including tunnels, and partial models for investigating localized behaviors. As materials for models, gelatin gel and acrylamide are used for ground, and silicone rubber materials for tunnels.

## 6. EARTHQUAKE-RESISTANT DESIGN

Since a submerged tunnel is comprised of structural components which show different response behaviors against earthquakes, in earthquake-resistant design the submerged tube portion would be calculated based on displacement of the ground during earthquake (displacement method) while vertical shafts, ventilation towers and retaining walls would have design calculations made by the seismic coefficient method or the modified seismic coefficient method. Needless to say, design and examination based on dynamic analyses must be made for the entire submerged tunnel as previously described. Since the seismic coefficient method and the modified seismic coefficient are already well-known, only special applications will be touched upon, and the discussion here will be chiefly in regard to the displacement method.

6.1 Displacement Method For computing the section forces produced during earthquake on the structural parts of the tunnel consisting of submerged tube section and approaches, and the earth pressures acting on the tunnel, the distribution of displacements during earthquake of the ground along the tunnel axis must be obtained. With regard to earthquake response of surface layer ground, there have already been many research works carried out with response velocities of ground having natural periods up to several sec having been obtained, and it is considered that in a major earthquake components of low-order natural shearing vibration are predominant with regard to displacement. Therefore, it would be possible to compute the response displacement of the

surface layer if the earthquake motion of the bedrock were to be known. However, it is not an easy task to determine how ground displacements will be distributed at the same instant along the axial line of the tunnel. According to the results of earthquake observations, it is seen that vibration components of relatively long periods are propagated at fairly high velocities to the ground surface. It is also known that the submerged tube portion does not respond well to wave motions of short wave length. Thereupon, using the models for dynamic analysis given by the authors, and with the principal objective of investigating the influence of variations in ground conditions on stresses in tunnels, response calculations were carried out for more than 260 cases under various conditions, and data for designing were obtained. The ground conditions considered for calculations were those indicated in Fig. 12, and the earthquake records of Hachinohe (Off-Tokachi Earthquake, 1968), El Centro Earthquake NS (1940) and Taft Earthquake EW (1952) were input from the bedrock and responses of the tunnels computed. The fundamental shearing vibration periods of the land and sea bed portions,  $T_1$  and  $T_2$ , were made up in various combinations, the gradients and shapes of the sloped sections were varied in many ways, and further, the stiffnesses of the tunnels against deformation and the spring relationships between ground and tunnels were varied. The response stresses of the tunnels determined from calculations were standardized through the equations below.

$$\sigma_t = \frac{\sigma_t}{D_L + D_S} \text{ (kg/cm}^2\text{/cm)}$$

$$\sigma_B = \frac{\sigma_B}{D_L + D_S} \text{ (kg/cm}^2\text{/cm)}$$

In these equations,  $\sigma_t$  and  $\sigma_B$  are the maximum axial strain and maximum fiber strain due to axial-direction deformation and bending deformation, respectively, obtained in response calculations, where  $D_L$  and  $D_S$  are the response displacements (relative displacements) of land and sea bed parts replaced by one-masspoint-spring systems, respectively.

Figs. 13 and 14 indicate the relationships between various combinations of  $T_1$  and  $T_2$ , and  $\sigma_t$  and  $\sigma_B$ . With this model, in case of  $T_1 = T_2$ , both  $\sigma_t$  and  $\sigma_B$  will be zero, but considering that grounds of  $T_1 = T_2$  do not actually exist, that earthquake wave motion is propagated through the bedrock, and that various wave motions are produced at the ground surface, from a practical standpoint the broken line is taken as the lower limit and only values above this line are taken up.

**6.2 Stability of Transverse Cross Section of Submerged Tube Section** The force acting on the spring between the submerged tube section and the ground may be calculated by the method proposed by the authors. Although designing has been done for this force to be resisted by passive earth pressure of ground surrounding the tunnel, since there is still room remaining for consideration, it was made permissible in the Specifications for calculations to be made by the seismic coefficient method. With regard to the design seismic coefficient in the seismic coefficient method, this is to be selected taking into account the topographical and geological conditions of the site and importance factor of the tunnel, and referring to the criteria of other related earthquake-resistant design standards.

**6.3 Earthquake-Resistant Design of Shafts and Ventilation Tower Sections** Since shafts and ventilation tower sections are considered normally to indicate dynamic behaviors similar to buildings, they are to be designed for earthquake resistance by the seismic coefficient method. In this design,

giving consideration to the fact that the submerged tube section and the approach sections show different dynamic behaviors, it is necessary for attention to be paid to the connections between these sections. It is possible to reduce stresses produced near joints during earthquakes by providing movable joints and sections high in flexibility and expandability in connections with the submerged tube section. In some cases, it is conceivable for shafts and ventilation towers to be built apart from the tunnel to break off the mutual influences of the two. Further, it is necessary for care to be exercised that uneven settlement — uneven settlement of the tunnel section — will not occur, not only during earthquake, but also at all times. In case there are comparatively large displacements of shafts and ventilation towers at underground portions, it will be advisable for dynamic analyses to be made of the structural parts including the submerged tube section.

Fig. 15 indicates the joints adopted at Tokyo Port Tunnel in connecting a shaft end with the submerged tube. The left half is the joint of a shaft with the first submerged element with primary water cutoff by rubber gaskets, and with secondary and tertiary cutoff measures provided. The right half is the joint between the last submerged element and a shaft with the primary water cutoff made by W-shaped rubber seals. By using these methods, the elements can move freely in the axial direction, up and down, right and left, and in rotation.

6.4 Effects of Joints Flexible joints are used at times in order that joints between elements will have sufficient strength against forces caused by earthquakes and ground settlement after pressure-jointing the elements, and in addition, to reduce the forces produced by these phenomena. Fig. 16 shows the joints adopted for Tokyo Port Tunnel which are provided with shear keys to prevent divergences between elements in the horizontal and vertical directions, while  $\Omega$ -shaped steel sheets form flexible springs in the axial direction.

By installing suitable joints between tunnel and shaft-ventilation tower sections, and between elements, the flexibility and the expandability of the tunnel are heightened, and as a result section forces of the tunnel can be reduced, but the range in which the effects are felt is determined by the relativity between the rigidity of the tunnel and the rigidity of soil, and is in a comparatively narrow range. Accordingly, it is necessary for studies to be made in the locations of the joints, intervals, and number.

Fig. 17 indicates the results of investigations on the effects of joints in the previously-mentioned analysis model. Case 1 is for no joint, Case 2 is for a single hinge joint, Case 3 is for 2 hinge joints, and Case 4 for when all joints are connected by springs with low spring coefficients. It may be seen that axial forces and bending moments are greatly lowered in Case 4.

6.5 Case of Variation in Dynamic Properties of Ground When there has been a change in the dynamic properties (natural period, vibration mode, etc.) of the ground along the tunnel axis, it has been clarified by experimental results and analytical results that an extremely large section force is produced in the tunnel at that portion. Fig. 18 is an example of the distribution of response section forces determined for four kinds of earthquake waveforms normalized at maximum acceleration of 100 gal using the previously mentioned vibration model. Although the absolute values of the response quantities may differ, it can be seen that the tendency for a large section force to be produced at the slope is not changed by earthquake. This is the same for the direction of depth also. Therefore, when the submerged tunnel route passes through such a location it is conceivable to aim for reduction in section force by measures such as adopting sections high in flexibility and installation of movable joints as necessary.

6.6 Influence on Tunnel Section Force of Non-Linearity of Stress-Strain Relationship of Soil Surrounding Tunnel Using the models for dynamic analysis previously described, and carrying out response analyses under various conditions and considering the properties of the springs connecting ground and tunnel, in effect, the relation of displacement and force between the surrounding ground of the tunnel and the tunnel considered as being of bi-linear type, the distribution of maximum values of section force will be as indicated in Fig. 19. According to this figure, the coefficient of deformation after yielding of springs does not exert so much influence on section force, but the size of strain at the yield point of the spring has a great effect, and when this value becomes small, it is seen that section force is reduced.

## 7. SAFETY MEASURES DURING EARTHQUAKE

With regard to the position and importance of safety measures during earthquake in earthquake-resistant design of a submerged tunnel, these matters are as described in Chapter 3 and Chapter 5. The safety measures during earthquake may be broadly divided into two kinds, one consisting of what might be called "hardware" facilities, such as evacuation passageways during emergencies, facilities to prevent entrance of water due to tsunamis, and facilities for water cutoff, which must be taken into consideration at the planning and designing stage. The other kind consists of so-called "software-type" facilities such as instrumentation for detection of earthquake motions, communication facilities, drainage facilities and traffic control facilities.

Adequate considerations must be given that these facilities will not lose their functions due to secondary trouble such as inundation, water leakage and uneven settlement of ground at time of earthquake, and considering that this type of tunnel is to be constructed at river beds or sea beds, measures against water leakage and inundation are of particular importance.

Safety measures for tunnels constructed recently will be of reference, while the Specifications require the following as facilities for safety during earthquakes.

- Facilities for detecting, recording and reporting earthquake motion
- Facilities for detecting, recording and reporting tide level and wave height
- Traffic control facilities during and immediately after earthquake
- Facilities for detecting, recording and reporting settlement and leakage
- Evacuation and guidance facilities
- Emergency electric power facilities
- Traffic monitoring facilities
- Drainage facilities and inundation prevention facilities
- Others (strain meter, reinforcing bar stress transducer, stress meter, etc.)

The types and numbers of these facilities would be decided as suited in accordance with the size and importance factor of the submerged tunnel, while depending upon the use of the tunnel, for example, an automobile tunnel, it will of course be necessary to consider facilities to cope with automobile fires.

The Specifications do not clearly stipulate at what level of earthquake these safety facilities should be activated, but do cite "Conduct of Train Operation during Earthquakes" for the Shinkansen lines of the Japanese National Railways as reference. This specifies standards for train operation control, on-ground patrol, in-train patrol, etc., to be carried out on action of earthquake sensors of 40 gal and 80 gal. The Specifications do stipulate that when subjected to earthquakes of seismic intensity 4 or higher, patrols are to be made to

check for earthquake effects on the various parts of the submerged tunnel and other abnormalities.

#### REFERENCES

1. JSCE: Specifications for Earthquake Resistant Design of Submerged Tunnels, 1975.
2. TAMURA, C., OKAMOTO, S., KATO, K. and NAKAGAWA, Y.: Earthquake Observation on Trench Type Subaqueous Tunnel, SEISAN-KENKYU, Vol. 23, No. 1, January 1971.
3. OKAMOTO, S. and TAMURA, C.: Behavior of Subaqueous Tunnel during Earthquakes, Earthquake Engineering and Structural Dynamics, Vol. 1, No. 3, 1973.
4. OKAMOTO, S., TAMURA, C., KATO, K. and HAMADA, M.: Behavior of Submerged Tunnel during Earthquakes, Proc. of 5th WCEE, 1973, Rome.
5. TAMURA, C., OKAMOTO, S. and HAMADA, M.: Dynamic Behavior of a Submerged Tunnel during Earthquakes, Report of the Institute of Industrial Science, University of Tokyo, Vol. 24, No. 5, March 1975.
6. KIYOMIYA, O., NAKAYAMA, S. and TSUCHIDA, H.: Observations of Dynamic Response of Kinuura Submerged Tunnel during Earthquakes and Dynamic Response Analysis, Technical Note of Port and Harbor Research Institute, No. 221, June 1975, 77 p.
7. TAMURA, C. and OKAMOTO, S.: On Earthquake Resistant Design of a Submerged Tunnel, Proceedings of the International Symposium on Earthquake Structural Engineering, University of Missouri, Rolla, August 1976.
8. METROPOLITAN EXPRESSWAY PUBLIC CORPORATION: General Report of Tokyo Port Tunnel, JSCE, March 1977.
9. JSCE: Earthquake Resistant Design for Civil Engineering Structures, Earth Structures and Foundations in Japan, 1977.



Table 1 Submerged tunnels in Japan, completed and under construction

Name <sup>a</sup>	Location	Use	Elements						Period for construction
			Length <sup>aa</sup> (m)	Num- ber	Length (m)	Width (m)	Height (m)	Sectional shape	
Aji River Tunnel	Osaka	2 lane road	49.2	1	49.2	14.0	7.0	Rectangular	1935-1944
Haneda Tunnel	Tokyo	4 lane road	56	1	56	20.1	7.4	Rectangular	1963-1964
Haneda Tunnel	Tokyo	2 track monorail	56	1	56	10.95	7.4	Rectangular	1963-1964
Dojima River Tunnel	Osaka	2 track railway	70.5	2	36.0 36.5	11.00	7.18	Rectangular	1967-1969
Dotonbori River Tunnel	Osaka	2 track railway	24.9	1	24.9	9.65	6.96	Rectangular	1967-1969
Keiyo-line Haneda Tunnel (Tama River)	Tokyo	2 track railway	480	6	80	13.0	7.95	Binocular	1968-1971
Keiyo-line Haneda Tunnel (Morigasaki)	Tokyo	2 track railway	328	4	82	12.74	7.99	Binocular	1969-1971
Atsumi Power Plant Intake Channel	Aichi Prefecture	Cooling water intake channel for power plant	36.01	1	36.01	8.4	4.0	Rectangular	1970
Dokai Bay Tunnel	Kita-kyushu	2 belt conveyors for iron ore and coke	1363.2	18	30 80.1	8.218	4.55	Rectangular	1970-1972
Kinura Port Tunnel	Aichi Prefecture	2 lane road	480	6	80	15.6	7.1	Rectangular	1969-1973
Ogishima Tunnel	Kawasaki	4 lane road	664.3	6	110	21.6	6.9	Rectangular	1971-1975
Tokyo Port Tunnel	Tokyo	6 lane road	1035	9	115	37.4	8.80	Rectangular	1969-1975
Sumida River Tunnel	Tokyo	2 track railway	201.5	3	67.5 67.0	10.30	7.80	Rectangular	1973-1976
Kawasaki Port Tunnel	Kawasaki	4 lane road	840	8	110 100	31.00	8.54	Rectangular	1972-(Under construction)
Tokyo Port 2nd Fairway Tunnel	Tokyo	4 lane road	744	6	124	28.40	8.80	Rectangular	1973-(Under construction)

<sup>a</sup> Tentative English names  
<sup>aa</sup> Lengths submerged structures

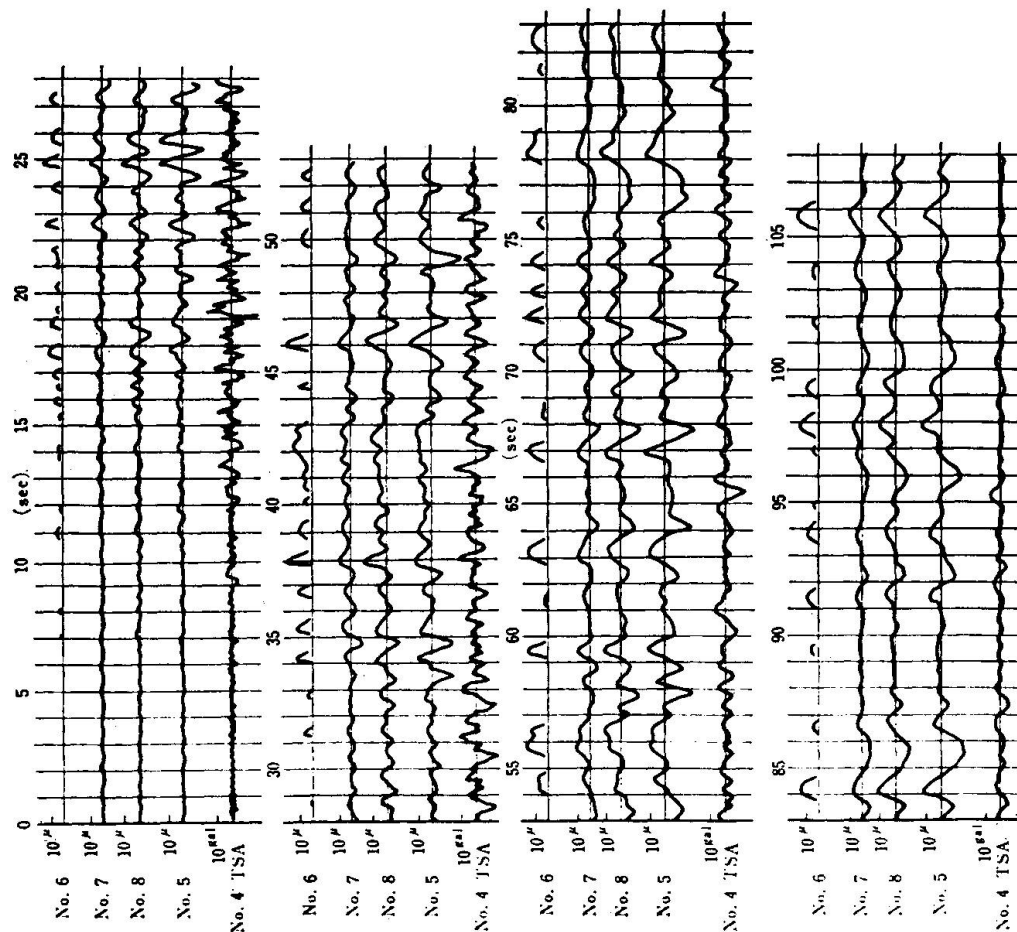


Fig.1 Earthquake records (December 4, 1972)

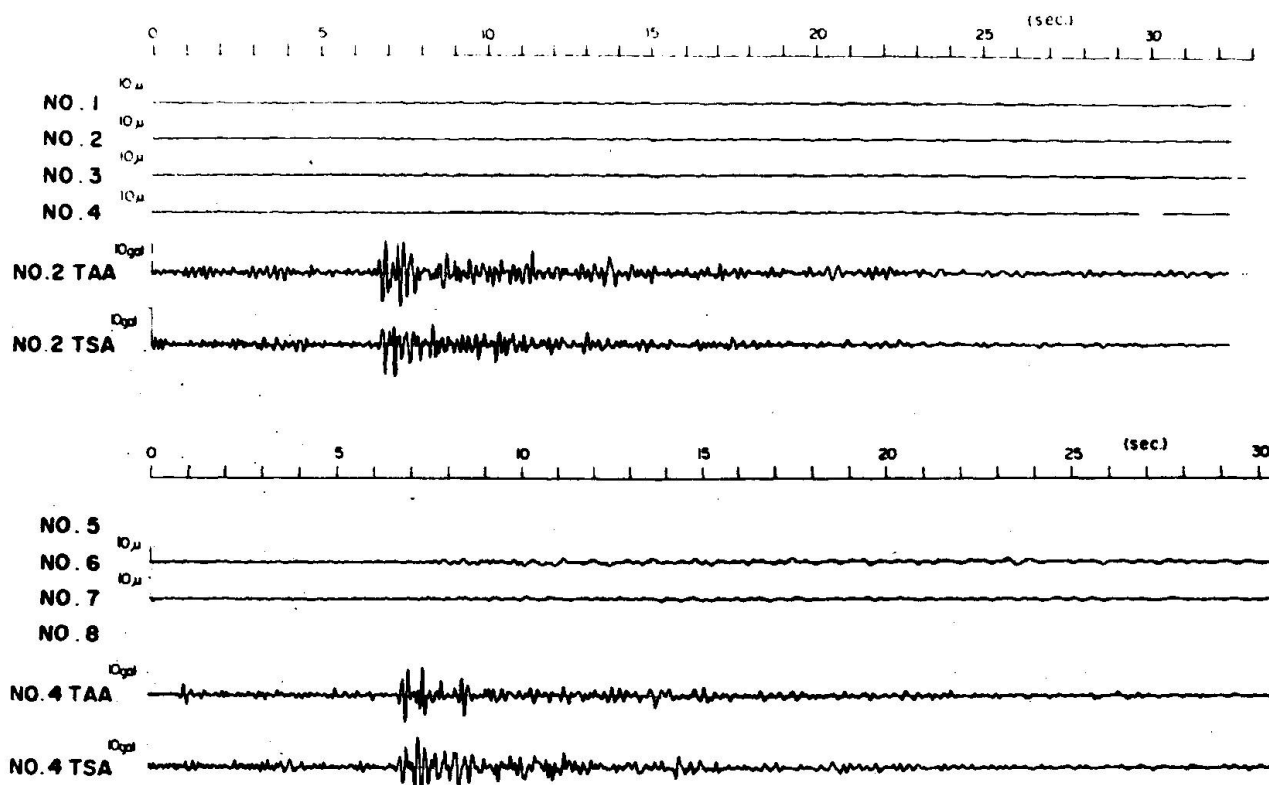


Fig.2 Earthquake records (March 27, 1973)

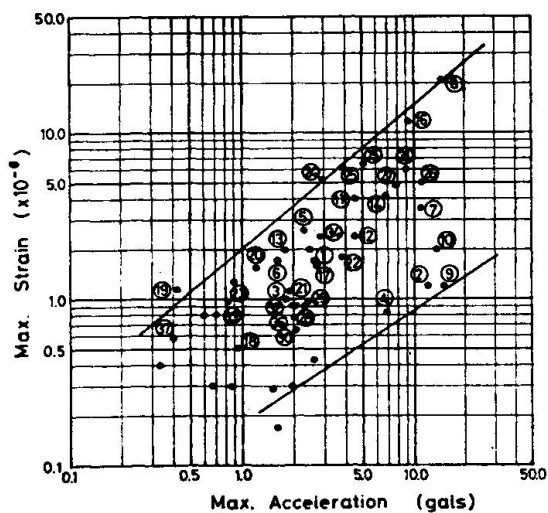


Fig.3 Relation between max. acceleration and max. axial strain at Haneda Tunnel (J.N.R.)

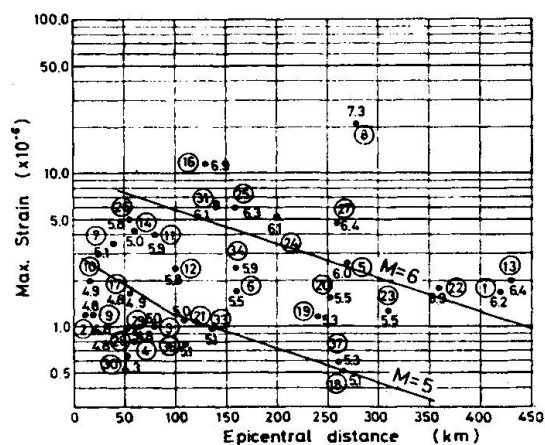


Fig.4 Relation between epicentral distance, magnitude of earthquake and max. axial strain at Haneda Tunnel (J.N.R.)



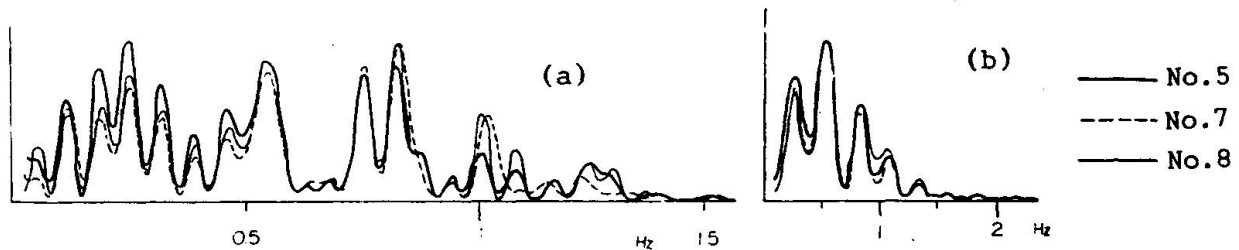


Fig.5 Power spectra of strain records of earthquake (December 4, 1972) at Haneda Tunnel (J.N.R.)

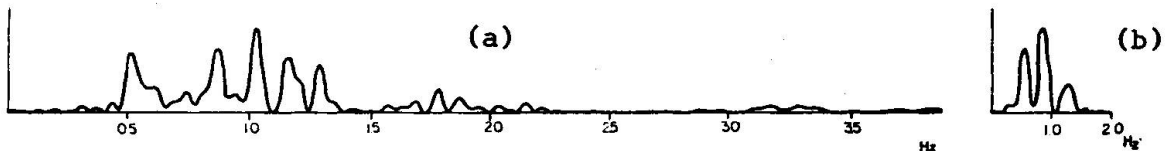


Fig.6 Power spectra of acceleration record (No.4 TSA) of earthquake (December 4, 1972) at Haneda Tunnel (J.N.R.)

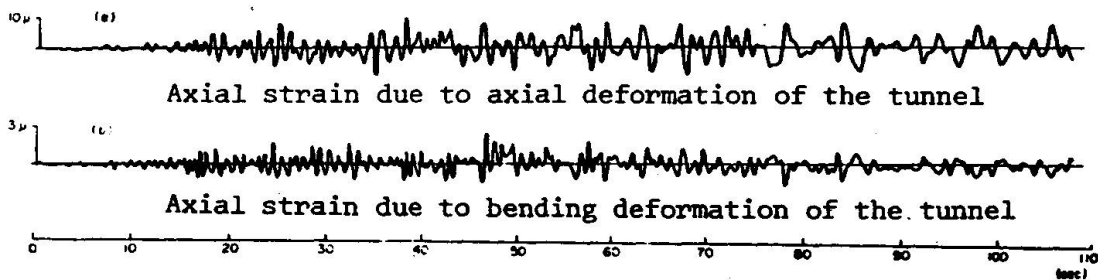


Fig.7 Strain waves generated by axial deformation and bending deformation of tunnel (Haneda Tunnel) during earthquake (December 4, 1972) and their power spectra

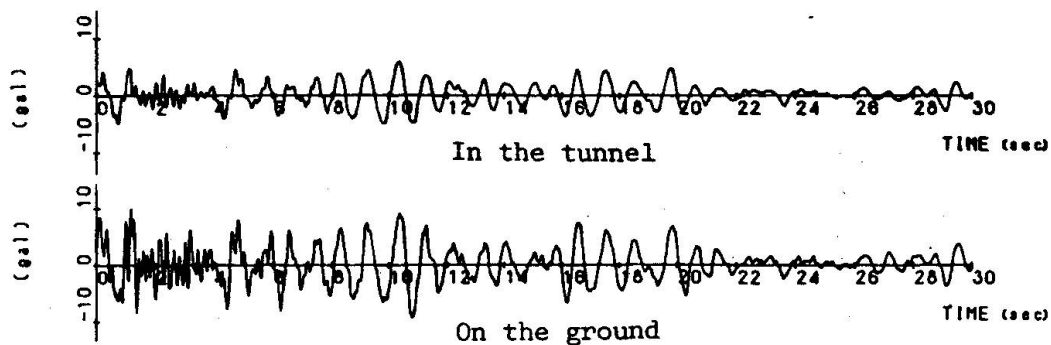


Fig.8 Earthquake records recorded simultaneously on the ground surface and in the tunnel (Kinuura Port Tunnel)

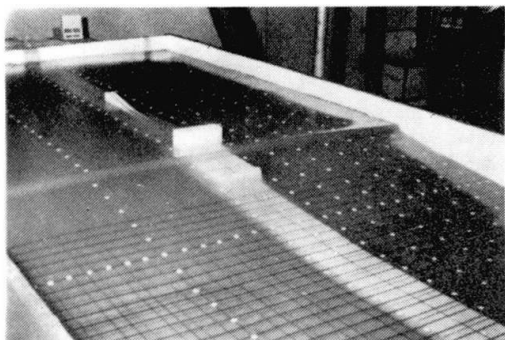


Fig.9 A model of tunnel

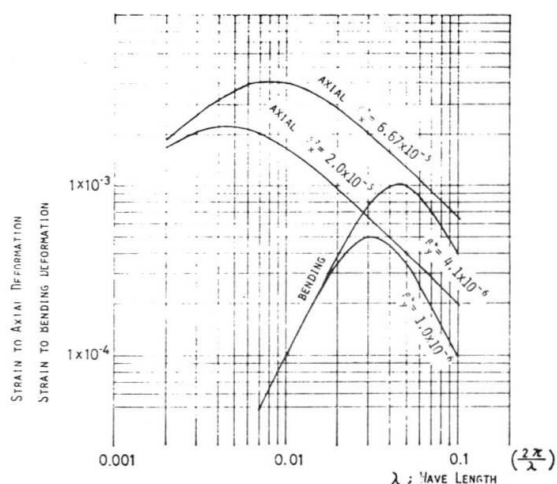


Fig.10 Relation between wave length and axial strain of tunnel

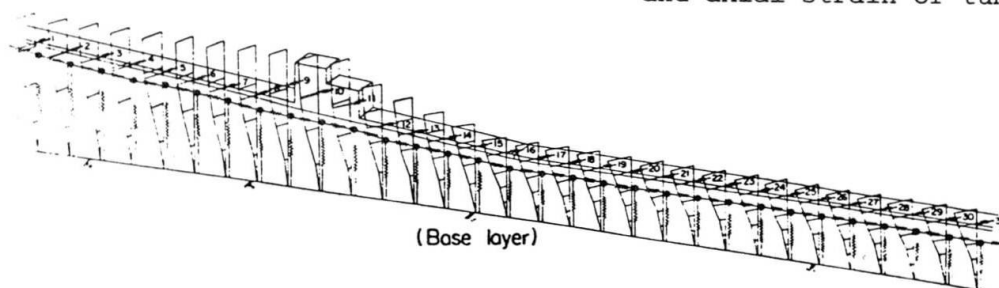


Fig.11 Mathematical model of tunnel

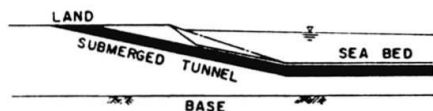


Fig.12 Typical profile of ground and tunnel for analysis

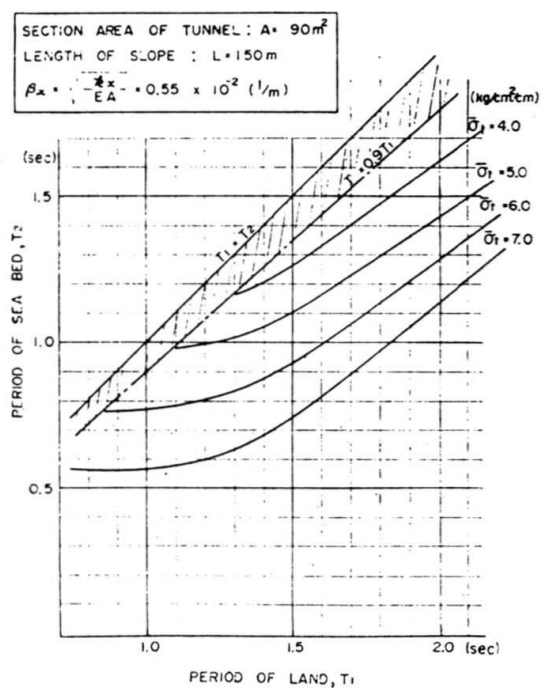


Fig.13 Max. response axial stresses of tunnel normalized by response displacement of ground

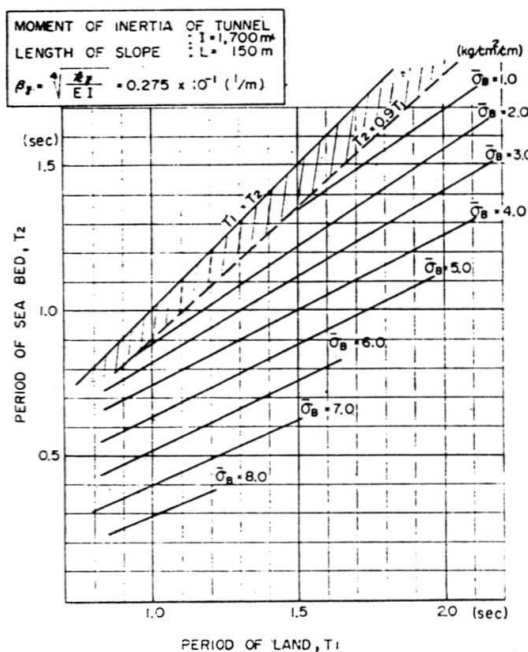


Fig.14 Max. response fiber stresses of tunnel normalized by response displacement of ground



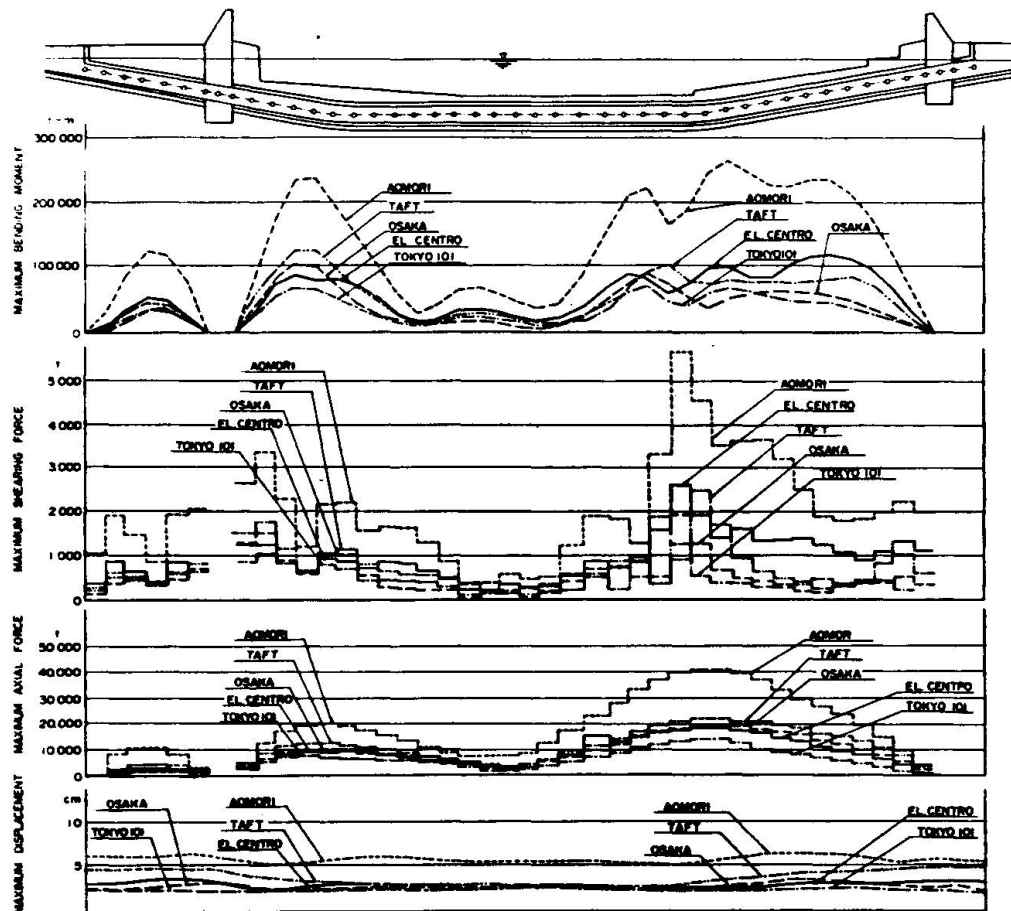


Fig.18 Distribution of response displacement and response cross-sectional force of tunnel to 5 earthquake records which are normalized by max. acceleration of 100 gals (Tokyo Port Tunnel)

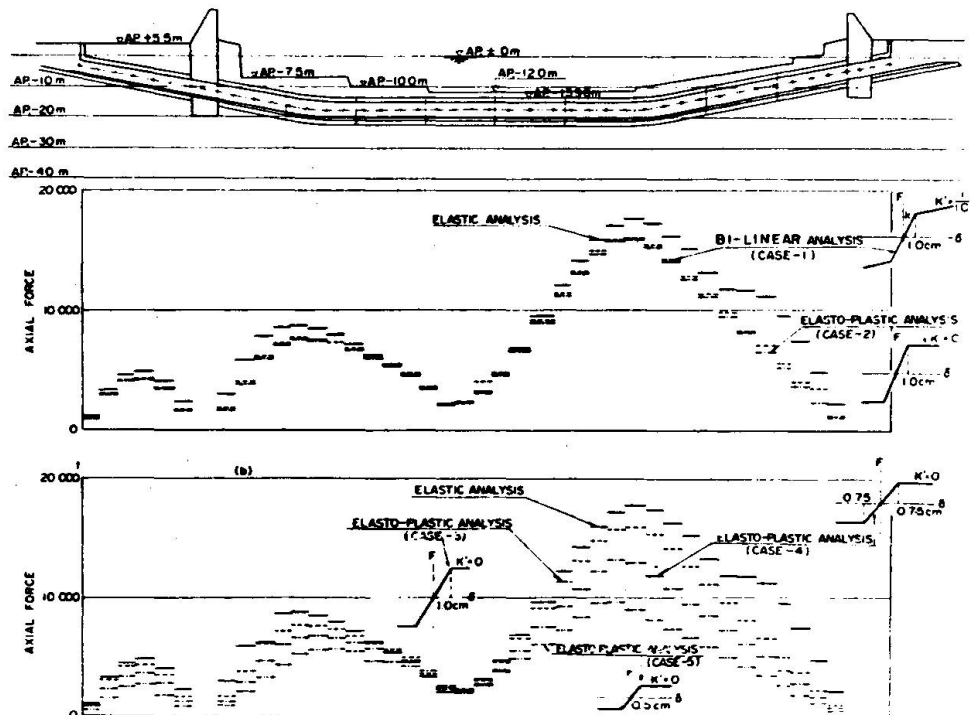


Fig.19 Max. response axial force of tunnel for bi-linear model of spring K which connects tunnel and ground (Tokyo Port Tunnel)

Leere Seite  
Blank page  
Page vide

On the modelling of sea-bed resistance for seismic response analysis of offshore pipelines in contact with the sea-bed.

Établissement de modèles de la résistance du fond de la mer en vue d'une analyse de la réaction sismique de pipelines sous-marins en contact avec le fond de la mer.

Über Modelle des Meeresbodenwiderstandes für die Analyse der seismischen Reaktion von Unterwasserrohrleitungen im Kontakt mit dem Meeresboden.

By

B Nath Ph D and C H Soh

Both in the department of Civil engineering, Queen Mary College, University of London, London, England.

## SUMMARY

This paper contains a study of the seismic behaviour of marine pipelines in contact with the sea-bed, with particular reference to the mechanics at the contact region between the pipe and the sea-bed. Assuming seismic excitation to be transversely horizontal to the pipeline the problem has been solved by the finite element method for three different types of idealized sea-bed soil behaviour. Results show that pipe response depends upon the sea-bed resistance model and, as expected, the response of the segment in contact with the sea-bed is less than when there is no contact.

## SOMMAIRE

Cet article contient une étude du comportement sismique de pipelines sous-marins en contact avec le fond de la mer et traite particulièrement la mécanique aux zones de contact entre pipeline et le fond de la mer. Le problème a été traité par la méthode d'éléments finis pour trois types différents de comportements schématisés du sol marin en admettant que l'excitation sismique est transversalement horizontal au pipeline. Les résultats montrent que la réaction du pipeline dépend du modèle de résistance du sol marin. Comme attendu, la réaction d'un segment de pipeline en contact avec le fond de la mer est moindre que dans le cas où il n'y a pas de contact.

## ZUSAMMENFASSUNG

Diese Abhandlung untersucht das seismische Verhalten von Unterwasserrohrleitungen im Kontakt mit dem Meeresboden, mit besonderer Beziehung auf die Mechanik an den Kontaktstellen zwischen Rohr und Meeresboden. Unter Voraussetzung einer zur Rohrleitung transversal-horizontalen seismischen Erregung wird das Problem durch Anwendung der Methode der endlichen Elementen für drei verschiedene Arten von idealisierten Verhalten des Meeresbodens gelöst. Die Ergebnisse zeigen, dass die Rohrreaktion von Modell des Meeresbodenwiderstandes abhängt, und dass, wie zu erwarten, die Reaktion eines Rohrteiles im Kontakt mit dem Meeresboden kleiner ist als im Falle in dem ein solcher Kontakt nicht besteht.

## 1. INTRODUCTION

For various reasons pipelines are extensively used for gathering offshore oil and gas resources throughout the World including seismic regions. Usually these pipes are buried into jet-blasted channels in the sea-bed, although, when conditions do not permit this, they may be secured to the sea-bed in suitable lengths by means of concrete anchor blocks or screw piles. However, depending upon the composition of the sea-bed sediment and the prevailing marine conditions, a pipe segment which was initially buried may subsequently be exposed by the transportation of sediment away from the pipe location during periods of high scouring activity [1]; in a reverse of this process an initially exposed segment may also be totally or partially buried by the "duning" of the sea-bed. Clearly, an important design criterion here is therefore that the pipeline should be safe and stable under either of these two possible conditions.

In the context of offshore energy exploitation pipelines usually represent a substantial proportion of the total capital investment (in the Bombay High field, India, for example, a pipe network totalling over 140 km is envisaged). For this reason alone an accurate assessment of the safety and stability of offshore pipelines against seismic hazards is of paramount importance, particularly in regions where such hazards may be expected. Unfortunately, an accurate prediction of seismic behaviour with a view to formulating appropriate design criteria is usually a difficult proposition here, since system response in this problem is determined by the structural, hydrodynamical and soil mechanical aspects of the system, not to mention the complex dynamic interactions that may also take place between these aspects.

At the moment little published material on the dynamic/seismic behaviour of offshore pipelines appears to be available, understandably perhaps considering the relative infancy of this branch of technology. Over the years considerable research effort has been directed, on the other hand, to the solution of terrestrial pipeline problems including seismic response studies (references 2-9 contain a selection of research papers on the subject). Although it may be possible, *prima facie*, to extrapolate some of the findings/criteria of terrestrial pipelines to offshore pipelines, the fact remains however that current design practice relating to terrestrial pipelines is basically inadequate [5,10]; indeed, this inadequacy, as underlined by the aftermath of the San Fernando (1971, Richter magnitude 6.6) and the Managua (1972, Richter magnitude 6.25) Earthquakes, led to a series of recommendations by various prestigious committees [10,11]. Clearly therefore, a considerable research effort is still needed for formulating generally acceptable design criteria for terrestrial pipelines and, the need is even greater and perhaps more urgent in the case of offshore pipelines.

## 2. THE PROBLEM AND ITS ASPECTS

The problem to be investigated in this paper can be briefly stated as follows:

An offshore pipeline segment, supported between two anchor blocks (Fig.1a) is in contact with the sea-bed at one or more points or over a portion of its length. The segment is subjected to a transverse, horizontal and uniform seismic excitation which is transmitted to it, without dissipation, via the anchor blocks. To analyze the response of the segment with particular reference to the idealized sea-bed impedance parameters.



It would be instructive at this stage to focus attention onto the various aspects of the problem and also the assumptions which have to be made in order to construct a workable mathematical model of what is inherently a very complex system.

## 2.1 The structural aspect

Offshore pipelines are usually constructed of concrete coated enamelled steel pipe sections (Fig. 1b). The function of the enamel is to protect the steel pipe against external corrosion; the enamel, in turn, is protected by the concrete coating against accidental damage. As we have assumed seismic excitation to be transversely horizontal to the pipeline, it is clear that pipe response will be exclusively in the bending (in the Euler-Bernoulli sense) mode. It would be reasonable therefore to treat the segment as a beam in bending. However, as the concrete coating is likely to undergo progressive structural/chemical degradation with time [12,13], its contribution to the overall stiffness of the segment will be ignored. Furthermore, the pipe will be assumed to respond in a linearly elastic fashion ---- an assumption which is more likely than not to be valid in practice.

An important determinant of system response here is the nature of the end constraints of the pipe segment; a given segment will have greater response and pressure drag effects [12] with simply supported ends than with fixed ends. For this reason the test segments to be analyzed here will be assumed to have simply supported ends, although, in practice the end constraints are likely to lie somewhere between the fixed and simply supported conditions.

## 2.2 The hydrodynamical aspect

From the point of view of its physics the offshore pipeline problem belongs to a well-known class of coupled structure-fluid problems [14-18] in which the structural and fluid aspects interact, the extent of interaction depending upon the dynamic properties (e.g, natural frequencies, mode shapes, etc.) of the uncoupled aspects comprising the system. Systems, in which the structure is relatively flexible (as in pipeline systems), are negligibly affected by fluid compressibility; consequently the inviscid coupled behaviour of such systems can be studied merely by adding the so called added mass [14] to the structure mass in the system equation(s) of motion. If, on the other hand, non-linear pressure drag effect is significant, then the total hydrodynamic resistance to motion must be included in the system equation(s) in terms of both drag and fluid inertia forces. Following the Morison equation [19], for example, the drag and inertia forces, which are implicitly independent, can then be expressed in terms of appropriate drag ( $C_D$ ) and inertia ( $C_M$ ) coefficients. This is the usual approach in problems of this type and, in the case of offshore pipelines computed response is found to depend substantially on the value of  $C_M$  and to a much lesser extent on that of  $C_D$  [12].

Under conditions of potential flow the value of  $C_M$  can be shown [20-22] to decrease from a maximum of 2.29 for  $d/D = 0$  (Fig. 1b) to an asymptotic minimum of 1.00 for  $d/D = \text{infinity}$ . For drag also experimental evidence indicates a significant correlation between  $C_D$  and the  $d/D$  ratio. In the case of a relatively smooth pipe for which  $d/D > 1.5$ , for example, Wilson and Caldwell [23] report  $C_D = 1.7$  and  $1.2$  for Reynold's number equal to 33,200 and 56,600 respectively; under identical conditions but with  $d/D <$

1.0 these  $C_D$  values were found to decrease by about 15%. Furthermore, both these parameters are likely to be significantly modified in practice by the structural/chemical degradation of the pipe coating [12] and also by the marine fouling on the pipe surface [12,24]. Unfortunately, published data relating to the in-situ values of these parameters do not appear to be available as of now. We will therefore use the classical (potential theory) values of  $C_M$ ; in all cases the value of  $C_D$  will be taken as 1.5, which is probably realistic considering the complex flow condition around the pipe and also the possible environmental effects on the pipe surface.

Although the inertial and drag forces are assumed to be implicitly independent, in a complex separated flow such as this as yet little understood dynamic interaction(s) may take place between these forces [25,26]. Furthermore, in the presence of an ambient stream the pipe will undergo self induced (Strouhal) vibrations in the vertical plane; such vibrations may also lead, particularly at high Reynold's numbers, to a time-dependent wake and this may affect the pipe's drag and inertia coefficients relating to its transverse horizontal vibrations. A hydrodynamic coupling of this type between the horizontal and vertical vibrations of the pipe is a manifestation of the well-known "wake-body" interaction phenomenon [27,28]. As the mechanics of this complex phenomenon is not yet fully understood, we will ignore such interactions in this work.

For small values of the  $d/D$  ratio the pipe will also experience a significant lift force [20,21,23]. However, as we have ignored possible coupling between the horizontal and vertical vibrations of the pipe and as we are interested only in its transverse horizontal response, this lift force is no longer relevant here.

### 2.3 The soil-mechanical aspect

Considering the complex behaviour of sea-bed soil including possible thixotropy and soil-liquefaction effects under dynamic/cyclic conditions of loading, it is clearly difficult to devise a general mathematical model to represent accurately the mechanics at the pipe-seabed interface. Here again the inadequacy of published data relating to the in-situ behaviour and properties of sea-bed soil seriously inhibits any attempt at realistic model studies. We will nevertheless examine a number of models based on idealized soil behaviour; clearly, their practical validity would depend very much on the extent to which in-situ behaviour corresponds with idealized behaviour.

We will assume that the resistance offered by the sea-bed against pipe motion can be idealized in the elasto-plastic sense by means of a kinetic coefficient of friction ( $\mu$ ) between the pipe and the sea-bed, and parameter  $Q$  which denotes the maximum elastic ground displacement. For simplicity both  $\mu$  and  $Q$  will be assumed to be constant although in practice they are both likely to vary, particularly with time.

The pipeline problem with ground contact considered here is basically one of pipe-seabed interaction. Figs.2a and b show the deformed pipe geometry with a single central contact point and the forces active at that point. For conceptual simplicity if the pipe is now represented by a linear elastic spring of stiffness  $k_p$  and the sea-bed by an elasto-plastic spring of stiffness  $k_s$  (which is a function of displacement), then it is clear that the coupled response of the pipe will be a function of both  $k_p$  and  $k_s$ . It

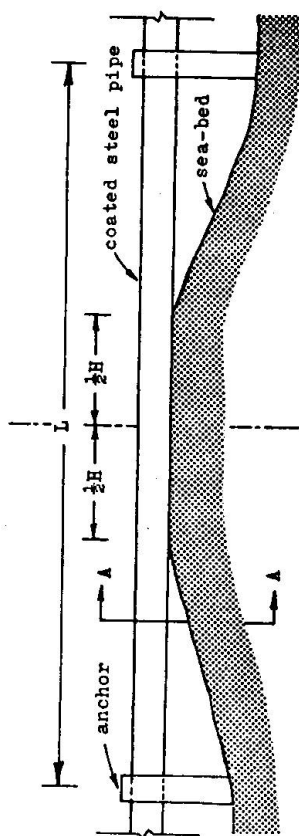


FIG. 1a Pipe-seabed configuration under consideration.

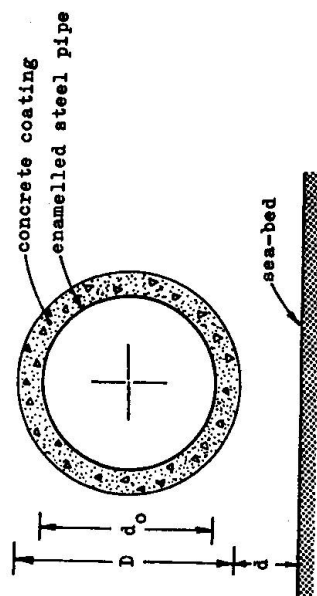


FIG. 1b Magnified pipe section at A-A in FIG. 1a.

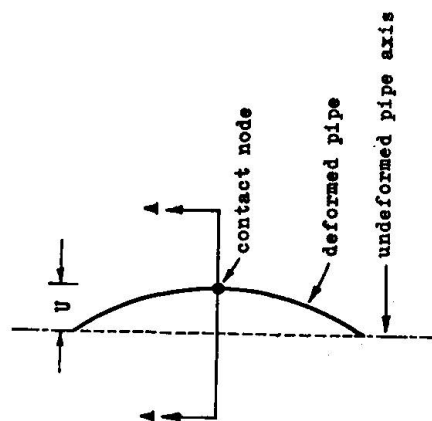


FIG. 2a Deformed pipe geometry with a single central contact node.

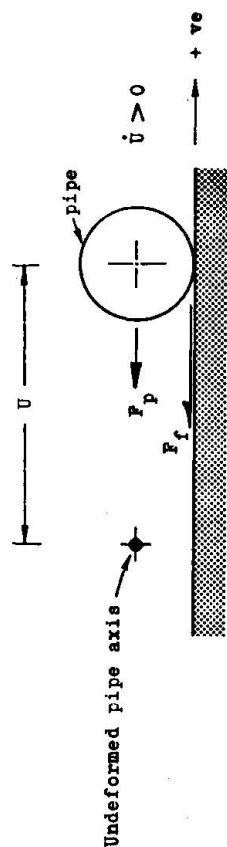


FIG. 2b Magnified section at A-A in FIG. 2a showing forces at the contact node.

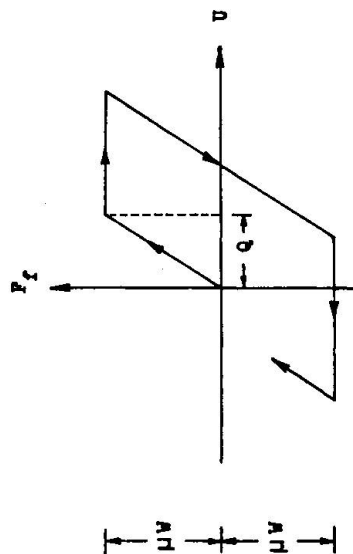


FIG. 2c Sea-bed resistance model "A".

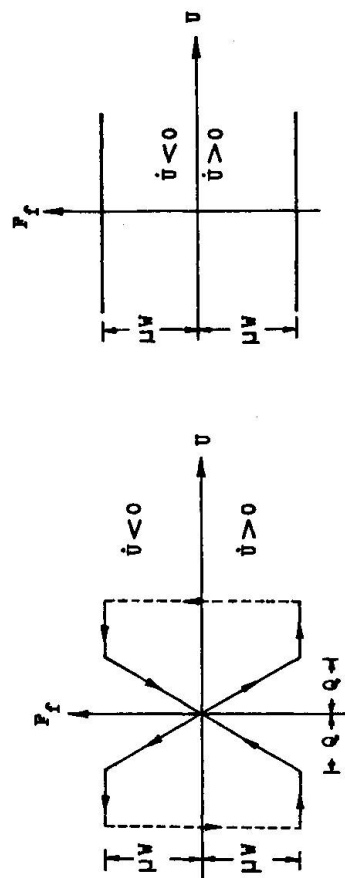


FIG. 2d Sea-bed resistance model "B".

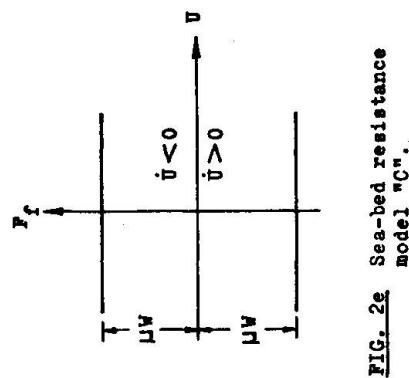


FIG. 2e Sea-bed resistance model "C".

is also clear from the mechanics of the coupled system that these springs act in parallel. Consequently, when  $k_s$  dominates, i.e.,  $k_s \gg k_p$ , the pipe is likely to undergo irrecoverable deflections caused by large plastic forces that will now be mobilized by the sea-bed. In this situation the sea-bed resistance model (model A), shown in Fig. 2c, is likely to be valid. If, on the other hand,  $k_p \gg k_s$ , then the pipe will not undergo significant irrecoverable deflections, and consequently, the sea-bed resistance model (model B), shown in Fig. 2d, is more likely to be valid. In another model (model C), shown in Fig. 2e, which is also worth considering, the contact point(s) is assumed to move only when the force in the pipe ( $|F_p|$  in Fig. 2b) becomes equal to  $\mu W$ . The validity of this model is difficult to justify, except perhaps when the peculiarity of the sea-bed (caused, for instance, by the presence of rocky obstacles or displaced sand-bags initially placed upon the pipe in order to increase its stability) constrains the pipe to move in this way.

### 3. THEORY

Following a spatial discretization of the pipe segment consisting of  $(n-1)$  finite elements interconnected by  $n$  nodes of which  $m$  nodes ( $m < n$ ) represent the pipe-seabed interface, the implicit equation of motion of the segment can be written with reference to Fig. 2b as [29]

$$\{F_p\} + \{F_f\} \operatorname{sgn} \{\dot{U}\} = \{0\} \quad (1)$$

in which, considering seismic excitation only, we can show that [12,17,19]

$$\{F_p\} = [K]\{U\} + [C]\{\dot{U}\} + [M + M_a]\{\ddot{U}_t\} + \frac{1}{2}\rho C_D[A]\{\dot{U}_t|\dot{U}_t|\} \quad (2)$$

Here vector  $\{F_f\}$  lists the sea-bed resistances concentrated at the  $m$  contact nodes.  $[K]$ ,  $[M]$  and  $[C]$  denote stiffness, submerged mass and viscous damping matrices of the segment, respectively, while  $[M_a]$  denotes its added mass matrix (both  $[M]$  and  $[M_a]$  are diagonal matrices).  $\{U\}$  lists pipe deflections relative to the moving undeformed pipe axis while  $\{U_t\}$  lists total pipe deflections from a fixed reference. Dots denote differentiation with respect to time,  $\rho$  the mass density of water and  $[A]$  the diagonal matrix of pipe areas projected along the direction of motion. Then, substituting

$$\{U_t\} = \{U_g\} + \{U\} \quad (3)$$

into Eq.(2), where  $\{U_g\}$  lists ground displacement history, we now obtain from Eqs.(1) and (2)

$$\begin{aligned} [K]\{U\} + [C]\{\dot{U}\} + [M + M_a]\{\ddot{U}\} + \{F_f\} \operatorname{sgn} \{\dot{U}\} \\ + \frac{1}{2}\rho C_D[A]\{(\dot{U} + \dot{U}_g)|(\dot{U} + \dot{U}_g)|\} = -[M + M_a]\{\ddot{U}_g\} \end{aligned} \quad (4)$$

The response of the pipe to a given ground excitation record will now be found by solving Eq.(4) with appropriate initial and boundary conditions.

#### 4. SOLUTION DETAILS

The pipe segment, supported between two anchor blocks (Fig. 1a) was represented by 6 finite beam elements and its rotational degree-of-freedom was condensed-out in order to minimize the size of matrices to be processed. Structural damping of the pipe was taken as 5% of critical which appears to be usual in slender offshore structures of this type [17]. The thickness of the concrete coating was determined by requiring that the total submerged weight of the empty segment, including the coating, be 10% greater than its buoyancy so that the empty pipe was prevented from floating up to the surface. The stiffness of the coating was however ignored for reasons given in section 2.1. At all times the pipe was assumed to be completely filled with oil (mass density taken as 1.82 lb/cu. ft.) as its maximum response occurred in this condition.

A numerical algorithm was implemented for the solution of Eq.(4); in this the mass of the pipe was represented by nodal lumped masses while the time domain was discretized in the finite (central) difference sense. The processing in the time domain by this device basically amounts to an explicit forward integration procedure [30] in which pipe response at time  $(t + \Delta t)$  is calculated on the basis of already computed (or prescribed) responses at times  $t$  and  $(t - \Delta t)$ . An iterative loop was included in each time-step to deal with the non-linear pressure drag term in Eq.(4); convergence of the iterated solution was found to be rapid and a sufficiently converged solution was obtained with less than 6 iterations per step. The size of the time-step  $(\Delta t)$  to be used was optimized with respect to the convergence and stability of solution. The high degree of accuracy that this algorithm is capable of has been demonstrated in reference 12.

The nodal contact reactions,  $\{W\}$ , between the pipe and the sea-bed will obviously depend on the end-constraints of the segment and also on the elevations or settlements of the contact nodes with respect to the end supports. For the sake of simplicity  $\{W\}$  was calculated in this study by assuming the segment to be resting on a total of  $(m + 2)$  supports, all at the same level ( $m$  denotes the number of contact nodes).

For a given sea-bed resistance model the value of the ground resistance vector  $\{F_r\}$  to be used in a given time-step in Eq.(4) was found from the idealized plot of that model (Figs. 2c-2e).

#### 5. RESULTS AND DISCUSSION

The seismic response of a test pipe segment (details given in table 1) to the Taft earthquake of 1952 was calculated relative to the three sea-bed resistance models shown in Figs. 2c-2e. Table 1 contains a summary of the maximum (beam) bending moment response of the segment for various parametric combinations. Clearly, the overall effect of ground contact is to diminish response compared with the no-contact situation, as we might have anticipated and, the amount of response reduction depends on the type of sea-bed resistance model implemented.

In an elasto-plastic idealization of sea-bed behaviour, it is clear that the maximum sea-bed resistance retarding pipe motion will be mobilized in the plastic zone (whose threshold is defined by the parameters  $Q$  and  $\mu$ ). Consequently, response attenuation due to contact will be expected to be greater in the plastic zone than in the elastic zone. Therefore, for a given  $Q$  an increase in the value of  $\mu$  would diminish plastic response; consequently, at a given relative sea-bed stiffness ( $K_r$ ) response will be ex-



**Table 1** Peak bending moment response of a simply supported pipe segment to the Taft earthquake of 1952.

H/L	Q/L	$\mu$	Peak bending moment/ $10^4$ (lbf-ft)		
			Model A	Model B	Model C*
0**		0	36.00**		
0.167	0.00200	0.025	35.96	35.10	28.80
0.167	0.00200	0.050	35.82	34.92	7.20
0.167	0.00200	0.075	35.78	34.94	6.84
0.167	0.00200	0.100	35.71	35.10	7.92
0.167	0.00100	0.025	34.50	34.33	
0.167	0.00100	0.050	34.81	34.26	
0.167	0.00100	0.075	34.42	34.21	
0.167	0.00100	0.100	33.14	33.22	
0.167	0.00067	0.025	33.45	32.69	
0.167	0.00067	0.050	32.93	30.25	
0.167	0.00067	0.075	31.30	30.30	
0.167	0.00067	0.100	35.18	30.60	
0.500	0.00200	0.050	37.91	35.76	
0.500	0.00100	0.050	36.78	34.00	
0.500	0.00067	0.050	35.00	28.12	

\* The ratio  $Q/L$  is not relevant in this model; \*\* no contact between the pipe and the sea-bed and consequently, this value is not dependent upon any model.

**System details:** The pipe segment is simply supported between two anchor blocks.  $L = 100.00$  ft.,  $D = 3.65$  ft.,  $d_o = 3.00$  ft.,  $EI = 1.85 \times 10^9$  lbf-ft, structural damping = 5% of critical;  $C_D = 1.5$ ,  $C_M = 2.3$  for the contact zone and 1.5 elsewhere.

pected to increase with increasing values of  $\mu$ , since this would amount to increasing the size of the elastic zone. Secondly, and for the same reason, an increase in the value of  $Q$  will be expected to lead to increased response for a given  $\mu$ , since clearly an increased  $Q$  leads to an enlarged elastic zone.

Both the above aspects have been vindicated [29] in the case of model B. The second observation is also valid in the case of model A, as may be seen from Table 1; however, the first observation does not strictly apply to this model, as may be seen from Fig. 3.

It will be seen from Table 1 that response attenuation due to contact is maximum in the case of model C. It is interesting to observe that in this case response attenuation is very steep within the range  $\mu = 0 - 0.04$  and, for  $\mu > 0.04$  response increases slowly with increasing values of  $\mu$ , as can be seen from Fig. 4. This increase may be explained as follows: according to model C the contact node(s) will move relative to the sea-bed only when  $|F_p| = \mu W$  ( $|F_p|$  cannot be greater than  $\mu W$ ); otherwise the contact node(s) remains stationary relative to the sea-bed. Therefore, as long as  $|F_p| \neq \mu W$ , energy will be stored up in the segment due to the motion of the part of the segment not in contact with the sea-bed, and clearly, the amount of stored energy will be directly proportional to the value of  $\mu$ . Then, when the condition  $|F_p| = \mu W$  is fulfilled, the hitherto stationary contact node(s) will be jerked into motion causing the pipe to respond slightly more, depending on the value of  $\mu$ , than it would have done with a smaller value of  $\mu$ .

The effect of increasing the contact zone length on response at various values of the friction coefficient is worth noting (Table 1).



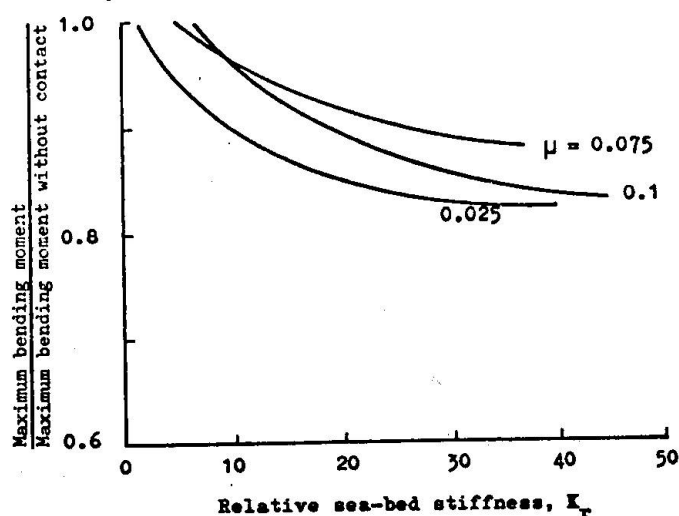


FIG. 3 Variation of the maximum bending moment response of the segment with relative sea-bed stiffness (model A).

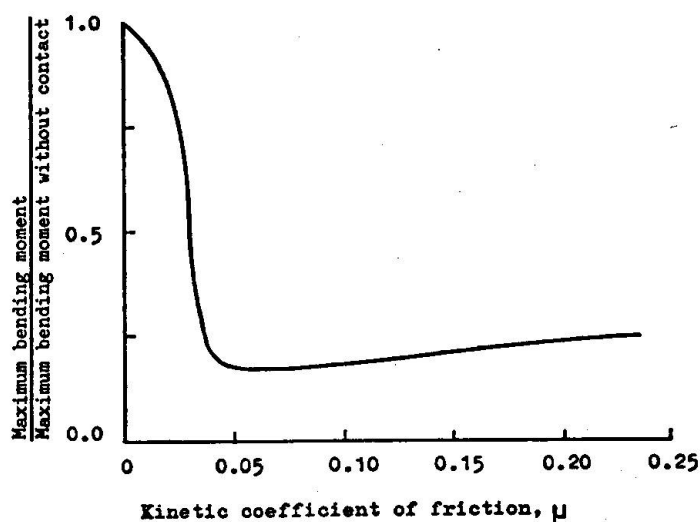


FIG. 4 Variation of the maximum bending moment response of the segment with the kinetic coefficient of friction (model C).

## 6. CONCLUSIONS

A computer coding has been developed for the seismic/dynamic analysis of offshore pipelines. This coding was implemented in this study to calculate the bending response of a typical offshore pipe segment, which is partially in contact with the sea-bed, to the Taft earthquake of 1952. Analysis was made by assuming ground excitation to be transversely horizontal to the pipe axis. Results show that for a given segment in a given hydrodynamic environment, pipe response is determined by the soil-mechanical behaviour of the sea-bed at the contact zone and the length of this zone. Testing of the system with three different idealized sea-bed soil resistance models showed that the overall effect of ground contact is to reduce response compared with the no-contact situation, as expected, the amount of reduction depending upon the model and the parameters defining it.

Despite the limited scope of this study two observations emerge from it and these may have important bearing on the design of such pipelines: firstly, models A and B are more likely to be valid in practice than model C, and, in A and B the response attenuation due to partial contact is not substantial over a realistic range of idealized sea-bed parameters. It would follow, therefore, that a design based on the no-contact assumption would not necessarily lead to a seismic over-design. Secondly, it is clear that in the interest of seismic safety against bending failure the amount of contact between the pipe and the sea-bed should be maximized. The buried pipe obviously represents the ideal situation in this respect. It would be prudent therefore to carry out a site survey with particular reference to scouring of the sea-bed; if high scouring activity is indicated then appropriate measures (e.g, sand-bagging, screw-piling, etc.) should be taken against it so that an initially buried segment is not subsequently exposed by sediment transport.

This study should be regarded as essentially a first step towards the understanding and solution of a very complex but important problem. A considerable amount of investigative work still remains to be done, particularly in the hydrodynamical and soil-mechanical aspects of the problem.

#### 7. NOTATION

[A]	Diagonal matrix of projected pipe areas.
[C]	Viscous damping matrix of pipe.
$C_D$	Drag coefficient = $2 \cdot \text{drag force} / (\rho \cdot \text{projected area} \cdot \text{velocity}^2)$
$C_M$	Inertia coefficient = added mass of pipe per unit length/mass of water displaced by pipe per unit length.
D	External diameter of pipe including concrete coating.
d	Clearance between the pipe and the sea-bed.
$d_o$	External diameter of pipe excluding concrete coating.
E	Young's modulus of steel pipe.
$\{F_f\}$	Listing of sea-bed resistance forces at the contact nodes ( $F_f$ refers to a single contact node).
$\{F_p\}$	Listing of restoring forces at the pipe nodes ( $F_p$ refers to a single node).
H	Length of contact zone.
I	Second moment of area of pipe.
[K]	Stiffness matrix of pipe.
$K_r$	Relative sea-bed stiffness = $(\mu W/Q)/(EI/L^3)$
L	Span of pipe segment
[M]	Submerged mass matrix of pipe.
$[M_a]$	Added mass matrix of pipe.
Q, $\mu$	Idealized sea-bed soil resistance parameters (Figs. 2c - 2e).
$\{U\}$	Listing of pipe deflections from the moving undeformed pipe axis.
$\{U_t\}$	Listing of pipe deflections from a fixed reference.
$\{U_s\}$	Listing of sea-bed displacement from a fixed reference.
$\{W\}$	Listing of nodal reactions between the pipe and the sea-bed ( $W$ refers to a single node).
$\rho$	Mass density of sea-water.

#### 8. BIBLIOGRAPHY

1. KING R: "Powerful eddy currents can play havoc with pipelines", Off-shore Engineer, London, December 1975, pp 42-43.
2. PARMELEE R A and CRAIG A L: "Seismic soil-structure interaction of buried pipelines", Proc. U.S National conf. on Earthquake engineering, Ann Arbor, June 1975, pp 406-415.

3. NEWMARK N M: "Seismic design criteria for structural facilities and the Trans-Alaska pipeline system", Proc. U.S National conf. on Earthquake engineering, Ann Arbor, June 1975, pp 94-103.
4. AYUB I and GOODLING E C: "Seismic design of buried pipes", Proc. 2nd. ASCE speciality conf. on structural design of Nuclear plant facilities, Vol. 1-A, 1975, pp 142-166.
5. ZASLAWSKY M et. al.: "Seismic safety considerations for buried pipes" Report no. UCRL-76977, Lawrence Livermore Laboratory, University of California, 1975.
6. BLAKE A: "Seismic protection of buried structures", Report no. UCID-16540, Lawrence Livermore Laboratory, University of California, 1972.
7. PATEL Y: "Pipeline design for seismic zones", Pipeline and Gas Journal, December 1975, Vol. 202, pp 24-32.
8. ANDERSON J C and JOHNSON S B: "Seismic behaviour of above-ground pipelines", Journal of Earthquake engineering and structural dynamics, Vol. 3, 1975, pp 319-336.
9. POWELL G H: "Seismic response analysis of above-ground pipelines", Journal of Earthquake engineering and structural dynamics, Vol. 6, 1978.
10. ----- "Protection of transport facilities against earthquakes", Report no. NTSB-ST-72-1, National transportation safety Board, Washington D C, 1972.
11. STEINBRUGGE K V et. al.: "Task force on Earthquake hazard reduction" Executive office of the President, Office of Science and Technology, 1970.
12. NATH B and SOH C H: "Transverse seismic response analysis of offshore pipelines in proximity to the sea-bed", Journal of Earthquake engineering and structural dynamics (to be published in 1978).
13. FRENCH W J and POOLE A B: "Deleterious reactions between dolomites from Bahrain and cement paste", Cement and concrete research, Vol. 4, 1974, pp 925-937.
14. NATH B: "Dynamics of structure-fluid systems", Advances in Hydroscience, Vol. 9, Academic Press, New York, 1973, pp 85-118.
15. LIAW C-Y and CHOPRA A K: "Dynamics of towers surrounded by water", Journal of Earthquake engineering and structural dynamics, Vol. 3, 1974, pp 33-49.
16. PENZIEN J et. al.: "Stochastic response of offshore towers to random sea waves and strong motion Earthquakes", Computers and structures, Vol. 2, 1972, pp 733-756.
17. PENZIEN J and KAUL H K: "Response of offshore towers to strong motion Earthquakes", Journal of Earthquake engineering and structural dynamics, Vol. 1, 1972, pp 55-68.
18. MALHOTRA A K and PENZIEN J: "Nondeterministic analysis of offshore structures", Journal of Engineering mechanics division, ASCE, EM-6, Vol. 96, December 1970, pp 985-1003.
19. MORISON J R et. al.: "The force exerted by surface waves on piles", Petroleum transactions, AIME, Vol. 189, 1950, pp 149-154.
20. YAMAMOTO T et. al.: "Wave forces on cylinders near plane boundary", Journal of the Waterways harbors and coastal engineering, ASCE, Vol. 100, WW-4, November 1974, pp 345-359.
21. YAMAMOTO T et. al.: "Yet another report on cylinder drag or wave forces on horizontal submerged cylinders", Bulletin no. 47, Engineering experiment station, Oregon State University, April 1973.
22. BUSHNELL M: ----- private communication.
23. WILSON J F and CALDWELL H M: "Force and stability measurements on models of submerged pipelines", Transactions of the ASME, Journal of Engineering for Industry, Vol. 93, series B, no. 4, 1971, pp 1290-1297.
24. MILLER B J: "The hydrodynamic drag of roughened circular cylinders", Proc. Royal Institution of Naval Architects, London, 1976, pp 55-70.
25. McNOWEN J S and KEULEGAN G H: "Vortex formation and resistance in periodic motion", Journal of the Engineering mechanics division, ASCE, EM-1, Vol. 85, part 1, January 1959, pp 1-6.
26. McNOWEN J S: "Drag in unsteady flow", Proc. IXth. International conf. on Applied mechanics, Brussels, 1957.
27. DAVIES M E: "A comparison between the wake structure of a stationary and oscillating bluff body, using a conditional averaging technique", Journal of fluid mechanics, Vol. 75, part 2, 1976, pp 209-231.
28. HARTLEN R and CURRIE I: "A lift-oscillator model for vortex induced vibrations", Proc. ASCE, Journal of the Engineering mechanics division, Vol. 96, 1970, p 577.
29. NATH B and SOH C H: "Seismic response analysis of offshore pipelines in contact with the sea-bed", International Journal of Numerical methods in engineering (to be published in 1978).
30. SHANTARAM D et. al.: "Dynamic transient behaviour of two and three dimensional structures including plasticity, large deformation effects and fluid interaction", Journal of Earthquake engineering and structural dynamics, Vol. 4, 1976, pp 561-578.

Leere Seite  
Blank page  
Page vide

CONTRIBUTION OF THE SURVEILLANCE TO THE EVALUATION OF THE  
SEISMIC EFFICIENCY OF DAMS. EXAMPLE OF THE AMBIESTA DAM

Dr. Aldo Castoldi - Director, Dynamic Department ISMES, Bergamo, Italy

SUMMARY

Present lack of information on site seismicity and approximation in usual design criteria require further research to be done in both theoretical and experimental directions to improve the knowledge on the seismic behaviour and, consequently, on the safety coefficient of large dams.

To this aim, an integrated research program, which includes in situ testing, mathematical models and seismic surveillance is proposed, and the technique adopted, as well as the results of a preliminary application of this program to the Ambiesta dam (Udine) during the aftershocks of the Friuli earthquake of 1976 are presented.

## 1. INTRODUCTION

Present criteria for the seismic risk analysis of a structure require on the one hand, the knowledge of the local seismicity, and on the other, the schematization by means of reliable mathematical models of the structural behaviour under seismic effects. These criteria have been satisfactorily applied for the nuclear plants and a well known procedure and regulation is now available in this field.

As far as the large dams are concerned, the problem of the seismic safety has been faced in these terms only in the last few years. Although the introduction of new methods has helped improve the computational techniques, theoretical difficulties still exist, particularly as regards the interaction between the dam and its foundation.

In order to achieve a correct set-up of the problem of the seismic risk evaluation for a dam, the checking of the reliability of available theories and procedures is required. In our view, this may be achieved through an approach which together with analytical computations and improved criteria for seismic surveillance, includes as well - at least in the most important cases - dynamic tests as a routine step of a research program for the long-term control and the safety-checking of a dam.

The following chapters illustrate a proposal for such a program, and describe the technique and the results of a preliminary application made on the Ambiesta dam for the recording of the Friuli earthquake aftershocks in October 1976.

## 2. PROPOSAL OF AN INTEGRATED PROGRAM FOR THE ANALYSIS OF THE SEISMIC EFFICIENCY OF A DAM

The analysis of the seismic risk of a dam and the evaluation of the effects of an earthquake have to be carried out by means of a series of operations which, notwithstanding their considerable validity even when taken singly, assume a most important significance if inter-related within the frame of an integrated program. The fundamental phases of this program should be the following:

- a) In situ testing to determine the dynamic characteristics of the dam.
- b) Setting up of a mathematical model for the calculation of the seismic response.
- c) Carrying out of the seismic surveillance, to collect data on site seismicity as well as on the response of the dam.
- d) Check up of the structure (both by the mathematical model or by testing) after a strong earthquake.

The close links among these phases are illustrated in fig. 1.

Phase a) has the aim of obtaining a sort of "identity card" of the structure, in which are listed the characteristics of its dynamic behaviour (possibly for different external conditions, such as the various levels of the impounded water).



These data can be obtained by different methods, such as forced or ambient vibrations, blast excitation, etc. The presently available recording and processing equipment assure highly precise results, as required for subsequent processing.

As regards phase b), although a mathematical model is usually developed in the design stage (this is not true, however, for dams designed several years ago), the above-mentioned theoretical complexity of the problem, together with the uncertainties of the design data (as to the geological and geophysical characteristics, and site seismicity) require that the model itself be carefully checked, and, if necessary, modified. To this aim, the experimental data obtained from phases a) and c) should be used as a reference stand, and the means to validate or to improve the reliability of the analytical schematization. It has to be underlined, however, that present experience on this subject is poor, and further investigations are necessary to fully exploit the experimental data for the above purposes.

The seismic surveillance of the dam (phase c)), is mainly intended to collect information on the seismicity of the site. Though a long term step, it is a necessary one, however, for the currently available data are usually unsatisfactory, and, especially for large reservoirs, local seismicity may be affected by the reservoir itself. Together with this aim, it should also allow the recording of shocks of medium or strong intensity and the determining of the structural response to these shocks. It is thus advisable to choose the recording points on the basis of the data supplied by the mathematical model, not only in order to simplify the interpretation of the results, but also in view of a possible further validation of the model itself.

The availability of a reliable mathematical model, as well as of significant data on the site seismicity, allow one both to meet and resolve in real terms the problem of the seismic risk analysis. Moreover, should a strong earthquake occur, as a consequence of which the structural integrity might be compromised, the problem arises of an immediate assessment of the structural safety. In this case the mathematical model, using as input the recorded seismic motion, can supply meaningful information on the state of stress induced by the earthquake in the structure; on the basis of this information it may be advisable to carry out a new phase of the program (phase d)), in which, through the repetition of the dynamic tests, the "identity card" of the structure is checked.

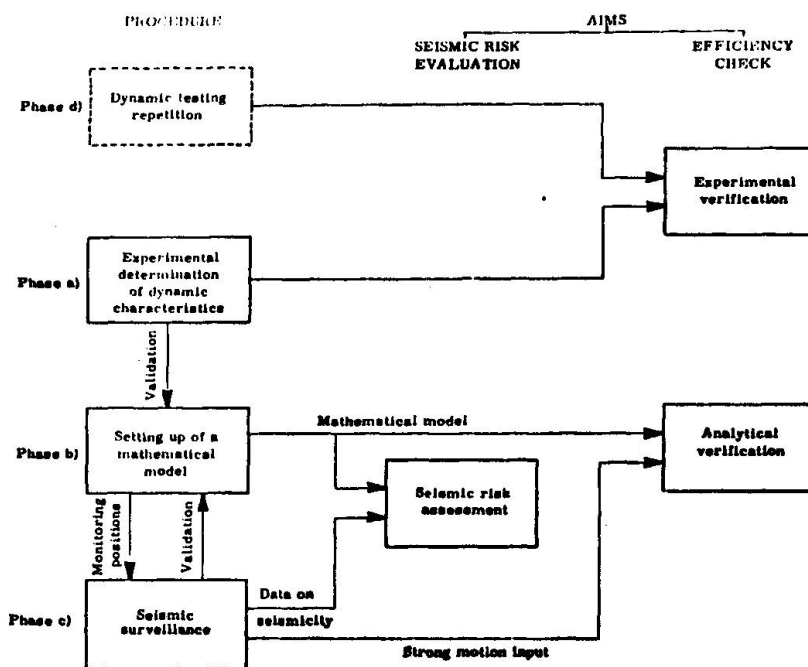


Fig. 1: Integrated program for the evaluation of the seismic efficiency of a dam.

Finally, another important outcome, which ought not to be disregarded, is that the data collected on the particular dam under control, may have a more general significance and may be profitably used both for theoretical analyses and for design or regulation purposes.

### 3. VIBRATION TESTS AND RECORDING OF AFTERSHOCKS ON THE AMBIESTA DAM

3.1. After the second main shock of the Friuli earthquake on September 15, 1976, ENEL entrusted ISMES with a program for the installation on the Ambiesta dam of an automatic system for the recording of the aftershocks, and for their processing. The Ambiesta dam is a small double-curvature arch dam, located near the epicentral area (fig. 2); the crest length is about 145 m, the maximum height is 60 m. Within framework of a research program supported by ENEL for the determination of the dynamic behaviour of the most important Italian dams, ISMES carried out forced vibration tests on the Ambiesta dam in 1975.

3.2. For the excitation of the dam, a mechanical vibration generator, delivering a sinusoidal force of up to 10 tons within the frequency range from 2 to 20 cps was used. This was placed in different positions on the crest arch, to allow a correct excitation of symmetric and antisymmetric modes. The response of the dam was recorded by means of 47 seismometers; the processing of the data carried out digitally by means of a Fourier analyzer, allowed the determination of the first resonance frequencies, modal shapes and damping coefficients. At the same time, a preliminary finite element mathematical model of the dam has been set up by ENEL. Since the dam is symmetrical, this model takes into account only half the structure; the foundation rock is considered of infinite stiffness. The main results of the vibrations tests as well as of the mathematical model are listed in table 1.

3.3. As to the practical application of the research program, examples of seismic surveillance, as previously discussed, or reference literature could not

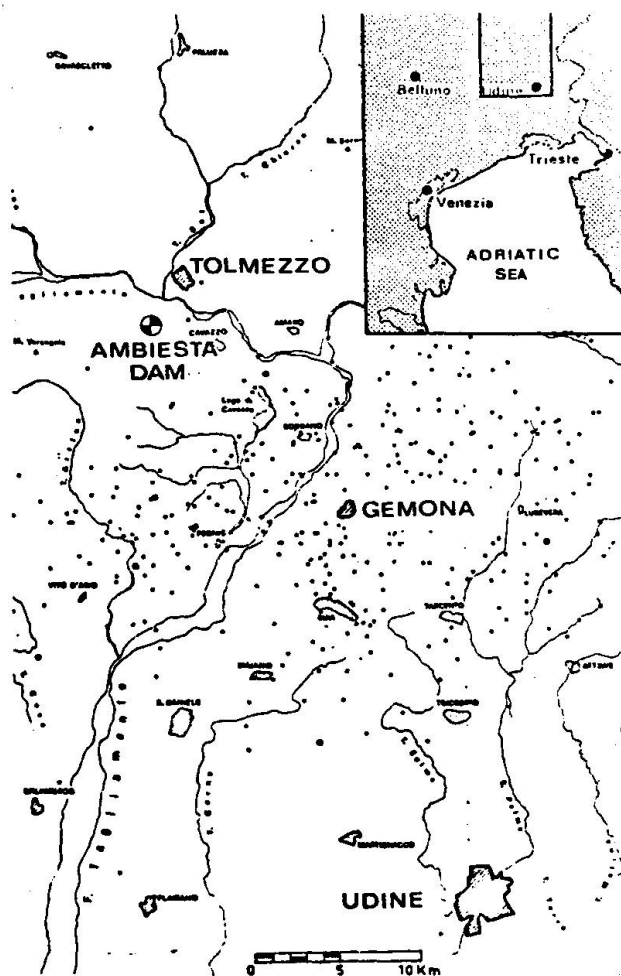


Fig. 2: Location of the Ambiesta dam (• : epicenters of shocks from 6.5.1976 to 16.6.1976).

be found. In effect, as far as is known, usually a single position on or near the dam is monitored by a single or three direction seismograph; obviously, this is not sufficient to carry out a seismic surveillance according to the criteria illustrated above.

In this preliminary phase of setting up of the criteria as well as of the most suitable procedure, the practical problems met with were as follows:

- to choose and set up a reliable and easy-to-handle digital equipment, for a continuous long term monitoring;

- to select the positioning of the recording instruments, and to establish the criteria of the data processing, in order to obtain the features of the earthquake excitation in several points along the foundation, as well as the characteristics of the response of the dam, to be compared with the results of the vibration tests.

In the particular case of the Ambiesta dam, 30 seismometers were used, 10 of which were placed along the foundation (two horizontal seismometers in each measuring position, oriented orthogonally to each other) and 20 on the downstream face in radial direction (fig. 3). This number is rather generous, and can be reduced for routine applications. However, it was justified by the lack of previous experience and by the need to avoid missing potentially useful information.

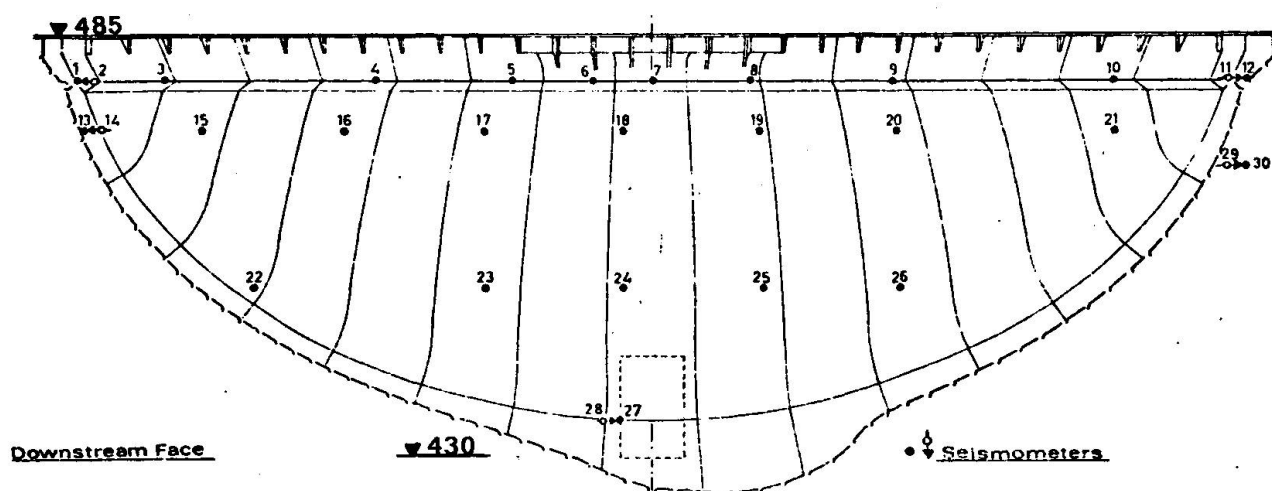


Fig. 3: Layout of the measuring points on the Ambiesta dam.

After digitization by an analog to digital converter, the signals coming continuously from the seismometers were sent to a minicomputer which stored on a magnetic tape only the seismic events exceeding a prefixed intensity threshold.

The intensity was checked out on the signal coming from the seismometer placed at the base of the central cantilever, in radial direction (position 27). In this way, electrical noise and other minor disturbances were disregarded, since only significant seismic events were recorded. Moreover, a single operator was required from time to time to replace the magnetic tapes.

3.4. The system was operative during the period from 8 to 27 October 1976, and 118 seismic aftershocks were recorded. Their intensity is very small since the maximum velocities recorded at point 27 ranged from  $5 \cdot 10^{-4}$  cm/sec to  $4 \cdot 10^{-2}$  cm/sec. Therefore, the processing was carried out on 35 records, showing maximum velocities larger than  $2 \cdot 10^{-3}$  cm/sec; the records of lower intensity were disregarded.

#### 4. PROCESSING AND ANALYSIS OF THE RECORDS

4.1. The analysis of the recorded data was intended to supply information able to enlight the phenomena connected with the energy exchange between the foundation and the dam, and to check the accuracy - and, consequently, the reliability - of the hypotheses currently adopted for the computing methods. As is well known, these methods, even the most sophisticated ones, take into account a three-dimensional continuum made up of the dam and a part of its foundation, and apply to its boundary an uniform excitation, equal to that of the "bed rock".

Under these hypotheses, and making use of the modal analysis techniques, it is easy to obtain the relationships between the response  $\{q\}$  of the dam and the input excitation. In particular, the expression of the transfer functions related to the upstream-downstream (x) and longitudinal (y) directions are:

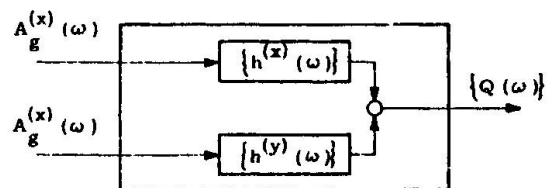
$$\begin{aligned} \{Q(\omega)\} / A_g^{(x)}(\omega) &= \{h^{(x)}(\omega)\} = \sum_{k=1}^{\infty} c_x^k \cdot \{\phi^{(k)}\} \cdot B^{(k)}(\omega) \\ \{Q(\omega)\} / A_g^{(y)}(\omega) &= \{h^{(y)}(\omega)\} = \sum_{k=1}^{\infty} c_y^k \cdot \{\phi^{(k)}\} \cdot B^{(k)}(\omega) \end{aligned}$$

where:  $c_{x,y}^k$  are the participation coefficients for the k-th mode in direction x and y respectively

$\{\phi^{(k)}\}$  is the modal shape of the k-th mode

$$B^{(k)}(\omega) = 1 / \left[ \omega_k^2 \left( 1 - \frac{\omega^2}{\omega_k^2} \right) + 2j\zeta \frac{\omega}{\omega_k} \right]$$

According to this procedure, the time histories  $\{q(t)\}$  recorded on the dam may be interpreted as being generated by two different inputs (the two components of the seismic excitation) as illustrated in the sketch. An estimation of the function  $\{h^{(x)}(\omega)\}$  and  $\{h^{(y)}(\omega)\}$  obtained through the theory of the linear systems and of the random processes, allows one to make an assessment of



the reliability of the assumptions by comparing these functions with those obtained employing the mathematical model.

In the present case, as a first approach to the problem, it was thought sufficient to proceed according to a simpler scheme, and to leave to future processing a further investigation, in case of interesting results being obtained from this approach. Such simplifications are justified by the following observations:

- The input motion, that is the components of the earthquake at the "bedrock", is obviously unknown; the time histories recorded at the bottom of the dam only as a first approximation may be considered as the inputs of the system.
- The contribution of the two components of the input motion to the response at a point of a dam has different weight depending on the frequency range considered, as it is determined by the transfer functions  $\{h^{(x)}(\omega)\}$  and  $\{h^{(y)}(\omega)\}$  which in turn depend on the participation coefficients  $c_x^*$  and  $c_y^*$ . As is known, these are rather different for the two components depending on the modal shape. According to this, for example as far as the first mode is concerned, when  $\omega \simeq \omega_1$  the following is obtained:

$$Q_i(\omega) = h_i^{(x)}(\omega) \cdot A_g^{(x)}(\omega) + h_i^{(y)}(\omega) \cdot A_g^{(y)}(\omega) \simeq h_i^{(x)}(\omega) \cdot A_g^{(x)}(\omega) = H(\omega) \cdot A_g^{(x)}(\omega)$$

It follows that the relationships between the response and the input motion can be replaced, at least in certain frequency intervals, by that relative to a single input linear system.

Therefore, the transfer function has been calculated by using the following relationship:

$$H(\omega) = G_{ab}(\omega) / G_{aa}(\omega)$$

where  $G_{ab}(\omega)$  is the cross-spectral density function between the input signal  $a(t)$  and the output signal  $b(t)$ ;  $G_{aa}(\omega)$  is the power spectral density of  $a(t)$ .

The coherence function  $\gamma(\omega)$  defined as:

$$\gamma^2(\omega) = |G_{ab}(\omega)|^2 / (G_{aa}(\omega) \cdot G_{bb}(\omega))$$

( $G_{bb}(\omega)$  being the power spectral density of  $b(t)$ ) is an indication of the correlation between the input and output signals. Low values of  $\gamma(\omega)$  indicate poor correlation, which may be due to different reasons, such as presence of noise or external disturbance in the signals, physical lack of correlation between the signals, inadequate description of the phenomenon through the assumed hypotheses.

Together with the calculation of  $H(\omega)$  it was thought that also the determining of the amplifications at several points of the foundation and the dam body (as ratios between the maximum values of the time histories recorded at these points and at the bottom of the dam) could supply an indication, even though rather approximated, of the reliability of the assumptions.

4.2. Some observations on the results of this preliminary processing are as

follows:

a) Motion at foundation

The records obtained at positions 1, 12 and 27 (transverse direction) and at positions 2, 11 and 28 (longitudinal direction) have been examined. Table 2 lists the average values of the maximum amplifications recorded at these points, from which the following consideration may be drawn:

- The two components of the motion at the bottom are, on the average, of the same intensity. Their values are, however, rather scattered, as it is obvious, owing to the large differences in the patterns of the records. This is clearly illustrated in fig. 4, which shows the Fourier transforms of some earthquakes recorded at position 27. As may be noted, the energy distribution over the frequency range differs greatly from earthquake to earthquake. This may be justified by the different hypocentral locations and by the varied paths of the travelling waves.

- The amplifications of the abutments are rather large (as shown in fig. 5, in which the time histories are given, and in fig. 6, which gives the response spectra at the same points), being respectively about 3 times and 2 times the motion in transverse and longitudinal direction. The attempt to calculate the transfer functions  $H(\omega)$  did not prove satisfactory, as may be seen from the fact that their patterns are dispersed, and the coherence very low (fig. 7). This could de

	Reference	Average of maxima	Standard deviation
Foundation	Pos. 1/Pos. 27	3.11	0.77
	Pos. 12/Pos. 27	2.75	0.71
	Pos. 2/Pos. 28	1.92	0.38
	Pos. 11/Pos. 28	1.88	0.42
	Pos. 27/Pos. 28	0.98	0.26
Crest arch	Pos. 7/Pos. 27	5.84	1.93
	Pos. 8/Pos. 27	7.93	2.44
	Pos. 9/Pos. 27	10.59	3.75
	Pos. 10/Pos. 27	6.88	1.84

Table 2: Average values of the ratios between the maximum velocities recorded.

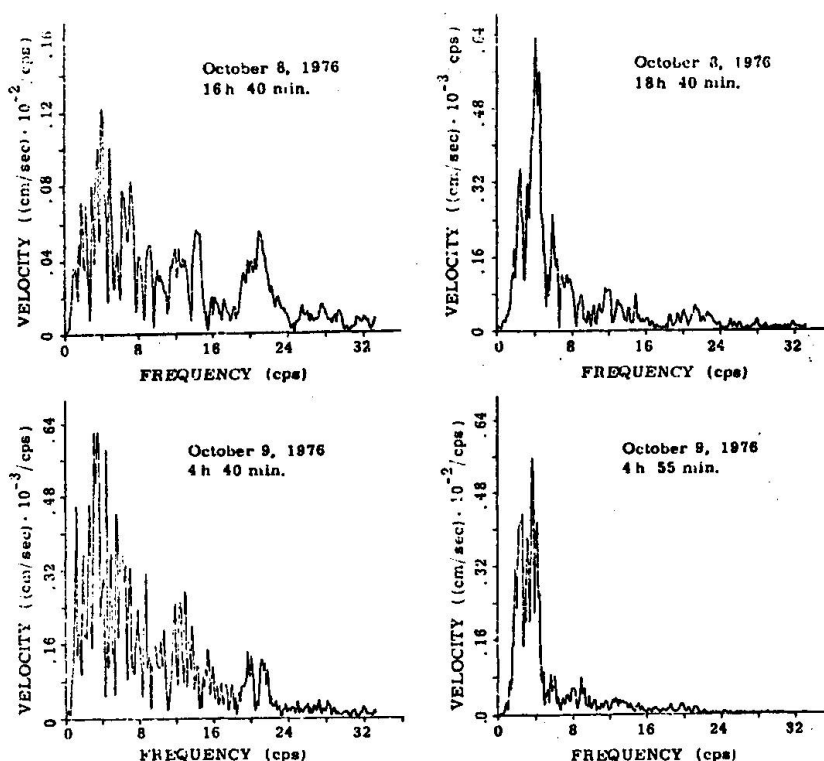


Fig. 4: Fourier transforms of different after-shocks at the bottom of the dam.



the reliability of the assumptions by comparing these functions with those obtained employing the mathematical model.

In the present case, as a first approach to the problem, it was thought sufficient to proceed according to a simpler scheme, and to leave to future processing a further investigation, in case of interesting results being obtained from this approach. Such simplifications are justified by the following observations:

- The input motion, that is the components of the earthquake at the "bedrock", is obviously unknown; the time histories recorded at the bottom of the dam only as a first approximation may be considered as the inputs of the system.
- The contribution of the two components of the input motion to the response at a point of a dam has different weight depending on the frequency range considered, as it is determined by the transfer functions  $\{h(x)(\omega)\}$  and  $\{h(y)(\omega)\}$  which in turn depend on the participation coefficients  $c_x^*$  and  $c_y^*$ . As is known, these are rather different for the two components depending on the modal shape. According to this, for example as far as the first mode is concerned, when  $\omega \simeq \omega_1$  the following is obtained:

$$Q_i(\omega) = h_i^{(x)}(\omega) \cdot A_g^{(x)}(\omega) + h_i^{(y)}(\omega) \cdot A_g^{(y)}(\omega) \simeq h_i^{(x)}(\omega) \cdot A_g^{(x)}(\omega) = H(\omega) \cdot A_g^{(x)}(\omega)$$

It follows that the relationships between the response and the input motion can be replaced, at least in certain frequency intervals, by that relative to a single input linear system.

Therefore, the transfer function has been calculated by using the following relationship:

$$H(\omega) = G_{ab}(\omega) / G_{aa}(\omega)$$

where  $G_{ab}(\omega)$  is the cross-spectral density function between the input signal  $a(t)$  and the output signal  $b(t)$ ;  $G_{aa}(\omega)$  is the power spectral density of  $a(t)$ .

The coherence function  $\gamma(\omega)$  defined as:

$$\gamma^2(\omega) = |G_{ab}(\omega)|^2 / (G_{aa}(\omega) \cdot G_{bb}(\omega))$$

( $G_{bb}(\omega)$  being the power spectral density of  $b(t)$ ) is an indication of the correlation between the input and output signals. Low values of  $\gamma(\omega)$  indicate poor correlation, which may be due to different reasons, such as presence of noise or external disturbance in the signals, physical lack of correlation between the signals, inadequate description of the phenomenon through the assumed hypotheses.

Together with the calculation of  $H(\omega)$  it was thought that also the determining of the amplifications at several points of the foundation and the dam body (as ratios between the maximum values of the time histories recorded at these points and at the bottom of the dam) could supply an indication, even though rather approximated, of the reliability of the assumptions.

4.2. Some observations on the results of this preliminary processing are as

follows:

a) Motion at foundation

The records obtained at positions 1, 12 and 27 (transverse direction) and at positions 2, 11 and 28 (longitudinal direction) have been examined. Table 2 lists the average values of the maximum amplifications recorded at these points, from which the following consideration may be drawn:

- The two components of the motion at the bottom are, on the average, of the same intensity. Their values are, however, rather scattered, as it is obvious, owing to the large differences in the patterns of the records. This is clearly illustrated in fig. 4, which shows the Fourier transforms of some earthquakes recorded at position 27. As may be noted, the energy distribution over the frequency range differs greatly from earthquake to earthquake. This may be justified by the different hypocentral locations and by the varied paths of the travelling waves.

- The amplifications of the abutments are rather large (as shown in fig. 5, in which the time histories are given, and in fig. 6, which gives the response spectra at the same points), being respectively about 3 times and 2 times the motion in transverse and longitudinal direction. The attempt to calculate the transfer functions  $H(\omega)$  did not prove satisfactory, as may be seen from the fact that their patterns are dispersed, and the coherence very low (fig. 7). This could de

	Reference	Average of maxima	Standard deviation
Foundation	Pos. 1/Pos. 27	3.11	0.77
	Pos. 12/Pos. 27	2.75	0.71
	Pos. 2/Pos. 28	1.92	0.38
	Pos. 11/Pos. 28	1.88	0.42
	Pos. 27/Pos. 28	0.98	0.26
Crest arch	Pos. 7/Pos. 27	5.84	1.93
	Pos. 8/Pos. 27	7.93	2.44
	Pos. 9/Pos. 27	10.59	3.75
	Pos. 10/Pos. 27	6.88	1.84

Table 2: Average values of the ratios between the maximum velocities recorded.

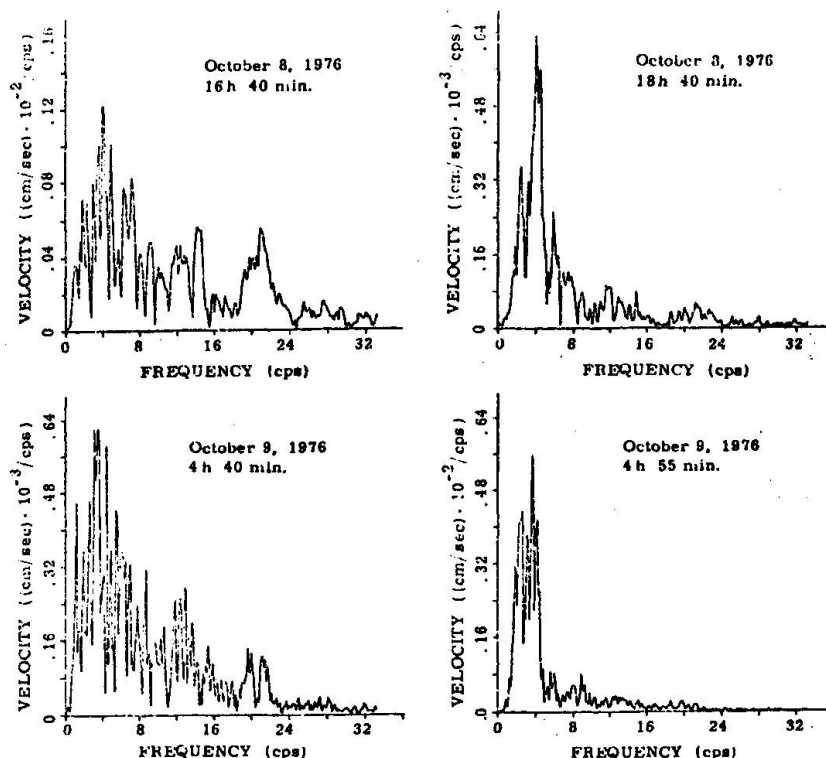
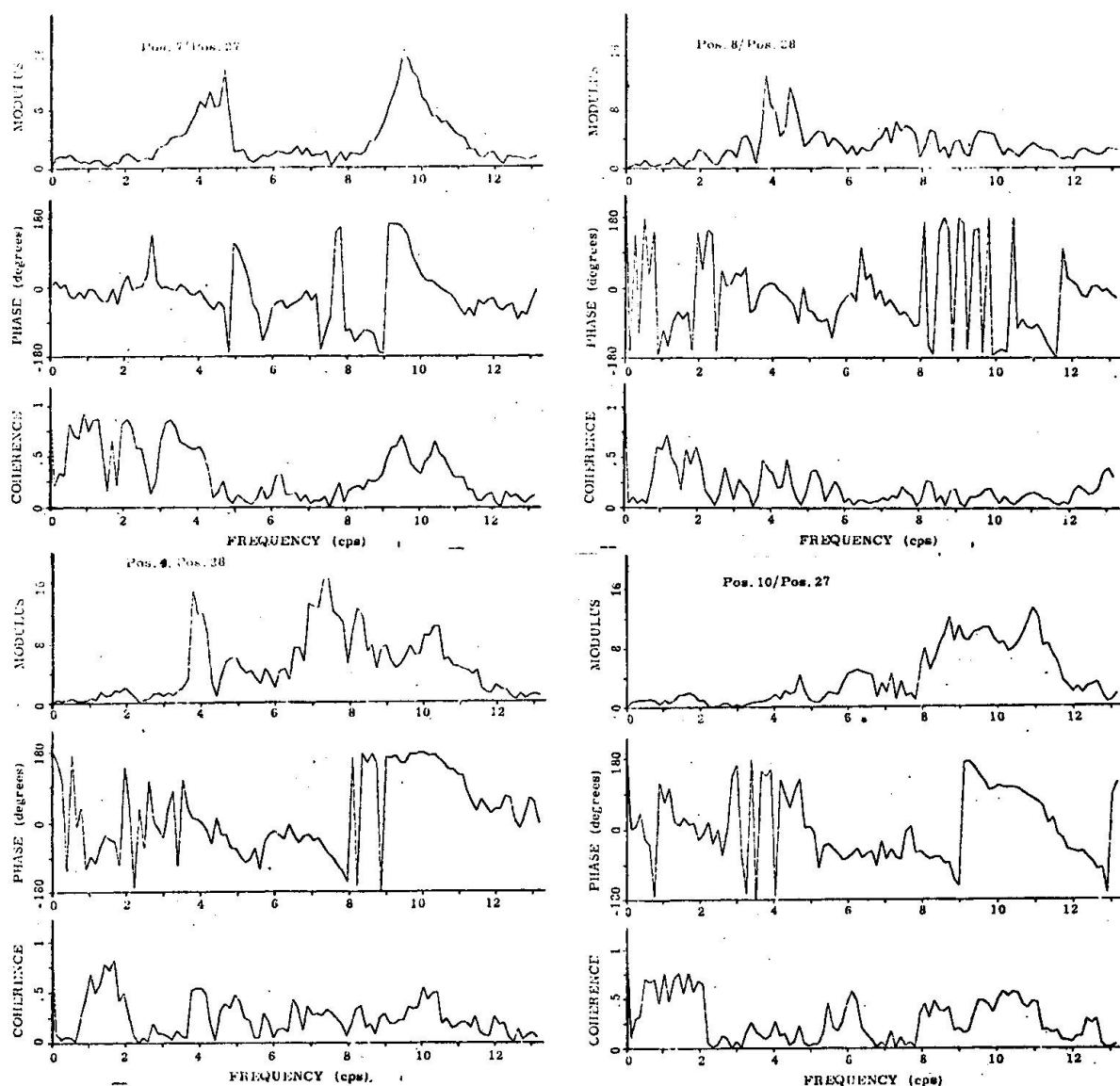


Fig. 4: Fourier transforms of different after-shocks at the bottom of the dam.



**Fig. 8:** Transfer functions  $H(\omega)$  relative to crest arch points.

Mode no.	Resonance frequencies (cps)	Amplifications recorded in position							
	R	T	7		8		9		10
			R	T	R	T	R	T	R
1	3.8 + 4.4	4.1	10.5	-	12.8	-	13.3	-	-
2	4.5 + 4.8	4.7	13.3	40.5	11.2	13.5	-	21.6	4.1
3	7.3 + 7.8	7.7	-	52.4	-	17.5	22.0	30.1	-
4	8.7	8.5	-	-	-	-	-	12.5	12.1
5	9.5 + 9.9	9.3	15.2	43.5	-	-	13.7	-	-

**Table 3:** Resonances and amplifications at the crest arch from records (R) and vibration tests (T).

## 5. CONCLUSIONS

Although still incomplete and with the processing of the data still at a preliminary stage, the experience gained from the program carried out in the particular case of the Ambiesta dam has nevertheless made it possible to draw up a series of useful clues concerning the validity of the proposed method.

As far as the single stages of the program are concerned, it may be concluded that both the determination of the modal characteristics of the structure as well as seismic surveillance are problems that by now have been solved - be it from the point of view of methodology or the instrumentation to be employed.

The cost as well may be considered altogether reasonable when compared with the financial commitment that the construction of a dam calls for.

The weightier problems present themselves in the stage involving the interpretation of the data in light of the behaviour models in use at present, which, in our view are not altogether adequate for the explanation of the phenomena as a whole and, therefore, are not able to duplicate analytically the experimental data.

In effect the lack of a direct correlation between the motion at the base of the dam and the response may be attributed only partly to the introduction of simplifications. It is probably explained, instead, by the fact that the behaviour model adopted assumes the existence of a physical link between the input and the output which in reality is absent. In other words, the motion at a point cannot be correlated with the hypothetical uniform motion of the bedrock, but it may be explained by taking into account rather more complex seismic wave propagation phenomena.

From this point of view, parameters such as the position of the hypocenter and the direction of wave propagation play an important role not only in that they determine the frequency contents of an earthquake but also because they are able to influence the manner with which the structure and its foundation exchange energy.

In conclusion, the extension of similar surveillance in future to other dams put up in seismic areas is to be recommended, not only for purposes of a better assessment of the seismic risk involved but also from the point of view of acquisition of data and information related to the characteristics of excitation and structural response.

The availability of further case histories can lead to a better understanding of the phenomena and thus make good the present deficiencies in the interpretation of the data.

## 6. ACKNOWLEDGMENTS

The author thanks the "Direzione Studi e Ricerche" of ENEL, which supported the research and allowed the publication of the results.

4th Session    SEISMIC EFFICIENCY OF LARGE STRUCTURES (RECOMMENDATIONS, CHECKING AND SURVEILLANCE)

DISCUSSION

Address to participants by R.G. T. LANE - ENGLAND

"Probelms in Assessing the Effects of Earthquake on Dams"

CLOUGH

Only five accepted examples of reservoir induced seismic events with magnitude  $M = 5$  have been reported. This is a very small number compared with the number of large dams in the world. Also, the accepted hypothesis is that reservoir induced seismicity (events) involve only the "triggering" of the existing strain fields - no significant increase of seismic energy is produced by the reservoir. In view of these facts, do you believe reservoir induced seismicity should have any influence on design criteria for dams?

LANE

On the question of statistics, the figures I have relate to very large dams defined as those higher than 100 m or with reservoir capacity exceeding one thousand million cubic meters.

Out of all such dams built in the world, 1 to 14 has shown induced seismicity. Now there are due to be built during the next few years another 140 dams of that size. That means that on the basis of statistics we can expect ten more cases of appreciable induced seismicity within the near future. That is the statistical position.

CLOUGH

I would like to comment on that, because the number you quoted is accepted as reservoir induced seismicity, but most of those are essentially micro-earthquakes or very small earthquake activities, and the only ones that might induce appreciable damage are those of magnitude 5 or greater. So the number of these is very much smaller.

LANE

The prefix "micro" is usually used for very small events. There have been two or three cases of induced seismicity of magnitude 6 (Richter). But

the point I raised is that these events are very close to structures and they are very shallow. Therefore, it is thought that the effect of even a small one could be appreciable, and this requires geological study also. I would recommend that for every large dam the question of induced seismicity should be seriously taken into account.

Your second question was related to factors causing induced seismicity. Various causes are suggested. Some people have referred to the weight of water but this is small compared with the weight of rock which once filled the valley. I do not think weight of water is in itself any problem. My own theory is that the water penetrates into the faults. Now these faults extend well beyond the reservoir area and they are also very deep. We are talking now of kilometres, of tens of kilometres or even more. Water is already in that fault and when you add to it a hundred metres of head, there is an elastic compression of water. This elastic compression of water takes time, but gradually the water down to great depths will be affected by this elastic compression; letting more water in and at the same time increasing compression. This accounts, in my opinion, for two things: it explains the long delay between the impounding and the effect; in the case of Kariba it was 5 weeks before it happened. But during that time, an area of perhaps tens of even hundreds of square kilometres has had its pressure increased by one hundred metres, and that is a lot of pressure. In my opinion that is the probable reason for induced seismicity.

#### CAPOZZA

I think it should be emphasized the particular role played by the actual state of stress on the arising of an induced seismicity. As a matter of fact, should the actual stresses be very near to the strength in a point of the rock mass, just a little increasing in the pore pressure could be required to allow the starting of a slip generating seismicity.

Whether this seismicity could attain high levels or not, it depends, among other things, on the amount of elastic energy stored in the rock mass, and so on conditions related again to the pre-existing state of stress.

Paper 4/1 R. PRISCU, A. POPOVICI, C. STERE - ROMANIA

"The Consequences of Partially Grouted Joints Upon the Arch Dam Seismic Behaviour"

#### CLOUGH

If I understand the paper correctly, the analysis of the dam response considers the ungrouted joints to be represented by reduced stiffness, but does not account for the non-linear effect of the joint opening and closing



during the dynamic response. In your opinion does the true non-linear response differ significantly from the assured linear partially grouted dam response?

PRISCU

When modelling the dam ungrouted joints with beam elements of reduced stiffness, some phenomena have been disregarded as: the shear effect in the dam joints, the non-elastic behaviour of the whole system, the damping variation with the intensity of the dynamic response.

The presented analysis has been carried out in the linear-elastic domain with the SAP IV computer program, elaborated by the University of Berkeley; that computer program has been adequately fitted out to the Romanian in use computers and it includes some routines written by us.

We know some computer programs performing some of the forementioned neglected phenomena (NONSAP, ADINA) do exist, but there is the unhappy situation that we do not still take advantage of it.

We are aware the proper consideration of some above disregarded phenomena could really yield some quantitative change of the dam static and dynamic response. In the paper, a qualitative comparison related to the dam monolithic structure has been sought for, that last variant being also analysed in the linear-elastic domain.

LANE

I believe that the ordinates of fig. 4 are all ten times too large and a decimal point should be added; also in fig. 7 I find it difficult to understand the large horizontal stresses in the area where the joints are ungrouted.

PRISCU

The values of the velocity potential function  $\psi$  presented in figure 3 are correctly represented. This fact could be properly noticed by making an analogy with the classical relationship of Westergaard. Let us consider for instance the network point (i) of the dam central cross-section, situated at the depth  $4 \cdot \Delta z = 132$  m below the crest, whereat the potential function is  $\psi_i = 99.6$  m.

The specific added mass normally directed to the dam upstream face comes out to be:

$$m_{hi} = \rho \cdot \psi_i = 0.102 \times 99.6 = 10.15 \text{ tf} \cdot \text{s}^2/\text{m}^3 \quad (1)$$

If, in the foreconsidered point (i), an acceleration of  $0.1 g \approx 1 \text{ m/s}^2$  normally directed to the dam surface ( $c_{ni}$ ) is being taken into consideration the hydrodynamic pressure will be:

$$p_{hi} = m_{hi} \cdot c_{ni} = 10.15 \times 1 = 10.15 \text{ tf/m}^2 \quad (2)$$

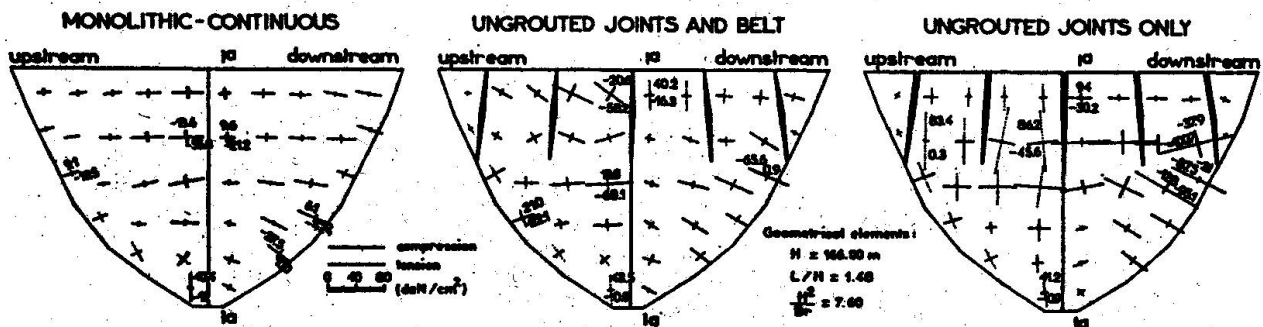
One comparatively gives the same hydrodynamic pressure by using instead the Westergaard relationship, with the same above data:

$$p_{hi} = a_{ni} \cdot C_p \cdot \sqrt{H \cdot z_i} = 0.1 \times 0.9 \cdot \sqrt{165 \times 132} = 13.20 \text{ tf/m}^2 \quad (3)$$

However, the values of the potential function take into consideration the dam and valley (reservoir) geometry and the earthquake wave direction.

The dam structure discretization has been carried out through Clough-Fellipa thin shell finite elements, according to the SAP IV program /6/. The computer program gives out stresses within the element centers. Therefore, in fig. 7, the horizontal and vertical stresses are represented for the medium cross-section of the dam central block (cross-section a-a).

As to have a more complete picture upon the stress distribution of the three considered schemes (monolithic, partial grouted joints with and without stiffening crest belt), in the hereby enclosed figure the principal stresses  $\sigma_1$ ,  $\sigma_2$  are presented, yielded by the hydrostatic pressure with the reservoir level up to the dam crest.



Principal stresses  $\sigma_1$ ,  $\sigma_2$  produced by hydrostatic pressure, according to the three analysed variants.

Paper 4/5 O. FISCHER - CZECHOSLOVAKIA

"Seismic Behaviour of Guyed Masts"

GROSSMAYER

I just wanted to ask if you can also make some considerations concerning dynamic excitation of the anchors of the guys, because if I understand you well, you consider only the excitation for the mast and static displacement for the guys.

FISCHER

In principle it would be possible to solve the effect of horizontal excitation of the guy-foundation similarly like that of the mast-foundation, described in the paper. The "influence-numbers" /7/

$$P_{(k)} = \frac{\int \mu v_o(x) v_{(k)}(x) dx}{\int \mu v_{(k)}^2(x) dx}$$

which depend on the product of the natural mode of the mast and the static deflection line caused by unitary displacement of the mast foundation, this static deflection line should be replaced by that corresponding to the unitary displacement of the guy-foundation. The rest of the solution remains the same.

LANE

I would like to ask if you have been able to check your theory on actual structures.

FISCHER

Till now we could check only the method for computation of natural frequencies and modes. Measuring the vibrations of a guyed mast in wind we have found the frequencies, which corresponded quite well to the calculated ones.

Paper 4/8 A. CASTOLDI - ITALY

"Contribution of the Surveillance to the Evaluation of the Efficiency of Dams. Example of the Ambiesta Dam"

CLOUGH

I would merely like to ask about the recent work using only two components of seismic input instead of three. Of course we all agree that even a three-component input is an over-simplification. But I was wondering why you did not include the vertical component in your representation.

CASTOLDI

The true reason for not having included the vertical component is that it has not been recorded. Since the number of seismometers was limited, and since it was therefore necessary to make a careful choice of the measuring points, it has been considered more important to determine the distribution along the dam foundation of the horizontal components (to which the seismic response of the dams is strictly related) than the vertical component. In any case, from a conceptual point of view, there are no difficulties in taking into account all the three components.

CLOUGH

There is one additional comment in that direction. As you probably know from the literature, Prof. Chopra's studies on the hydrodynamic interaction mechanism have demonstrated that in gravity dams, at least, the vertical component is or may be as important as the horizontal component in generating seismic response.

CASTOLDI

Yes, that is true. However, it should be pointed out that the Ambiesta dam, on which these recordings have been taken, is an arch dam, not a gravity dam.

CLOUGH

But I think the same might be true in the case of the arch as well.

CASTOLDI

This is a matter which should be checked. However, in my opinion, the

contribution of the horizontal components of the seism to the horizontal components of the response of an arch dam is by far more important than that of the vertical component. This statement is justified if one considers that the modal shapes of the arch dam usually show vertical components less than  $10 \div 20\%$  of the horizontal ones. It follows that the participation coefficients of the first vibration modes are smaller for a vertical seism with respect to a horizontal one.

GROSSMAYER

I would like to ask if you can draw any conclusion about the distribution of the excitation along the base and abutment of the Ambiesta dam.

CASTOLDI

Yes, 10 of the 30 instruments used were placed along the abutments of the dam at different levels and enabled to know the distribution of the excitation along the foundation.

Some data concerning the amplification factors are shown in the paper: they range between two and four, with a large dispersion around these mean values depending on the direction and frequency content of the motion. It has not been possible however to find a correlation among the records at different levels.

LANE

I do not know the Ambiesta dam, but I am wondering whether there is an other structure near the dam to enable a simple understanding of the site behaviour for comparison with the more complex behaviour of the dam. This would help to separate various effects.

CASTOLDI

I do not think that there is such a structure near the dam. We have monitored the dam and its foundation quite extensively, so that we have a good picture of the situation; yet we could not find correlation among the records. In my opinion, it may not be a matter of better knowing the site geology or the earthquake features, but how the energy spreads from its source and reaches the abutment and the dam.

Leere Seite  
Blank page  
Page vide